ELASTIC STABILITY CHARACTERISTICS ILLUSTRATED BY SIMPLE MODELS

BY

HARISHCHANDRA S. PATEL

Submitted in Partial Fulfillment of the Requirements

for the Degree of

Master of Science in Engineering

in the

CIVIL Engineering

Program

Paul X Bellini 6/6/74

Adviser Date

Dean of the Graduate School 6/10/74

Date

YOUNGSTOWN STATE UNIVERSITY

JUNE, 1974

ABSTRACT

ELASTIC STABILITY CHARACTERISTICS

ILLUSTRATED BY SIMPLE MODELS

HARISHCHANDRA S. PATEL

Master of Science in Engineering

Youngstown State University, 1974

The purpose of this thesis is to obtain a simple model, which gives the load-deflection relationship resembling the load versus lateral deflection plot for an axially-compressed thin cylindrical shell. Hence four simple mathematical models consisting of a rigid rod combined with a linear spring are investigated using the criteria of static and dynamic stability. Similarly, two more mathematical models consisting of a rigid rod combined with a linear and a torsional spring are also investigated.

The basic laws of elastic stability are also interpreted mathematically and geometrically for the suitable models. The mathematical solutions for both stable and unstable equilibrium states are illustrated graphically, in the statical case, by potential energy and load-deflection curves.In the case of dynamic analysis, the concept of phase-plane is utilised.

ACKNOWLEDGEMENTS

I wish to take this opportunity to convey my utmost thanks to my advisor, Dr. Paul X. Bellini, whose efforts, guidance, and advice contributed directly to the completion of this thesis.

I also wish to thank the review committee members, Dr. Michael K. Householder and Mr. John Ritter for their co-operation.

I wish to thank all my friends, who have immensely helped in my efforts to complete this thesis.

TABLE OF CONTENTS

LIST OF SYMBOLS

SYMBOL	DEFINITION
E_o	Total energy of the system, at time t = 0
k_1, k_2, k_3	Stiffness of the linear springs
k_T	Stiffness of the rotational spring
k	Stiffness ratio
L	Length of the rigid rod
L_o	Combined lenght of the rigid rod and undeformed spring
$\hat{L}$	Non-dimensional Lagrangian of the system
m	Combined mass of the system
P	Applied external vertical load
$\hat{P}$	Non-dimensional form of applied load P
$\hat{P}_{cr}$	Critical value of applied load
R	Radius of curved guide
r	Combined lenght of the rigid rod and deformed spring
$\hat{T}$	Non-dimensional kinetic energy of the system
u	Horizontal projection of the rigid rod
$\hat{U}$	u/L
$\dot{\hat{U}}$	$\dot{u}$/L
$\hat{U}_{cr}$	Non-dimensional form of the critical static displacement
V	Potential energy of the system
$\hat{V}$	Non-dimensional potential energy of the system
$\hat{V}'$	First derivative of the potential energy
$\hat{V}''$	Second derivative of the potential energy
α	R/L

α_0, α_1	Geometrical parameters
θ	Angular displacement
$\dot{\theta}$	Angular velocity

LIST OF FIGURES

LIST OF FIGURES (CONT.)

CHAPTER I

INTRODUCTION

Object:

The structural engineering elements have been studied extensively for the criteria of load stability. However stability of certain systems such as, an axially-compressed long cylindrical shell, have been observed to be governed by perturbing lateral deformations, which is explained by Panovko and Gubanova.[3] It follows from the above reference that, the critical compressive stress, based on Euler's method, was approximately given as,

$$\sigma_{cr} = \frac{0.6Eh}{R},$$

where,

E= The modulus of elasticity of the material of the shell,

h= The thickness of the shell, and

R= The radius of the cylinder.

The geometric shape, of shell upon loss of stability is shown dotted, in the figure (1-a). Subsequent experimental tests on the thin cylindrical shells have not supported the results, which were derived, on the basis of Euler's method, where the terminal axial displacements were not considered. The figure (1-c), shows the result of non-dimensional axial load versus, the longitudinal shortening ϵ magnified by the factor R/h, which is obtained by taking into consideration the terminal displacements. The segement O-A of the figure (1-c) shows that, in the begining the stress increases rapidly, following a linear law. Point A shows the critical stress given by Eulerian approach. At this

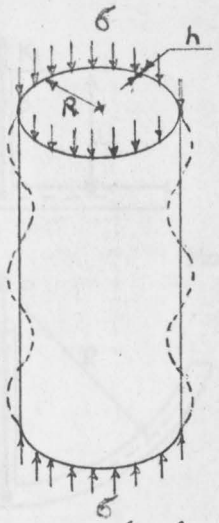

Figure (1-a)

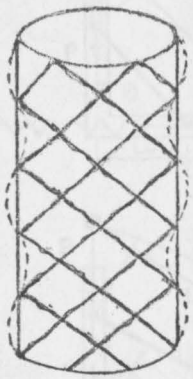

Figure (1-b)

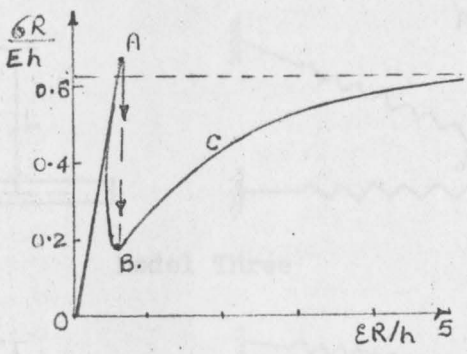

Figure (1-c)

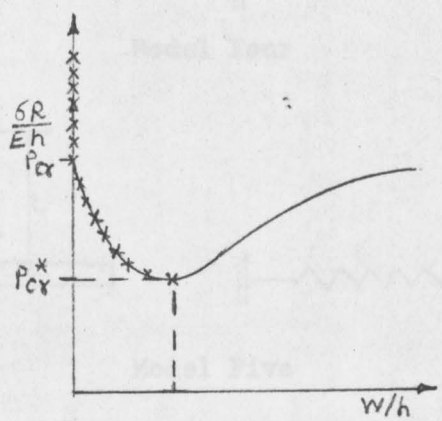

Figure (1-d)

Initial Configuration

Displaced Configuration

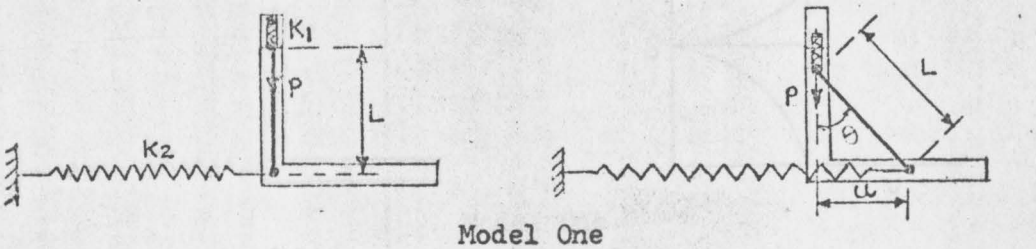

Model One

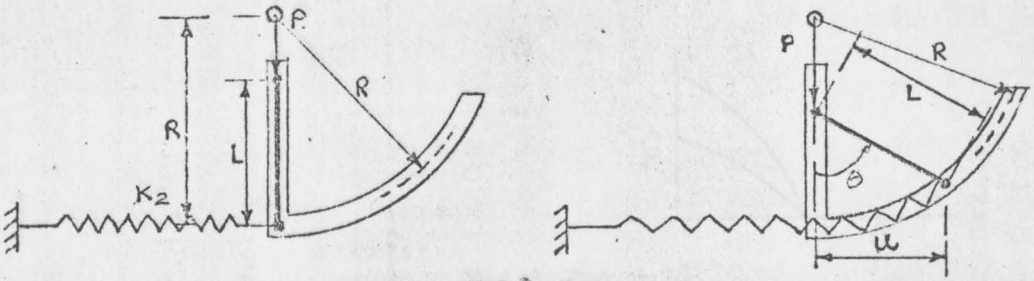

Model Two

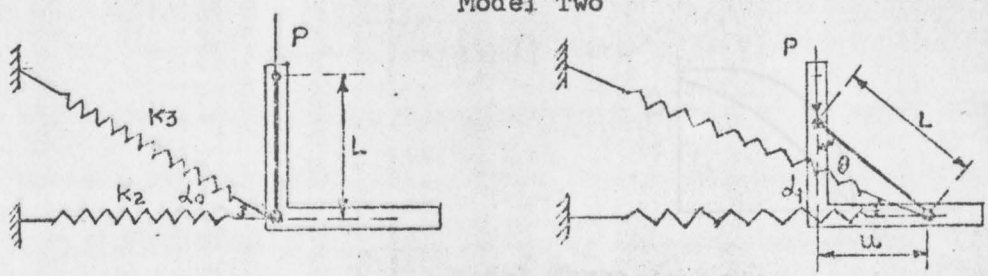

Model Three

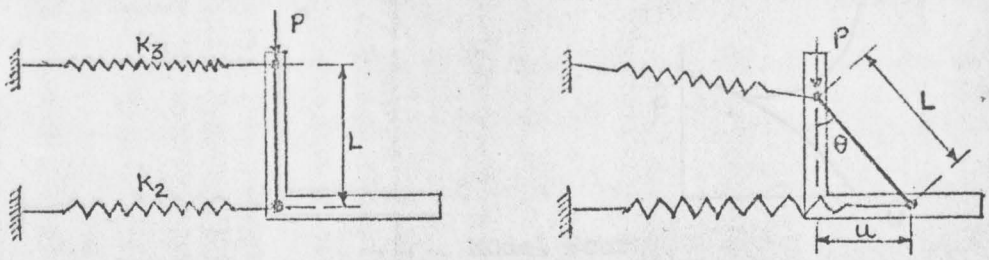

Model Four

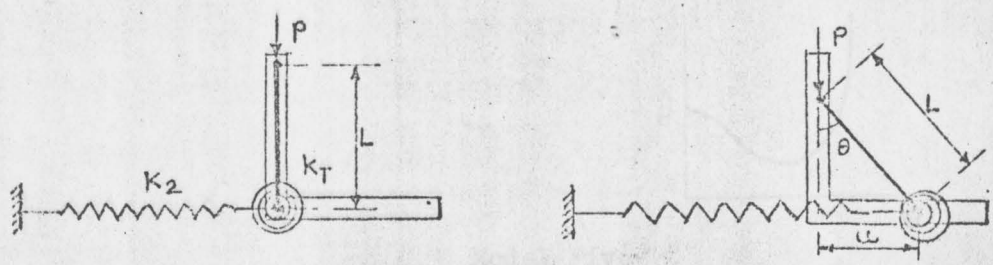

Model Five

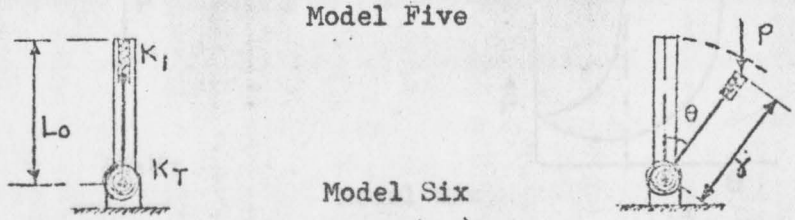

Model Six

Figure (1-e)

Geometry of Models

Load-Deflection Plots

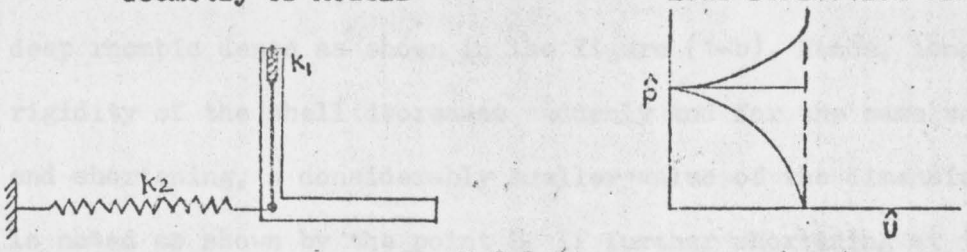

Model One

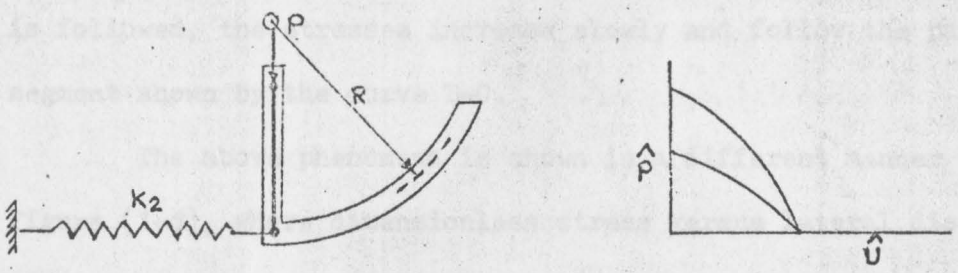

Model Two

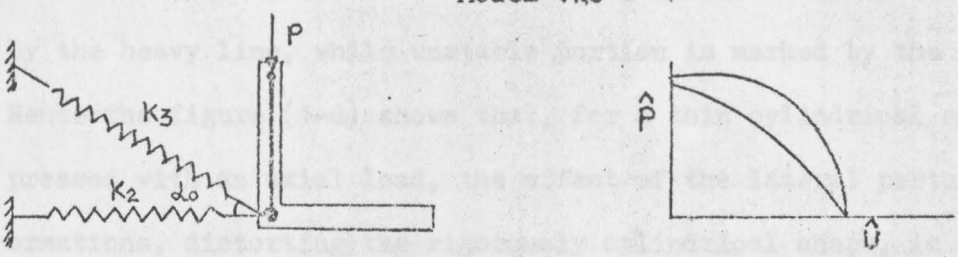

Model Three

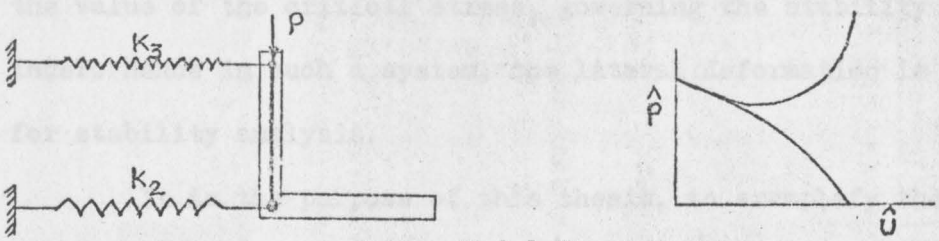

Model Four

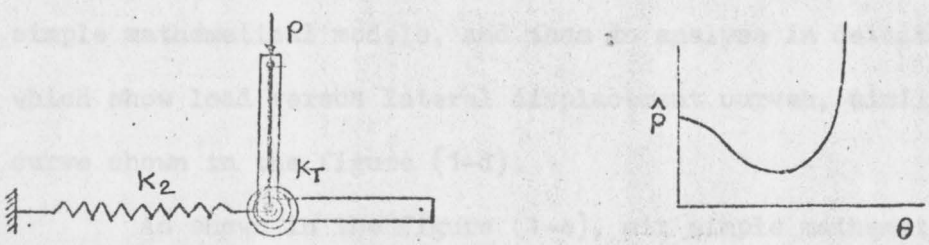

Model Five

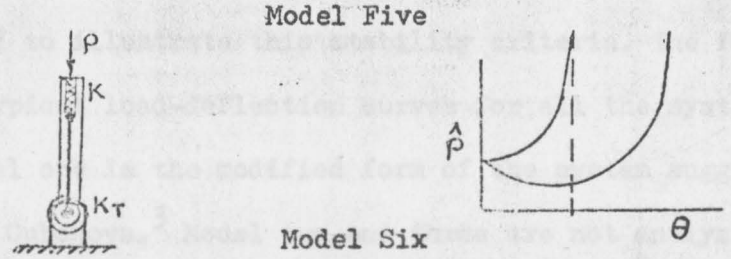

Model Six

Figure (1-f)

stage, the shape of the cylindrical surface gets distorted and shows deep rhombic dents as shown in the figure (1-b). Hence, longitudinal rigidity of the shell decreases suddenly and for the same value of the end shortening, a considerably smaller value of the dimensionless stress is noted as shown by the point B. If further shortening at the ends is followed, the stresses increase slowly and follow the path of the segment shown by the curve B-C.

The above phenomena is shown in a different manner in the figure (1-d), where dimensionless stress versus lateral displacement of the shell is presented. The stable portion of the curve is shown by the heavy line, while unstable portion is marked by the stars. Hence the figure (1-d) shows that, for a thin cylindrical shell, compressed with an axial load, the effect of the lateral perturbing deformations, distorting the rigorously cylindrical shape, is to lower the value of the critical stress, governing the stability of the cylinder. Hence in such a system, the lateral deformation is more important for stability analysis.

It is the purpose of this thesis, to exemplify the criteria of lateral deformations governing the elastic stability, by means of simple mathematical models, and thus to analyse in details, the models which show load versus lateral displacement curves, similar to the curve shown in the figure (1-d).

As shown in the figure (1-e), six simple mathematical models are selected to illustrate this stability criteria. The figure (1-f) shows the typical load-deflection curves for all the systems.

Model one is the modified form of the system suggested by Panovko and Gubanova.[3] Model two and three are not analysed in detail,

as load-deflection curves obtained, are similar to the specific case of model one.

Model one, four and five representing a single degree of freedom and model six of two degrees of freedom system are analysed in detail, for the stability characteristics.

Approach:

A complete analysis of a stability model includes,

1. Static stability analysis, and
2. Dynamic stability analysis.

Hence the stability models are analysed both statically and dynamically.

1. Static stability analysis:

The criteria for static stability is based on the potential energy function of the system designated as V. If the function must be atleast twice differentiable in (a,b) then a necessary condition for the existence of an equilibrium state at θ_o for which $\theta_1 < \theta_o < \theta_2$ is that, $dV/d\theta$ at$(\theta_o)=0$. This condition is not sufficient to guarantee that θ_o is a state of stable equilibrium. A sufficient condition for a stable equilibrium state or an unstable equilibrium state is determined by investigating the sign of the function $V''(\theta_o)=d^2V/d\theta^2$.

If $V''(\theta_o)<0$, This corresponds to a maximum point and thus an unstable state of equilibrium exists.

If $V''(\theta_o)>0$, This signifies a minium point exists and hence, a stable point of equilibrium.

Finally, if $V''(\theta_o)=0$, the point is neither a stable point nor an unstable point. This condition determines the critical positions of the system separating a stable and an unstable zone of equilibrium.

It is designated as neutral equilibrium.

2. Dynamic stability analysis:

Fundamental to dynamic stability analysis is the formulation of the differential equation of motion, which is usually of the non-linear type even for the most simplified stability problems. The equation of motion is reduced in order, into a set of first order differential equations which have inherent in them a form of the potential energy of the system. Secondly, an intermediate energy intigral equation which exists for a conservative force system, in which direction of an external applied force remains vertical throughout, is formed. This equation states the condition that the sum of the kinetic and the potential energies remain constant for all values of time t. For a one degree of freedom system, a function of the variables results which is plotted as a surface in three space, the variables being displacement, velocity and the potential energy. The projections of this surface onto the displacement-velocity plane define the phase-plane. A specified level of potential yields a single continuous trace or curve on the phase plane. A geometric interpretation of the phase plane plots yields the criteria for stable and unstable equilibrium configurations.

The various plots of the analysis of each model are included at the end of each chapter, showing the results of static analysis and dynamic analysis geometrically.

CHAPTER II

ANALYSIS OF STABILITY MODEL ONE

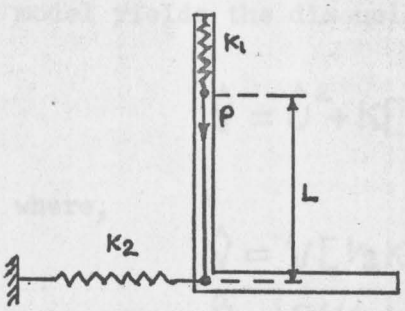

Initial Configuration
Figure (2-a)

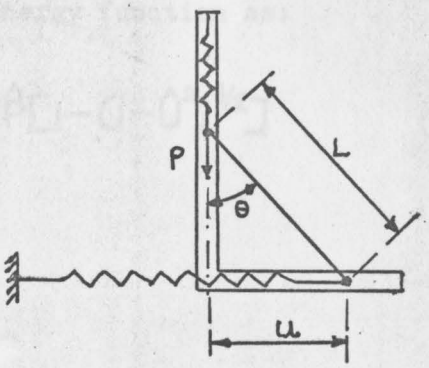

Displaced Configuration
Figure (2-b)

2.1 STATIC ANALYSIS

The geometrical configuration of the model, shown in figure (2-a), consists of a vertical and horizontal frictionless guide constraining the movement of the rigid rod. A vertical load P is applied as shown.

The following assumptions are made for the idealized mathematical model:

1. The bar is assumed to be a rigid body.
2. The springs are assumed to have a linear load-displacement relationship.

3. The external applied force P acts in the vertical direction for all values of the angular rotation θ and is thus a conservative force.
4. The weight of the bar is neglected.
5. The total mass of the bar m is assumed as a point mass located at the point of application of load P.

Refering to figure (2-b), the displaced configuration of the model yields the dimensionless potential energy function as:

$$\hat{V} = \hat{U}^2 + K[1-(1-\hat{U}^2)^{1/2}] - 2\hat{P}[1-(1-\hat{U}^2)^{1/2}] \qquad (1)$$

where,

$$\hat{V} = V[\tfrac{1}{2}K_2L^2]^{-1},$$
$$\hat{P} = P/K_2L \quad ,$$
$$\hat{U} = U/L \quad , \text{ and}$$
$$K = K_1/K_2 \quad .$$

It follows that,

$$\hat{V}' = 2\hat{U}[1+K(1-\hat{U}^2)^{-1/2} - K - \hat{P}(1-\hat{U}^2)^{-1/2}], \quad \text{, and} \qquad (2)$$
$$\hat{V}'' = 2[1+K(1-\hat{U}^2)^{-3/2} - K - \hat{P}(1-\hat{U}^2)^{-3/2}]. \qquad (3)$$

For static stability analysis, the necessary condition, for the existence of a possible equilibrium state at $\theta = \theta_o$ is that $\hat{V}' = 0$, this condition yields,

$$\hat{P} = [1-\hat{U}^2]^{1/2} + K[1-(1-\hat{U}^2)^{1/2}] \qquad (4)$$

Equation (4) gives a relation between dimensionless load $\hat{P}$ and dimensionless displacement $\hat{U}$.

The sufficiency condition for neutral equilibrium is given by the condition $\hat{V}'' = 0$, this condition yields

$$\hat{P} = (1-\hat{U}^2)^{3/2} + K[1-(1-\hat{U}^2)^{3/2}] \qquad (5)$$

Simultaneous solution of equations (4) and (5) yields the critical value of displacement $\hat{U}_{cr}$ and the critical value of load $\hat{P}_{cr}$ as

$$(\hat{U}_1)_{CR} = 0., \quad \text{and} \qquad (6)$$

$$(\hat{U}_2)_{CR} = 1, \qquad (6\text{-a})$$

and

$$(P_1)_{CR} = 1, \quad \text{and} \qquad (7)$$

$$(P_2)_{CR} = K. \qquad (7\text{-a})$$

A plot of the family of dimensionless load-deflection curves is shown in figure (2-c), for various values of the parameter K.

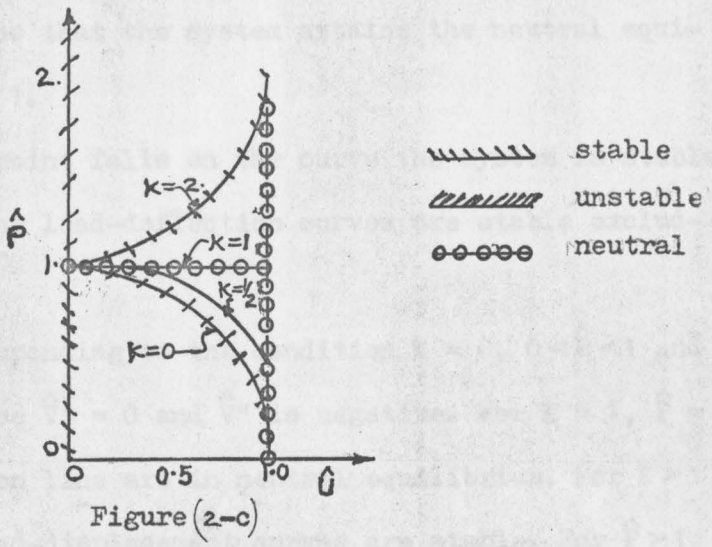

Figure (2-c)

From figure 2-c, it follows that for $K = 1$ and $0 \leq \hat{U} \leq 1$, load-displacement curve is a straight line.

For $K = 0$, the shape of the curve is the classical cosine function.

For $0 \leq K < 1$ and $0 \leq \hat{U} \leq 1$, the slope of the curve is negative and increasing.

For $K > 1$ and $0 \leq \hat{U} \leq 1$, the slope of the curve is positive and increasing.

For the case $\hat{U} = 0$, all points on the vertical axis are stable for $0 < \hat{P} < 1$; for $\hat{P} = 1$ neutral equilibrium exists, and for $\hat{P} > 1$ all points are unstable.

For $0 < \hat{P} < 1$, all points on curves for $0 < K \leq 1$, are unstable, for all values of $\hat{U}$, but excluding $\hat{U} = 1$, where neutral equilibrium exists. For given values of $\hat{P}$, $\hat{U}$ with $0 < K < 1$, if resulting point falls on the prescribed load-displacement curve, the system is unstable and motion occurs, so that the system attains the neutral equilibrium position at $\hat{U} = 1$.

If $K > 1$ and the point falls on the curve the system is stable. For $K > 1$ all points on the load-deflection curves are stable excluding $\hat{U} = 0$.

The points corresponding to the condition $K = 0$, $0 < \hat{P} < 1$ and $0 < \hat{U} < 1$ are unstable since $\hat{V}' = 0$ and $\hat{V}''$ is negative. For $K = 1$, $\hat{P} = 1$ and $0 < \hat{U} < 1$ all points on line are in neutral equilibrium. For $K > 1$, $0 < \hat{U} < 1$ all points on load-displacement curves are stable. For $\hat{P} > 1$, all points on vertical axis are unstable for all values of K.

2.2 DYNAMIC ANALYSIS

Assuming the mass of the bar 'm' as a point mass located at the point of application of load P, the Lagrangian of the system $\hat{L}$ is defined as $\hat{L} = \hat{T} - \hat{V}$,

where

$\hat{T}$ = kinetic energy of the system / $(\frac{1}{2} K_2 L^2)$, and

$\hat{V}$ = potential energy of the system / $(\frac{1}{2} K_2 L^2)$,

hence it follows that

$$\hat{L} = \hat{L}(\hat{U}, \dot{\hat{U}}, \hat{P}) = \tfrac{1}{2} M \dot{\hat{U}}^2 - [\hat{V}] \tag{8}$$

where,

$M = 2m/K_2$, and

$\dot{\hat{U}} = \dot{U}/L$.

The differential equation of motion satisfies the following Lagrange equation:

$$\frac{\partial \hat{L}}{\partial \hat{U}} - \frac{\partial}{\partial t}\left(\frac{\partial \hat{L}}{\partial \dot{\hat{U}}}\right) = 0. \tag{9}$$

which yields,

$$M \ddot{\hat{U}} + (\hat{V})' = 0. \tag{10}$$

where, $\hat{V}'$ denotes first derivative with respect to $\hat{U}$.

Equation (10) is reduced to a pair of first order differential equations in the form

$$\dot{\hat{U}}_1 = \hat{U}_2 \quad , \text{ and} \tag{11}$$

$$\dot{\hat{U}}_2 = -[\hat{V}']/M. \tag{12}$$

where,

$\hat{U} = \hat{U}_1$

$\dot{\hat{U}} = \dot{\hat{U}}_1 = \hat{U}_2$, and

$\ddot{\hat{U}} = \ddot{\hat{U}}_1 = \dot{\hat{U}}_2$.

Integration of equation (12) yields,

$$\tfrac{1}{2}M(\hat{U}_2)^2+\hat{V} = E_o(\hat{U}_1,\hat{P}) = CONSTANT, \tag{13}$$

that is, the sum of the kinetic energy plus the potential energy of the system remains constant, which is the special case of a conservative force field. The parameter $E_o\ (\hat{U}_1, \hat{P})$ represents the sum of the kinetic energy plus the potential energy evaluated at the time $t = t_o = 0$. Solving equation (13), yields

$$\hat{U}_2 = \pm[2/M(E_o-\hat{V})]^{1/2}. \tag{14}$$

where for convenience,

$$(2/M)^{1/2} = 1 \quad \text{, yields}$$

$$\hat{U}_2 = \pm[E_o-\hat{V}]^{1/2} \tag{15}$$

Equation (15) gives the relationship between angular displacement, the stability load, the initial energy of the elastic system at any time t, and the velocity of motion in non-dimensional form.

For this one degree of freedom system shown, the phase-plane diagram of the non-dimensional velocity versus displacement is plotted with the dimensionless potential energy on the third axis. The projections of this three dimensional surface on to the phase-plane produce the phase-plane trajectories. For each value of $\hat{P}$ a separate phase-plane diagram is produced. Noting the load-deflection curve in figure 2-c, the following values of $\hat{P}$ are investigated:

$\hat{P} = 0$, $\hat{P} = 0.8$, $\hat{P} = 1.0$, and $\hat{P} = 1.2$

For the special case K = 0, the phase-plane trajectories are shown in figure (2-Q) through (2-T).

Figure (2-6) represents phase-plane trajectories which are produced for load $\hat{P} = 0$. They are characterized by a stable point at the origin. Hence, all oscillatory motion about the origin is stable.

For load $\hat{P} = 0.8$, figure (2-7) illustrates the phase-plane trajectories. A stable point A at the origin, and an unstable point B on the $\hat{U}_1$ axis at the point $\hat{U} = \pm 0.6$ is shown in the figure (2-7).

For load $\hat{P} = 1$, figure (2-5) illustrates a set of trajectories showing point A, as unstable point of equilibrium.

Thus, for K = 0, as $\hat{P}$ increases the unstable point B moves to the left and approches the stable point A. Points A and B coincide for $\hat{P} = 1$, producing an unstable point.

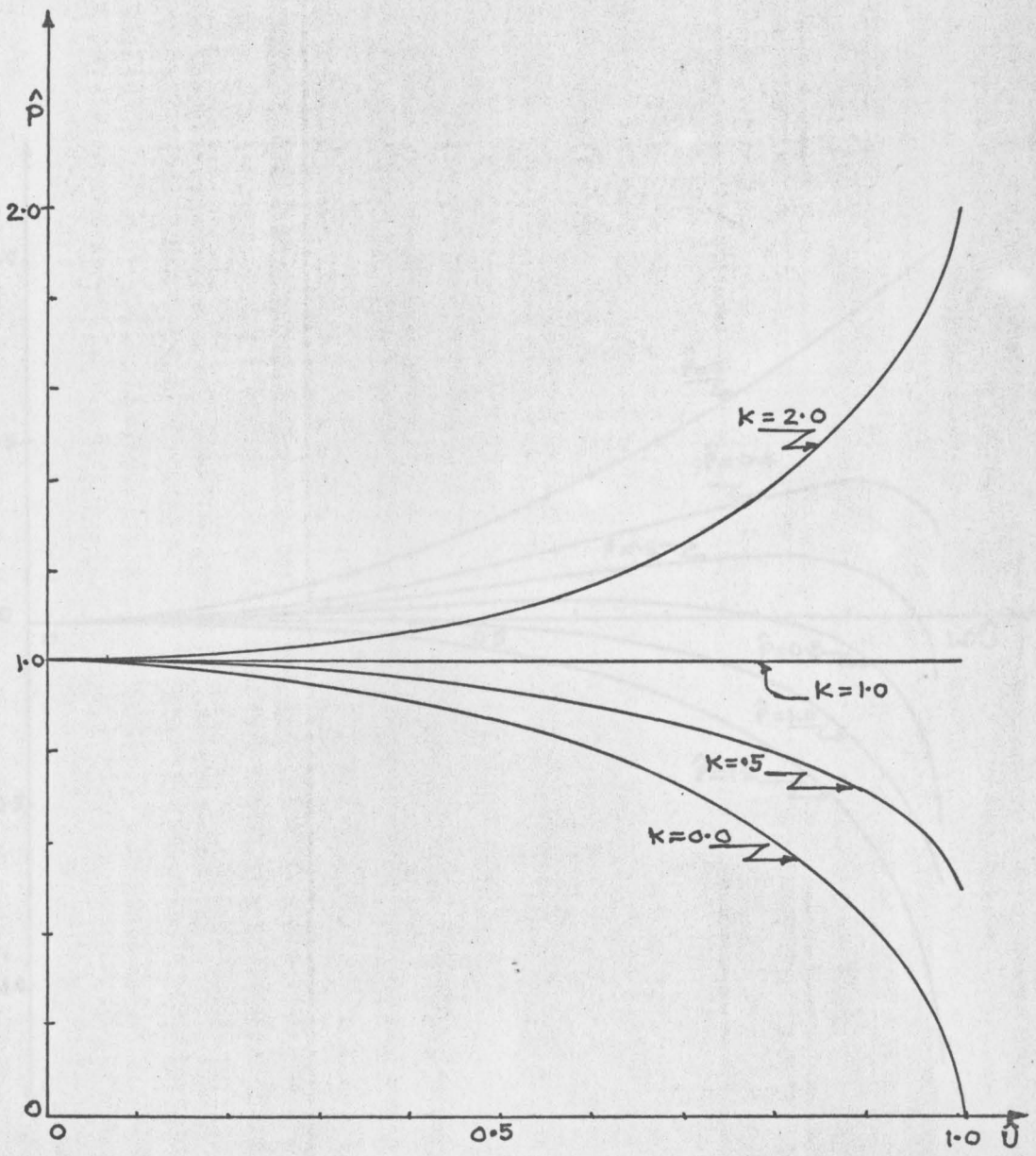

Load Vs Displacement

Figure (2-d)

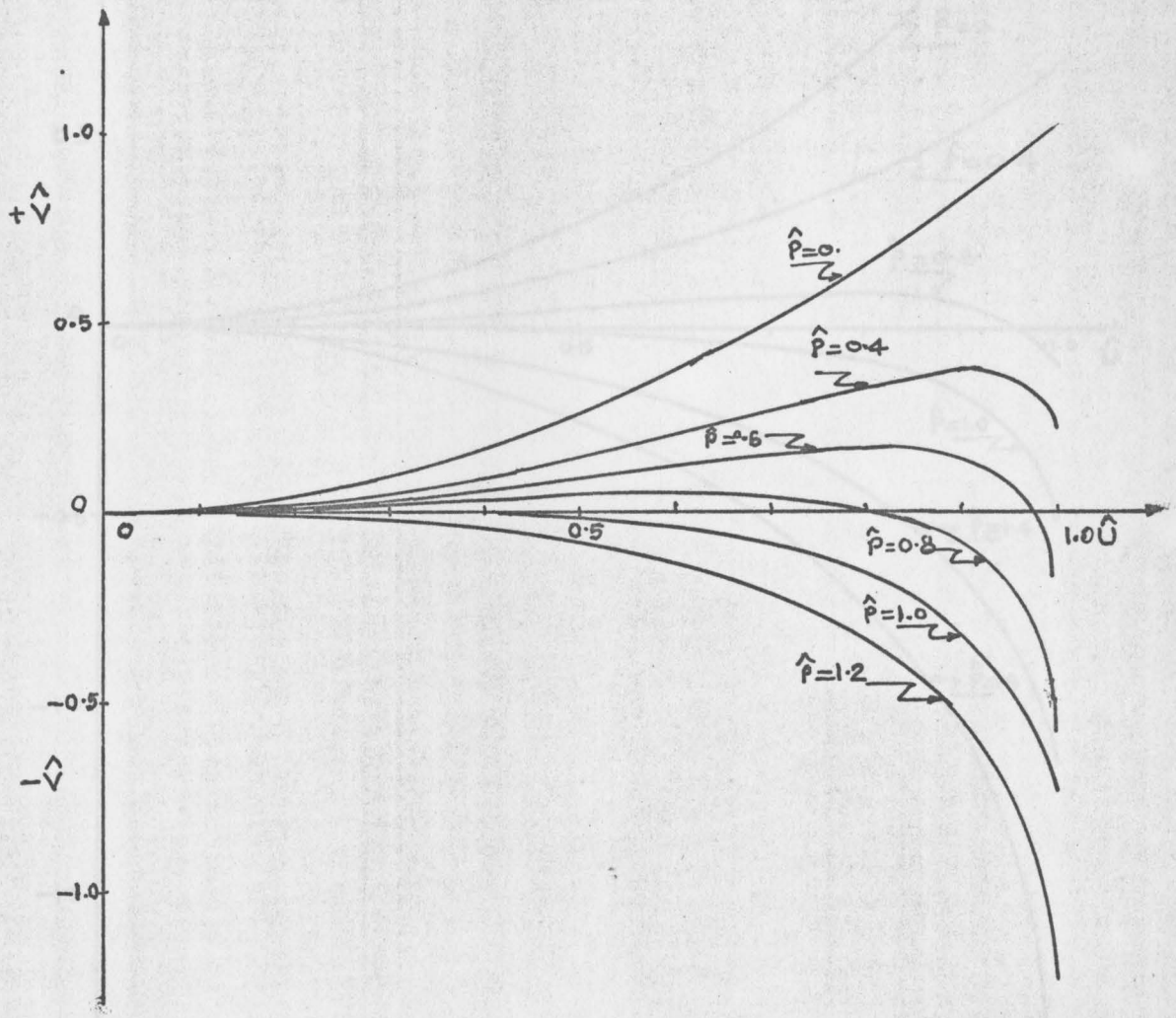

Potential energy Vs displacement for K=0

Figure (2-e)

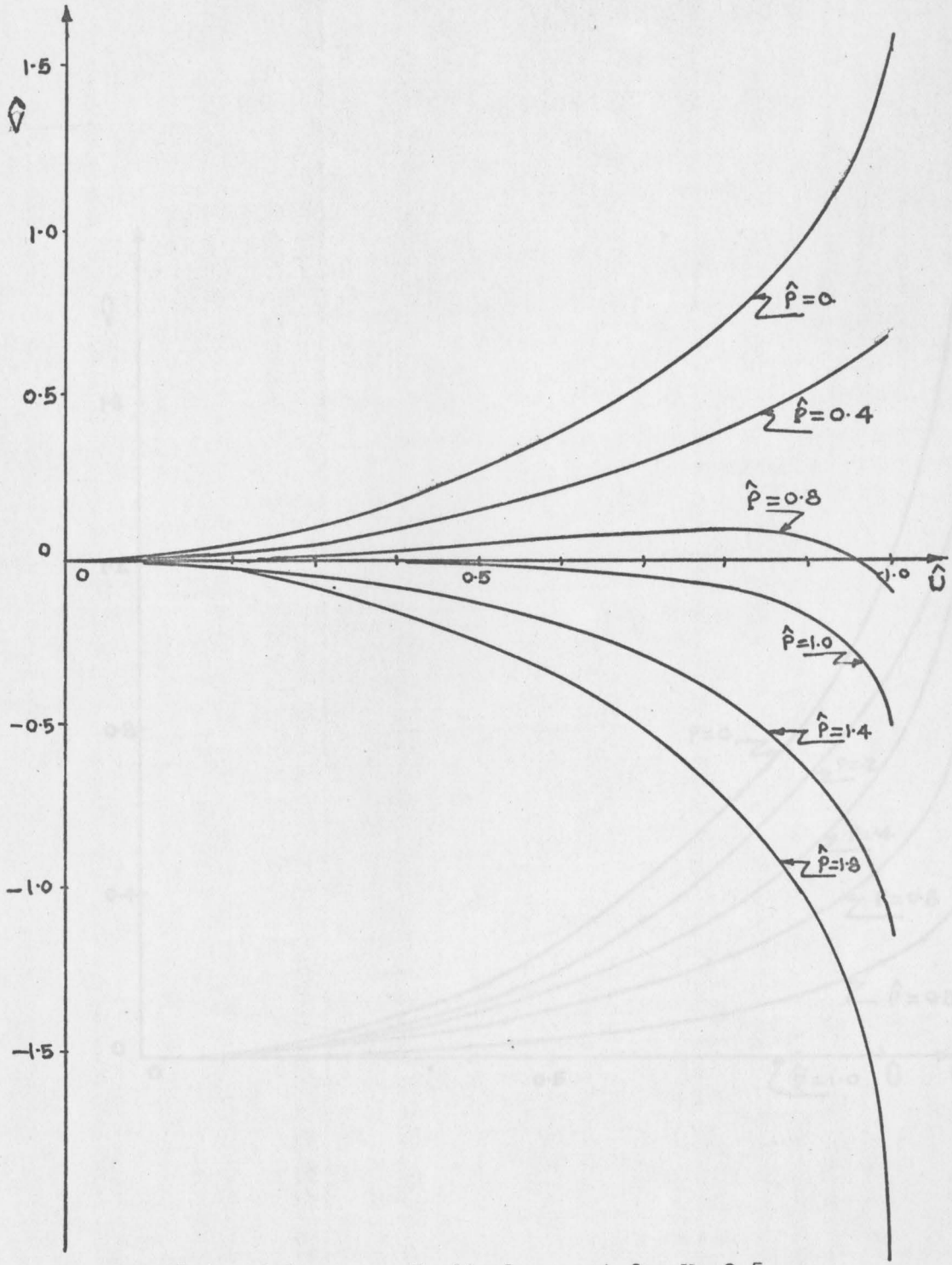

Potential energy Vs displacement for K= 0.5

Figure (2-f)

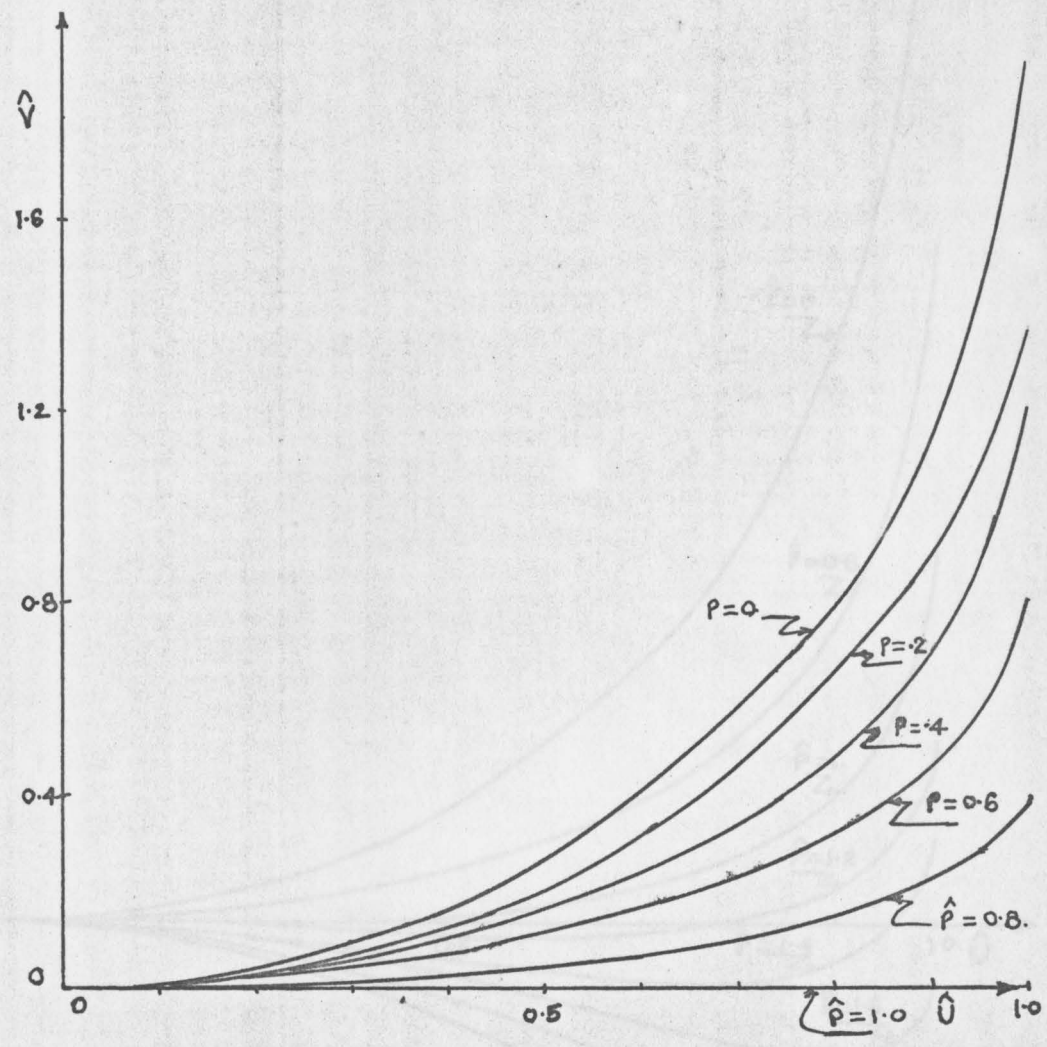

Potential energy Vs displacement for K=1.0

Figure (2-g)

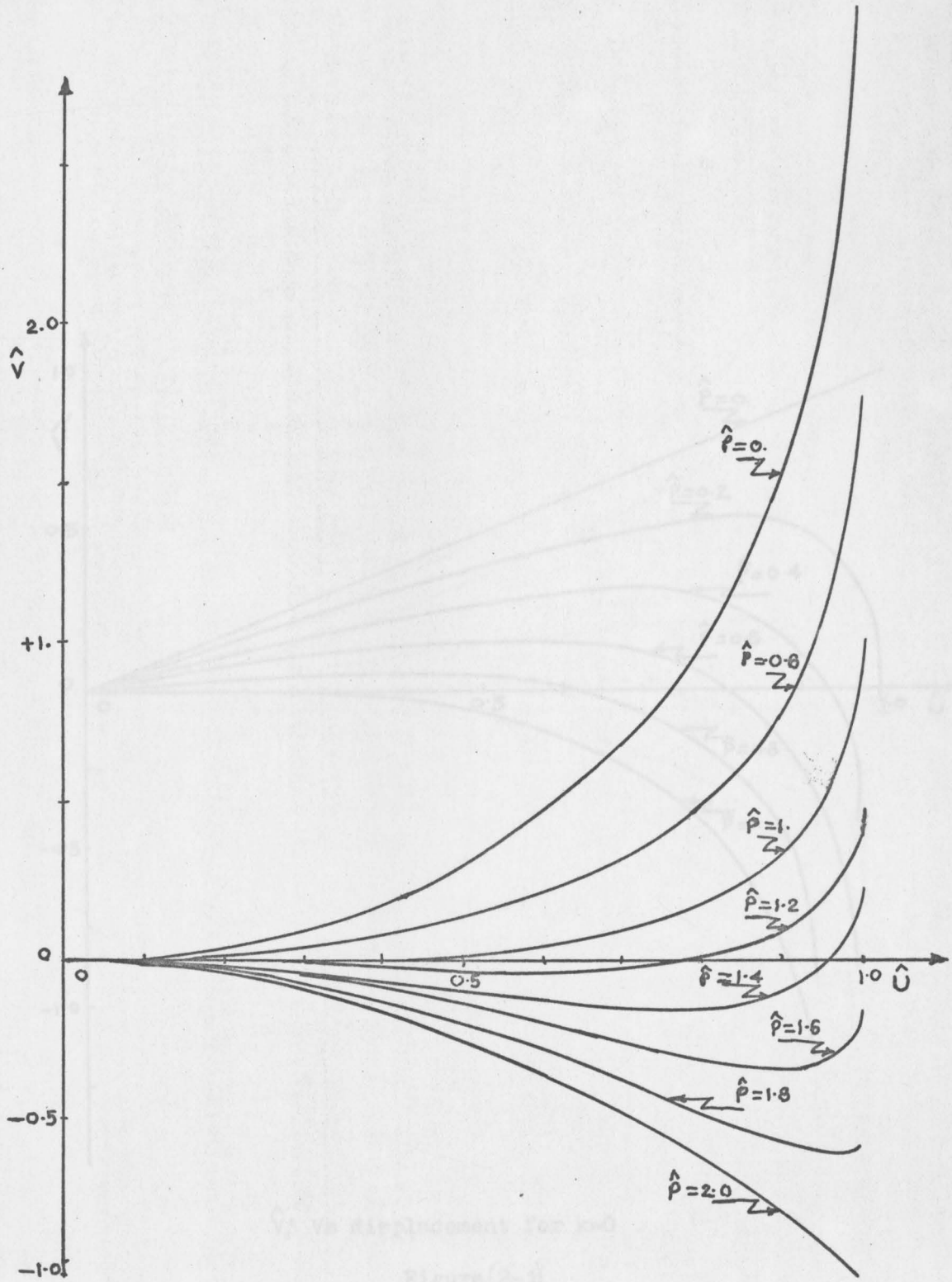

Potential energy Vs displacement for K=2.0

Figure (2-h)

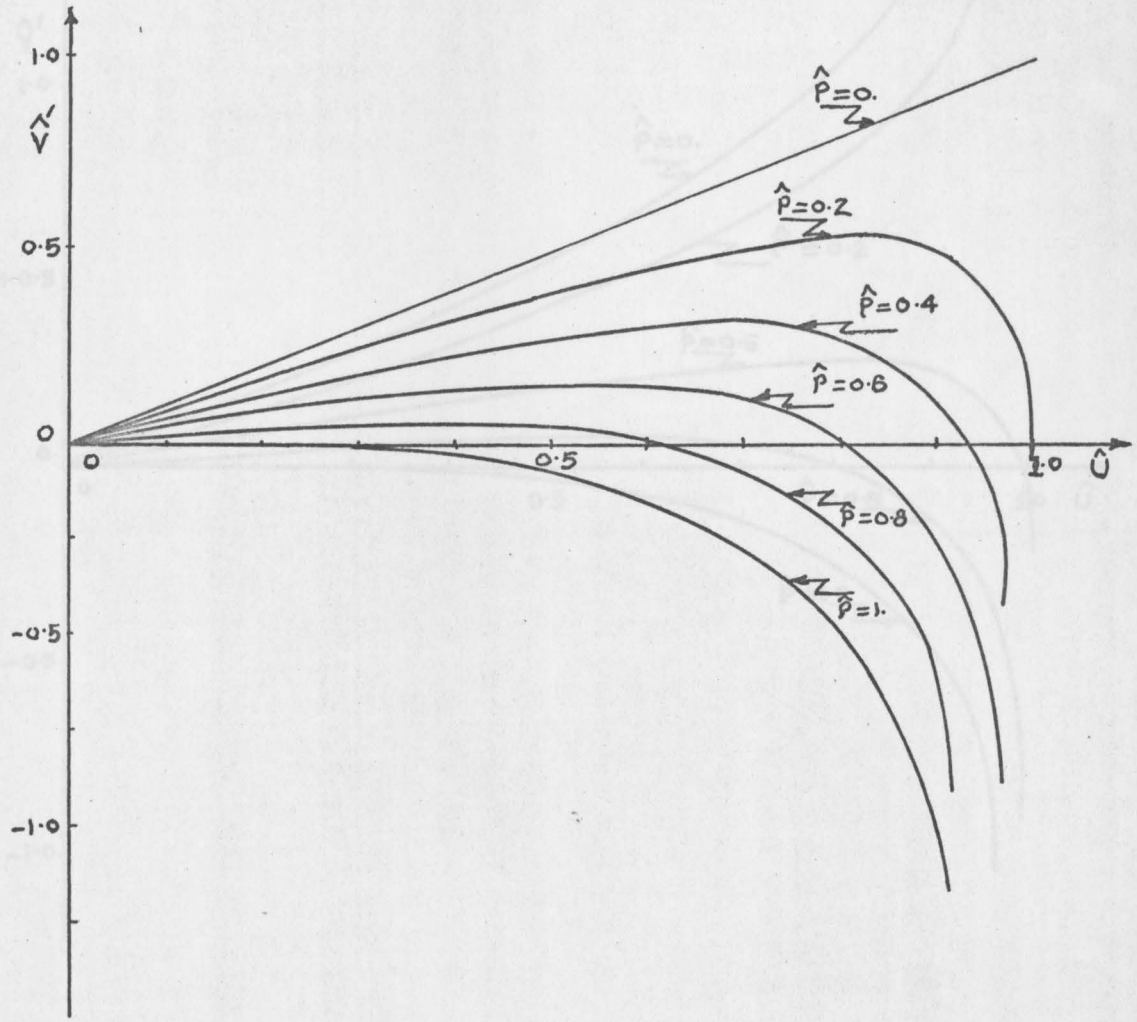

$\hat{V}_d'$ Vs displacement for k=0

Figure (2-i)

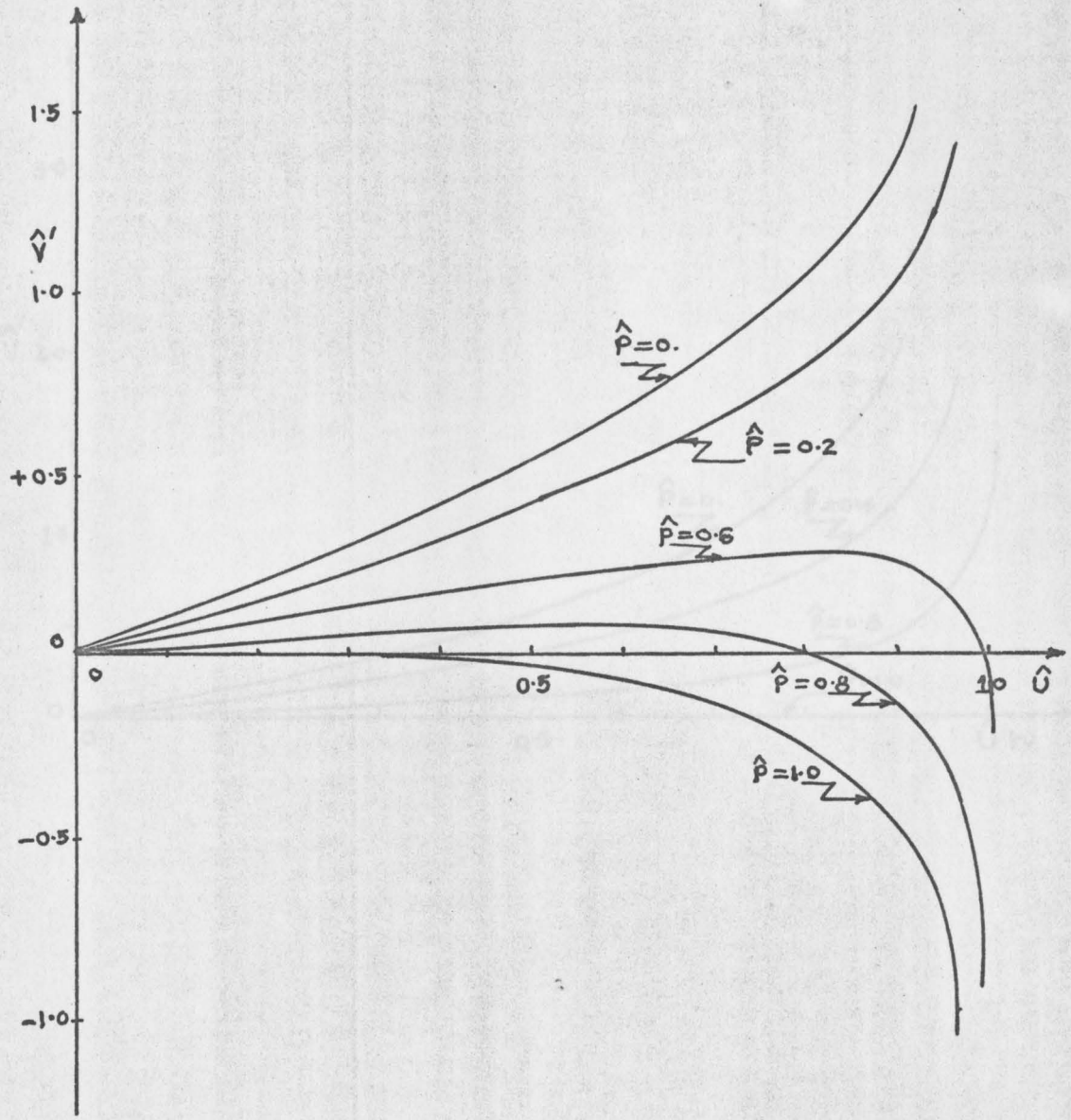

$\hat{V}'$ Vs displacement for K= 0.5 .

Figure (2-J)

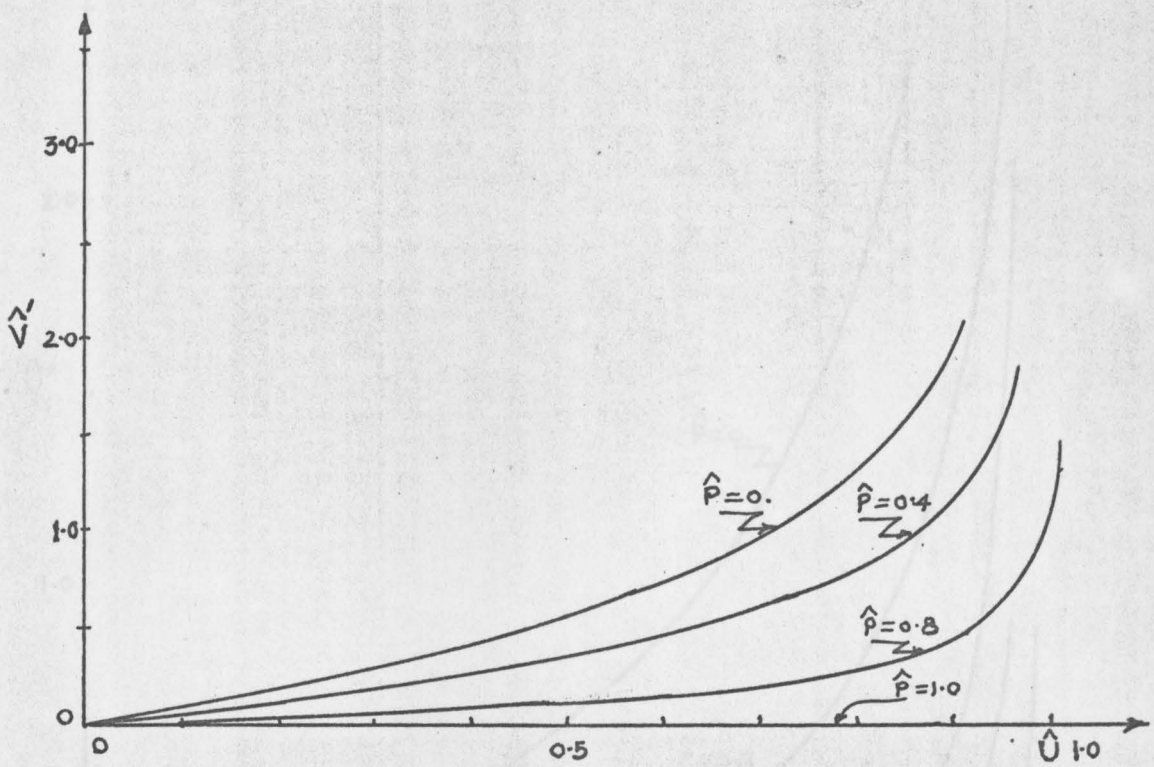

$\hat{V}'$ Vs displacement for K=1.0

Figure (2-K)

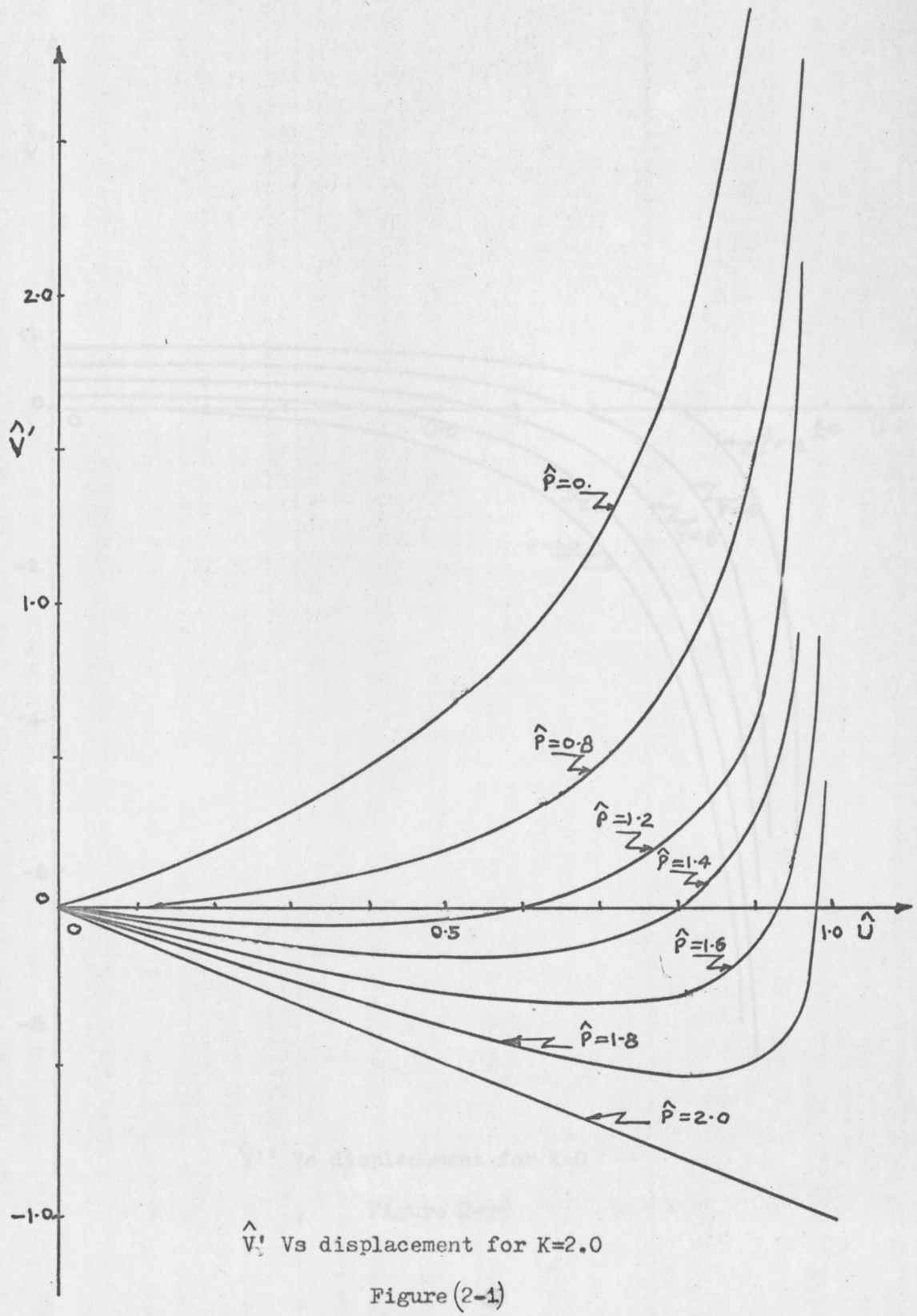

$\hat{V}'$ Vs displacement for K=2.0

Figure (2-1)

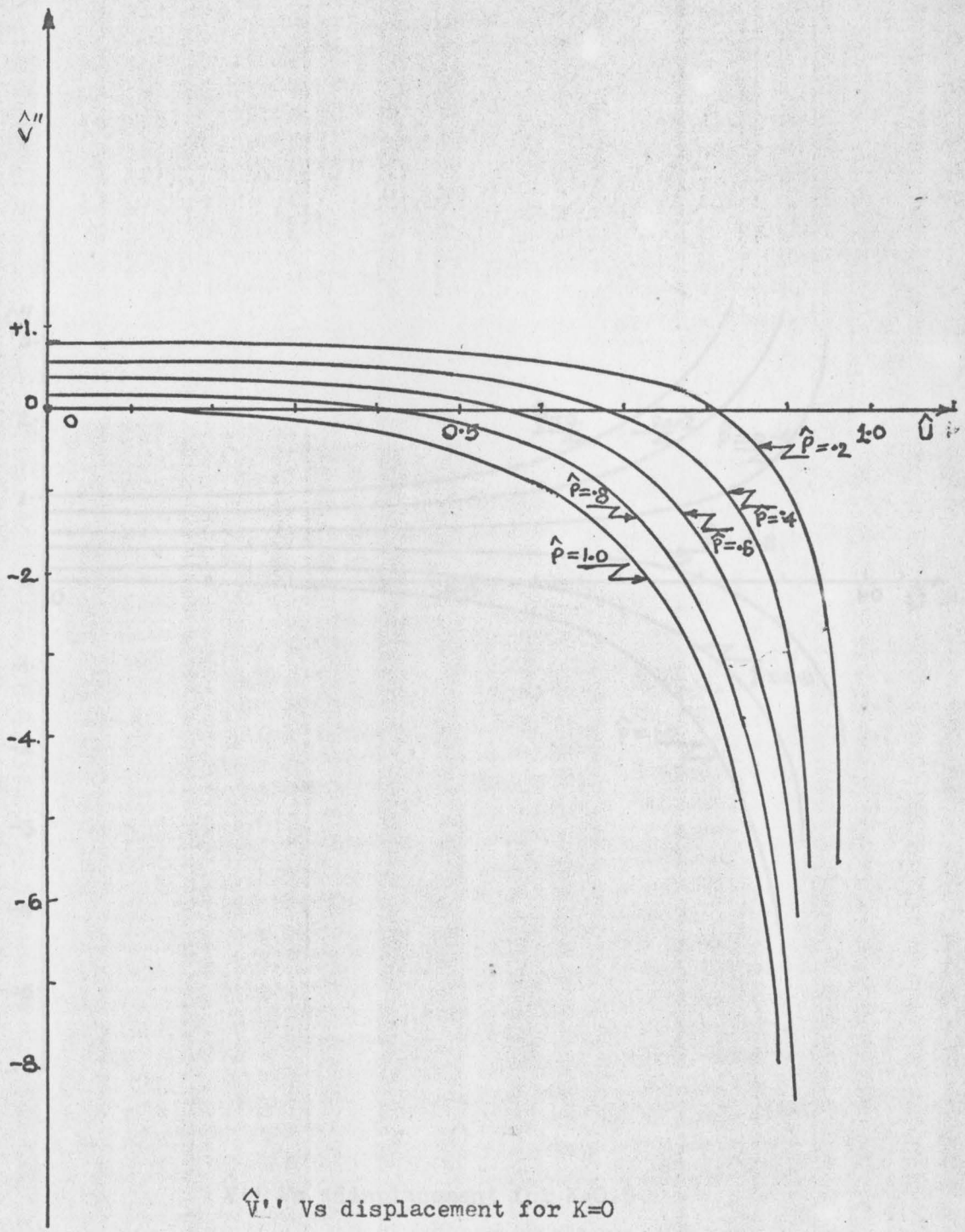

$\hat{V}''$ Vs displacement for K=0

Figure (2-m)

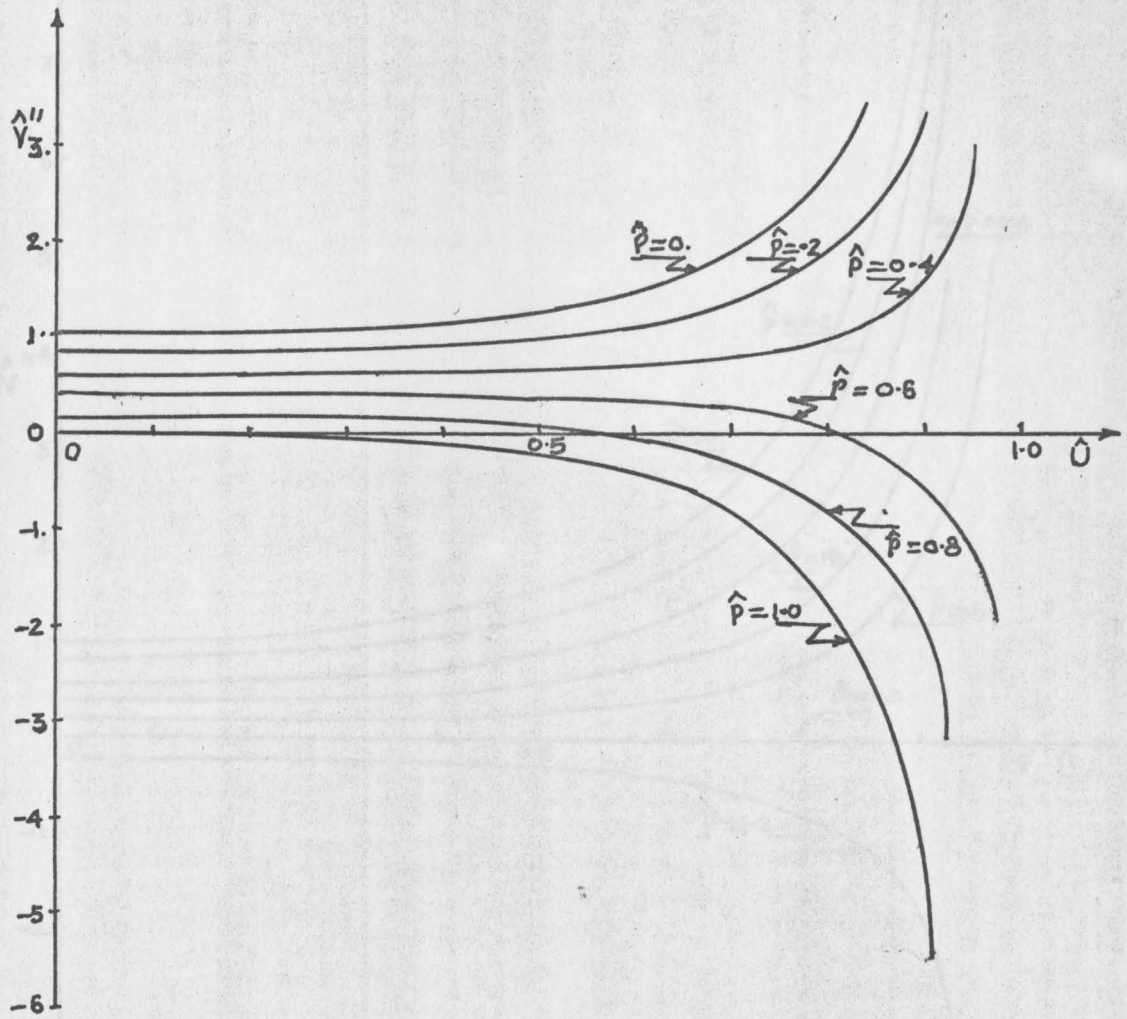

$\hat{V}''$ Vs kdisplacement for K=0.5

Figure (2-y)

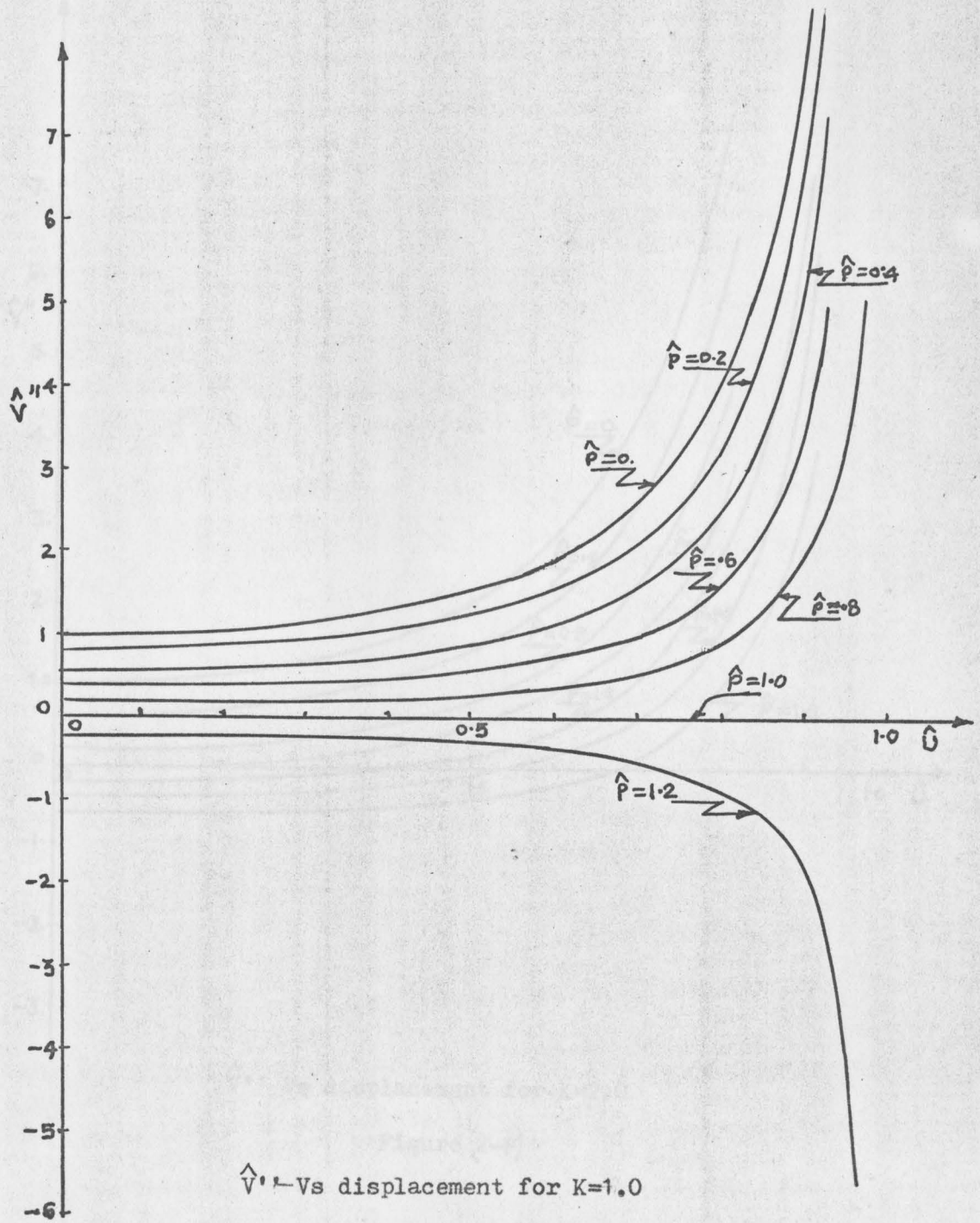

$\hat{V}$ Vs displacement for K=1.0

Figure (2-0)

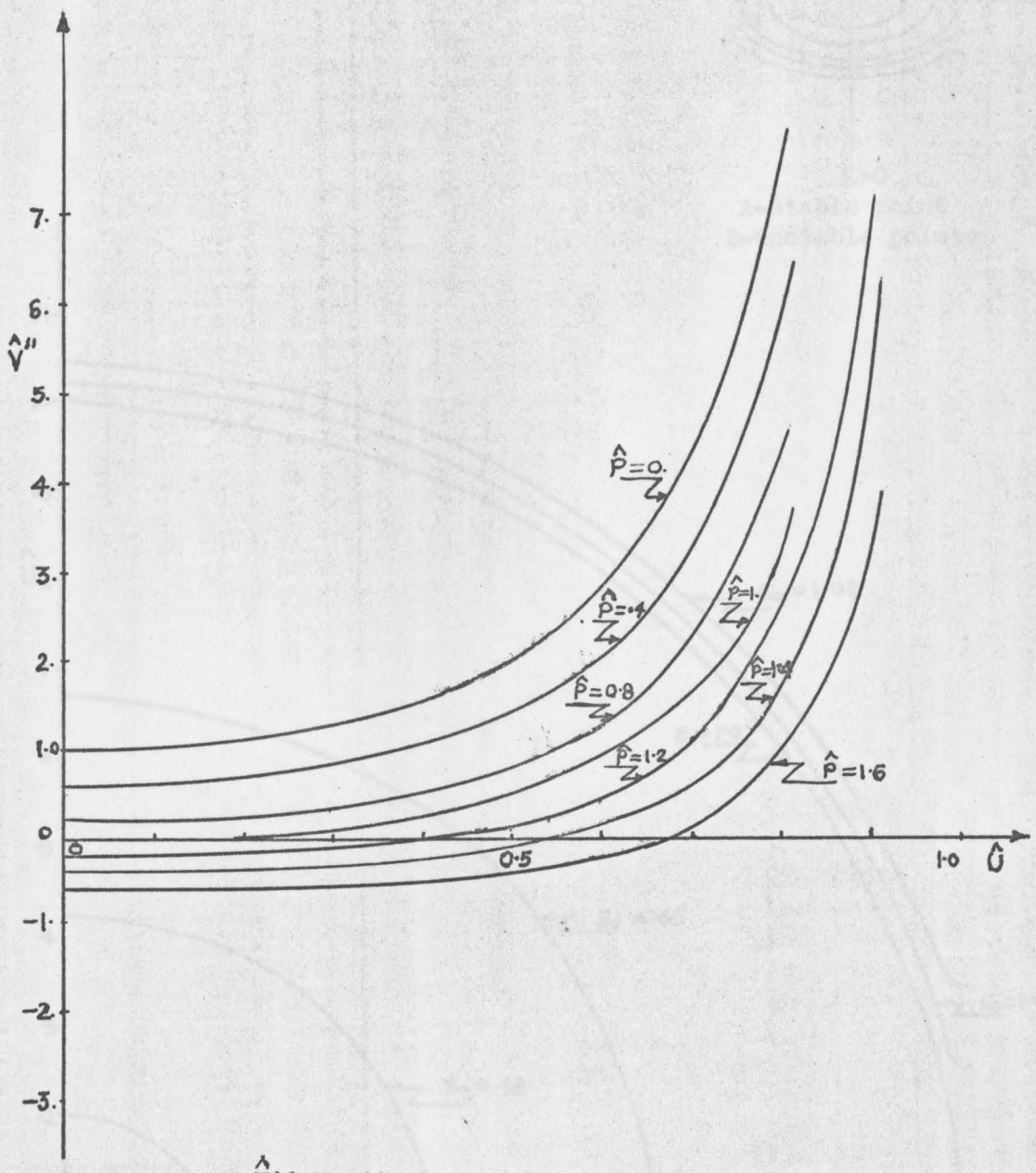

$\hat{V}''$ Vs displacement for K=2.0

Figure (2-p)

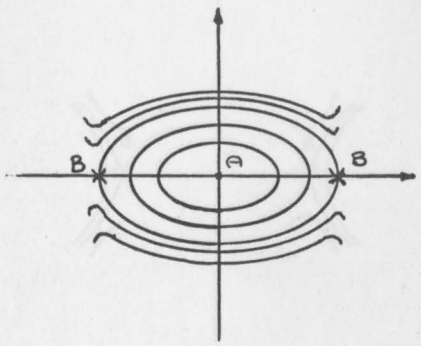

K=0
A-stable point
B-unstable points

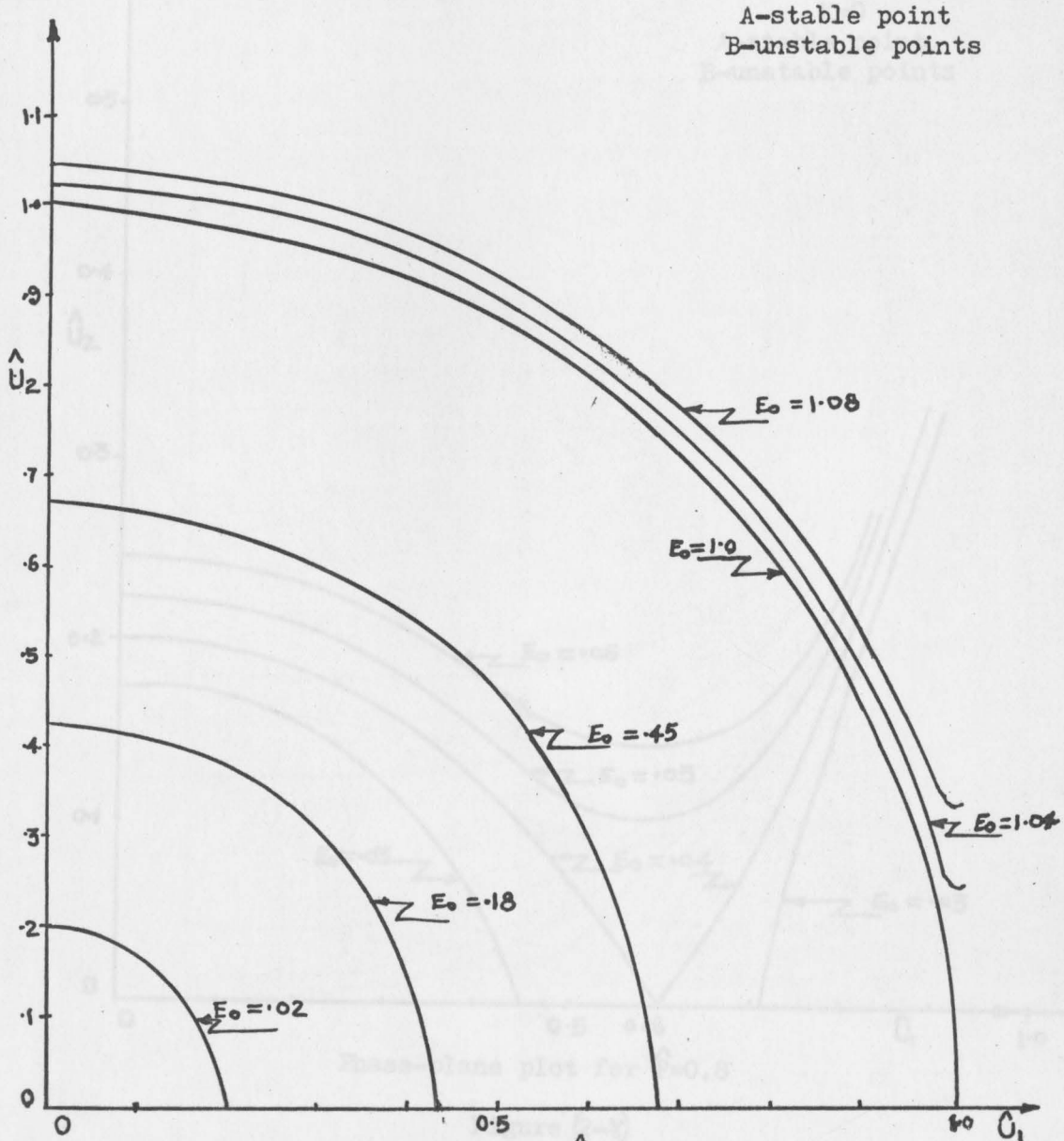

Phase-plane plot for $\hat{P}=0.0$
Figure (2-6)

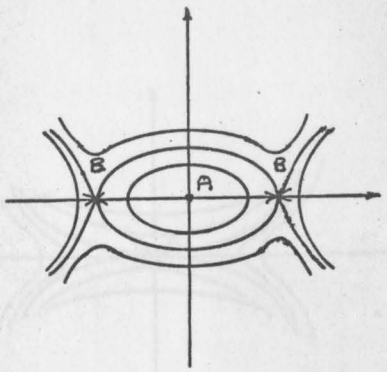

K=0
A-stable point
B-unstable points

Phase-plane plot for $\hat{P}$=0.8

Figure (2-8)

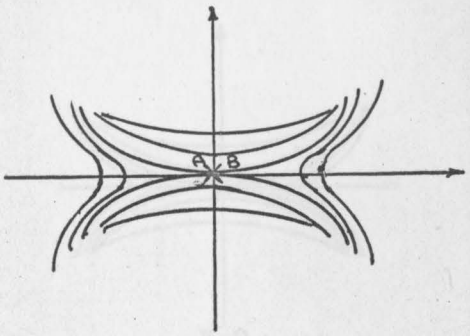

K=0
A, B-unstable point

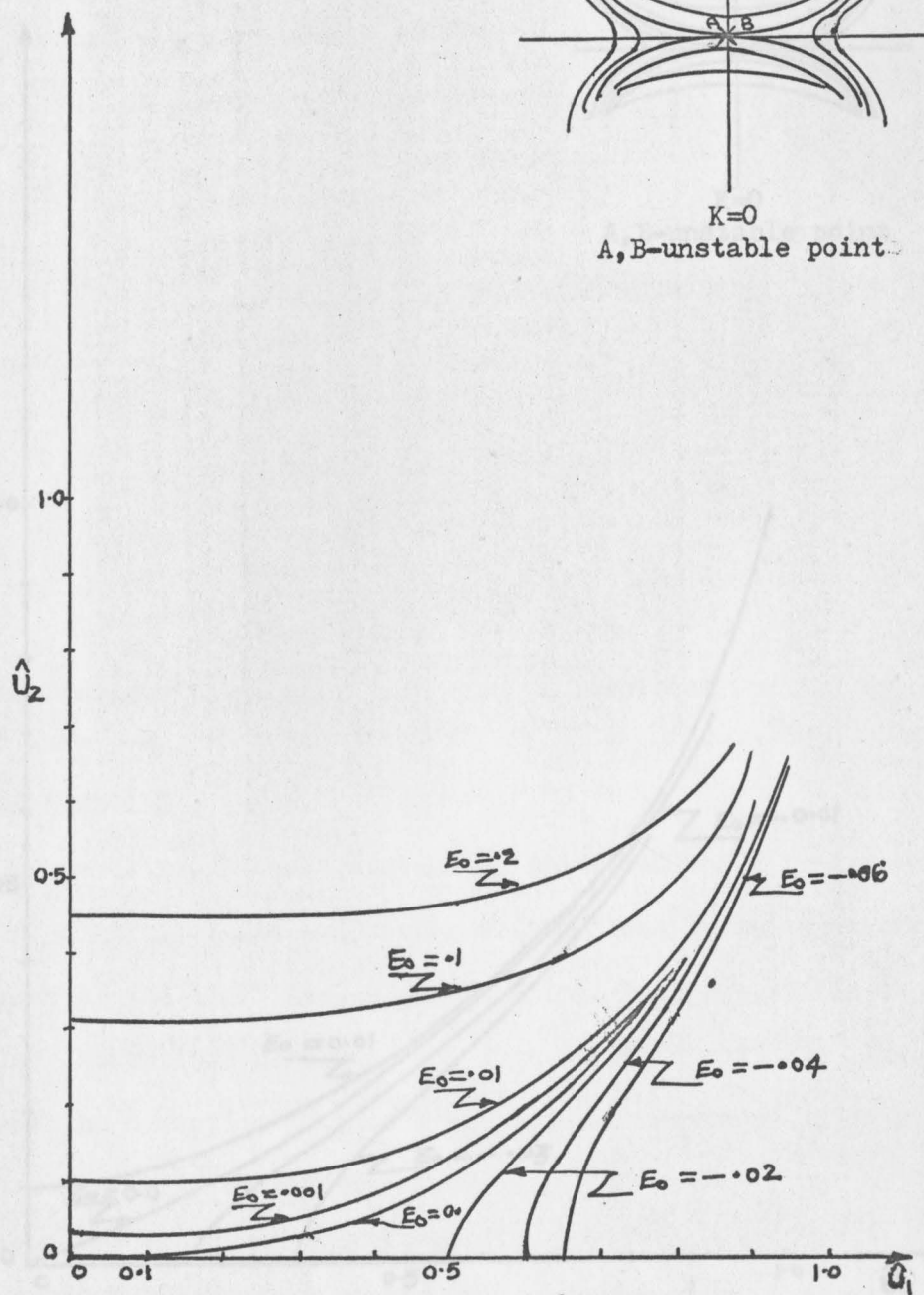

Phase-plane plot for $\hat{P}=1.0$

Figure (2-5)

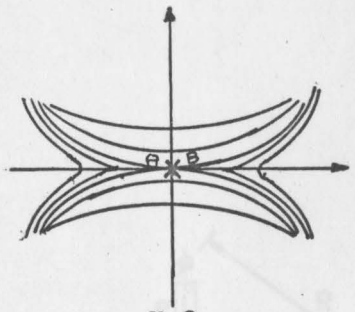

K=0
A,B-unstable point

Phase-plane plot for $\hat{P}=1.2$

Figure (2-t)

CHAPTER III

ANALYSIS OF STABILITY MODEL TWO

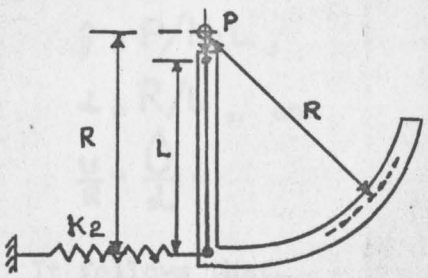

Initial Configuration

Figure (3-a)

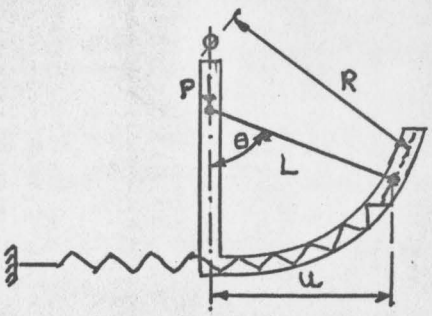

Displaced Configuration

Figure (3-b)

3.1 STATIC ANALYSIS

The geometrical configuration of the model shown in figure (3-a), consists of a vertical and a circular frictionless guide constraining the movement of the rigid rod. A vertical load P is applied as shown.

The assumptions regarding the type of rigid rod, the linear spring, and the direction of load P are same as mentioned in chapter two for the stability model one.

Refering to figure (3-b) the displaced configuration of the model yields the dimensionless potential energy function as

$$\hat{V} = \alpha^2\{\text{TAN}^{-1}[\hat{U}/\alpha(1-\hat{U}^2/\alpha^2)^{-1/2}]\}^2$$

$$-2\hat{P}[1-\alpha-(1-\hat{U}^2)^{1/2}+\alpha(1-\hat{U}^2/\alpha^2)^{1/2}]. \qquad (16)$$

where,

$\hat{U} = U/\alpha$,

$\hat{P} = P/K_2L$,

$\alpha = R/L$, and

$\frac{U}{R} = \frac{\hat{U}}{\alpha}$.

It follows that,

$$\hat{V}' = 2\alpha(1-\hat{U}^2/\alpha^2)^{-1/2}\text{x}\text{TAN}^{-1}[\hat{U}(\alpha^2-\hat{U}^2)^{-1/2}]$$
$$-2\hat{P}\hat{U}[(1-\hat{U}^2)^{-1/2}-(\alpha^2-\hat{U}^2)^{-1/2}], \qquad (17)$$

and

$$\hat{V}'' = 2\alpha^2(\alpha^2-U^2)^{-1}+2\hat{U}\alpha^2(\alpha^2-\hat{U}^2)^{-3/2}\text{x}\text{TAN}^{-1}[\hat{U}(\alpha^2-\hat{U}^2)^{-1/2}]$$
$$-2\hat{P}\hat{U}^2[(1-\hat{U}^2)^{-3/2}-(\alpha^2-\hat{U}^2)^{-3/2}]$$
$$-2\hat{P}[(1-\hat{U}^2)^{-1/2}-(\alpha^2-\hat{U}^2)^{-1/2}]. \qquad (18)$$

For static stability analysis, the necessary condition for the existence of a possible equilibrium state at $\theta = \theta_o$ is that $\hat{V}' = 0$, this condition yields,

$$\hat{P} = \text{TAN}^{-1}(\hat{U}/\alpha)[\hat{U}/\alpha\{(1-\hat{U}^2/\alpha^2)^{1/2}(1-\hat{U}^2)^{-1/2}-\alpha^{-1}\}]^{-1} \qquad (19)$$

Equation (19) gives a relation between dimensionless load $\hat{P}$ and dimensionless displacement $\hat{U}$ and a parameter α.

The sufficiency condition for neutral equilibrium is found by setting $\hat{V}'' = 0$, this condition yields,

$$\hat{P} = \alpha^2(\alpha^2-\hat{U}^2)^{-3/2} X$$
$$[(\alpha^2-\hat{U}^2)^{1/2}+\hat{U}\,TAN^{-1}(\hat{U}/(\alpha^2-\hat{U}^2)^{1/2})] X$$
$$[(1-\hat{U}^2)^{-3/2}-\alpha^2(\alpha^2-\hat{U}^2)^{-3/2}]^{-1} \quad (20)$$

Equations (19) and (20) are to be solved simultaneouly to evaluate the critical values of displacement $\hat{U}_{cr}$ and load $\hat{P}_{cr}$ in a non-dimensional form.

A set of curves for nondimensional load $\hat{P}$ versus dimensionless displacement for various values of parameter α, are shown in figure (3-c).

As figure (3-c) does not resemble the figure (1-d), further stability analysis for this model is not done.

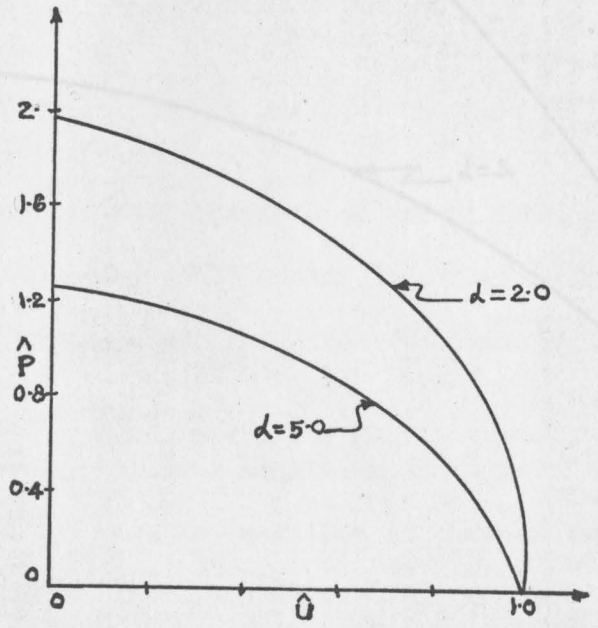

Typical load Vs displacement

Figure (3-c)

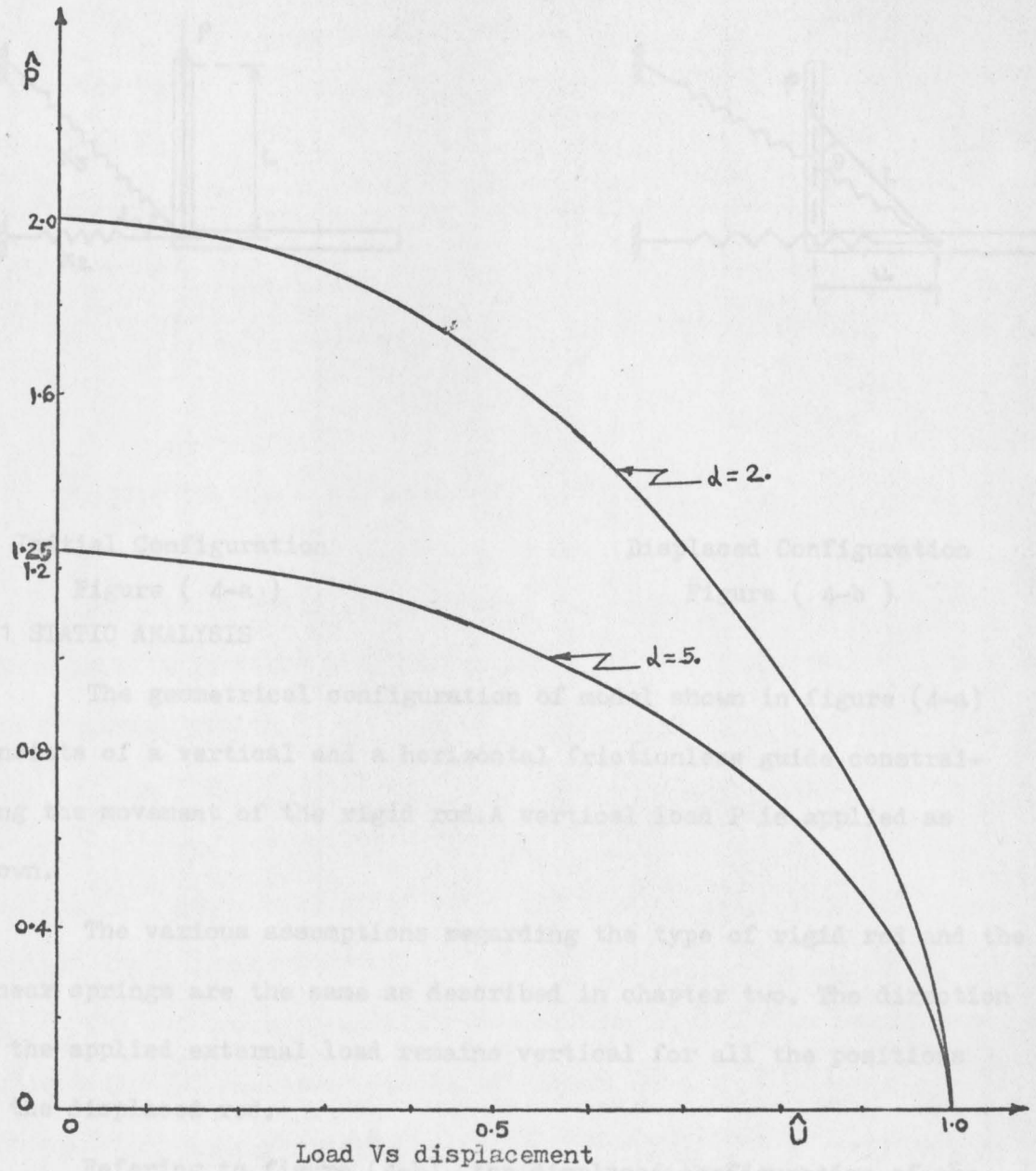

Load Vs displacement

Figure (3-d)

CHAPTER IV

ANALYSIS OF STABILITY MODEL THREE

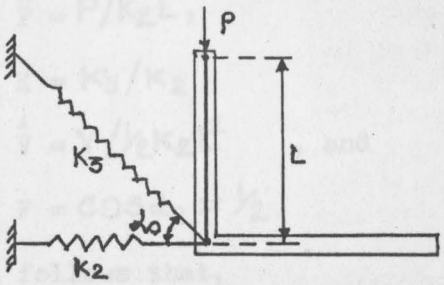

Initial Configuration

Figure (4-a)

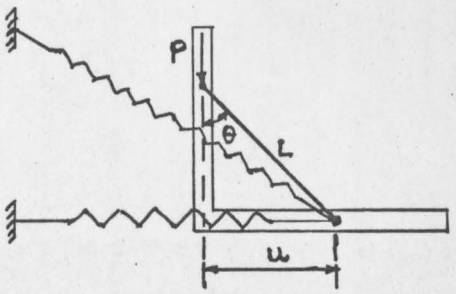

Displaced Configuration

Figure (4-b)

4.1 STATIC ANALYSIS

The geometrical configuration of model shown in figure (4-a) consists of a vertical and a horizontal frictionless guide constraining the movement of the rigid rod.A vertical load P is applied as shown.

The various assumptions regarding the type of rigid rod and the linear springs are the same as described in chapter two. The direction of the applied external load remains vertical for all the positions of the displaced rod.

Refering to figure (4-b), the displaced configuration of the model yields the dimensionless potential energy function as

$$\hat{V} = \hat{U}^2 + K\left[(\hat{U}^2 + 2\hat{U}F + 1)^{1/2} - 1\right]^2 - 2\hat{P}\left[1 - (1-\hat{U}^2)^{1/2}\right]. \tag{21}$$

where,

$\hat{U} = U/L$,

$\hat{P} = P/K_2L$,

$K = K_3/K_2$,

$\hat{V} = V/\frac{1}{2}K_2L^2$, and

$F = \cos\alpha_o = \frac{1}{2}$.

It follows that,

$$\hat{V}' = 2\left\{\hat{U} + K(F+\hat{U})\left[1 - (\hat{U}^2 + 2\hat{U}F + 1)^{-1/2}\right] - \hat{P}\hat{U}(1-\hat{U}^2)^{-1/2}\right\}, \tag{22}$$

and

$$\hat{V}'' = 2\left\{1 + K + K(F^2-1)\left[\hat{U}^2 + 2\hat{U}F + 1\right]^{-3/2} - \hat{P}(1-\hat{U}^2)^{-3/2}\right\}. \tag{23}$$

For static stability analysis, the necessary condition for the existence of a possible equilibrium state at $\theta = \theta_o$ is that $\hat{V}' = 0$, this condition yields,

$$\hat{P} = \left\{\hat{U} + K(F+\hat{U})\left[1 - (\hat{U}^2 + 2\hat{U}F + 1)^{-1/2}\right]\right\}(1-\hat{U}^2)^{1/2}\hat{U}^{-1}. \tag{24}$$

Equation (24) gives a relation between dimensionless load $\hat{P}$ and dimentionless displacement $\hat{U}$.

The sufficiency condition for neutral equilibrium is given by the condition $\hat{V}'' = 0$, this condition yields

$$\hat{P} = \left[1 + K + K(F^2-1)(\hat{U}^2 + 2\hat{U}F + 1)^{-3/2}\right](1-\hat{U}^2)^{3/2}. \tag{25}$$

Equations (24) and (25) are to be solved simultaneously to determine the critical values of displacement $\hat{U}_{cr}$ and the critical values of load $\hat{P}_{cr}$.

A plot of the family of dimensionless load versus dimensionless displacement curves is shown in figure (4-c), for various values of the parameter K.

As figure (4-c) does not resemble the figure (1-d), further stability analysis for this model is not done.

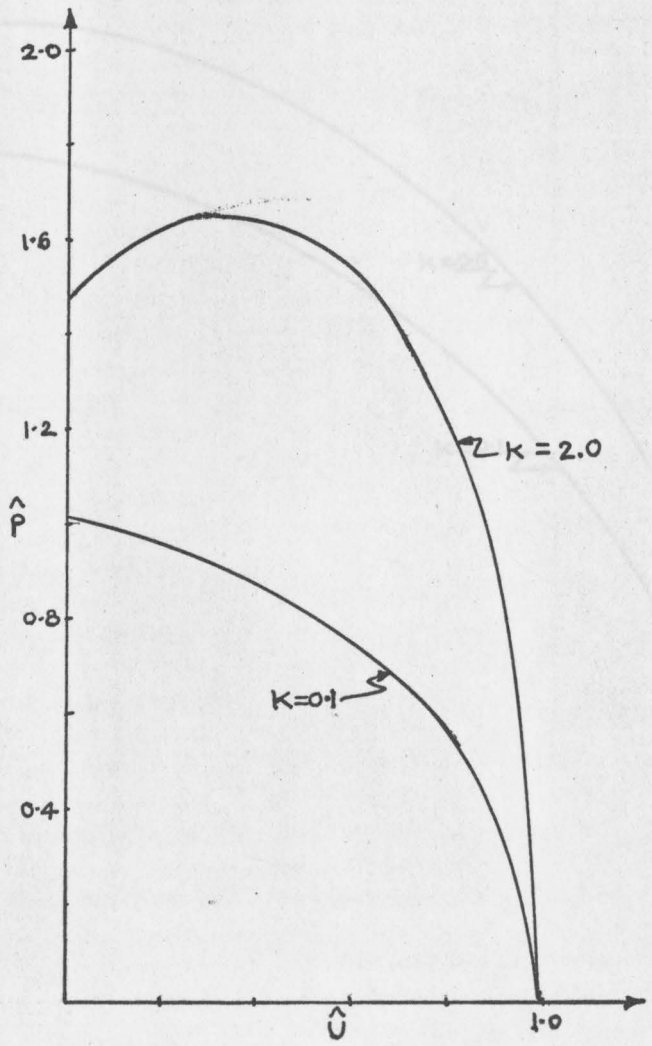

Typical load Vs displacement

Figure (4-c)

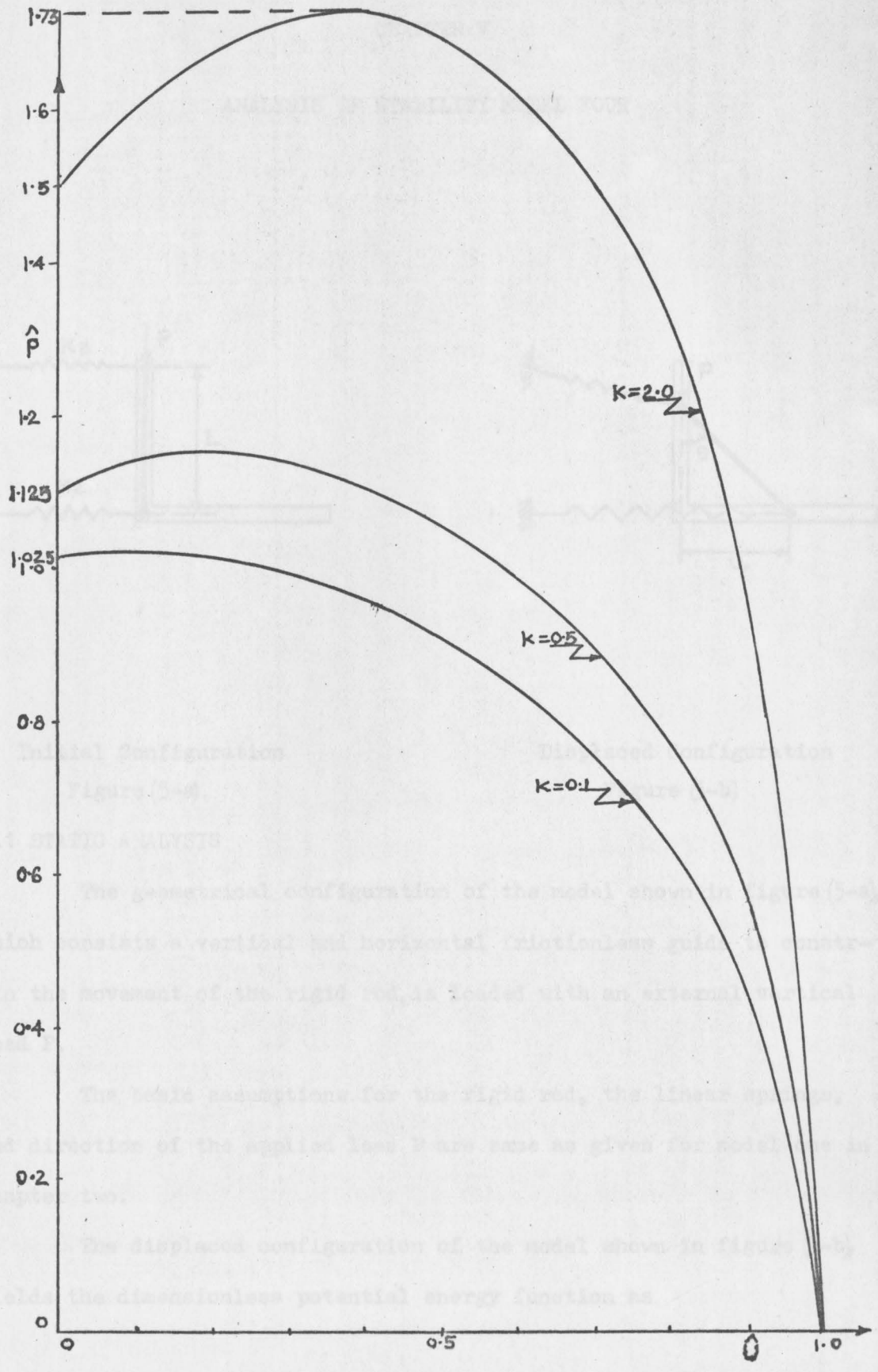

Load Vs displacement Figure (4-d)

CHAPTER V

ANALYSIS OF STABILITY MODEL FOUR

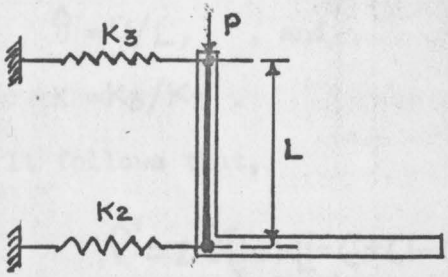

Initial Configuration
Figure (5-a)

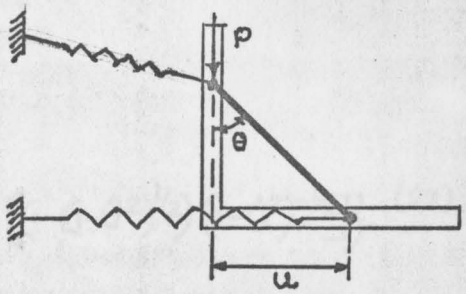

Displaced Configuration
Figure (5-b)

5.1 STATIC ANALYSIS

The geometrical configuration of the model shown in figure (5-a), which consists a vertical and horizontal frictionless guide to constrain the movement of the rigid rod, is loaded with an external vertical load P.

The basic assumptions for the rigid rod, the linear springs, and direction of the applied load P are same as given for model one in chapter two.

The displaced configuration of the model shown in figure (5-b), yields the dimensionless potential energy function as

$$\hat{V}=\hat{U}^2+K\{[3-\hat{U}^2-2(1-\hat{U}^2)^{1/2}]^{1/2}-1\}^2-2\hat{P}[1-(1-\hat{U}^2)^{1/2}]. \qquad (26)$$

where,

$\hat{V} = V/\frac{1}{2}K_2L^2$,

$\hat{P} = P/K_2L$,

$\hat{U} = U/L$, , and

$K = K_3/K_2$.

It follows that,

$$\hat{V}'=2\hat{U}\{1+K[-(1+(1-(1-\hat{U}^2)^{1/2})^2)^{-1/2}][(1-(1-\hat{U}^2)^{1/2})(1-\hat{U}^2)^{-1/2}]\} \qquad (27)$$
$$-[2\hat{U}\hat{P}(1-\hat{U}^2)^{-1/2}],$$

and

$$\hat{V}''=2[1-\hat{P}(1-\hat{U}^2)^{-3/2}]+2K\{[(1-\hat{U}^2)^{-3/2}-1]\times$$
$$[1-(1+(1-(1-\hat{U}^2)^{1/2})^2)^{-1/2}]+$$
$$\hat{U}^2[1-(1-\hat{U}^2)^{1/2}]^2[1-\hat{U}^2]^{-1}[1+(1-(1-\hat{U}^2)^{1/2})^2]^{-3/2}\}. \qquad (28)$$

For static stability analysis, $\hat{V}' = 0$, governs the necessary condition for the existence of a possible equilibrium state at $\theta = \theta_o$. This condition yields,

$$\hat{P}=(1-\hat{U}^2)^{1/2}+K[1-(1-\hat{U}^2)^{1/2}]\{1-[1+(1-(1-\hat{U}^2)^{1/2})^2]^{-1/2}\}. \qquad (29)$$

Equation (29) gives a relationship between dimensionless load $\hat{P}$ and dimensionless displacement $\hat{U}$, for a given value of parameter K.

The sufficiency condition $\hat{V}'' = 0$, governs the existence of neutral equilibrium. It follows,

$$\hat{P}=\{[(1-\hat{U}^2)^{-3/2}-1][1-(1+(1-(1-\hat{U}^2)^{1/2})^2)^{-1/2}]+ \hat{U}^2[1-(1-\hat{U}^2)^{1/2}]^2(1-\hat{U}^2)^{-1}[1+(1-(1-\hat{U}^2)^{1/2})^2]^{-3/2}\}\times [K(1-\hat{U}^2)^{3/2}]+[(1-\hat{U}^2)^{3/2}]. \quad (30)$$

Equations (29) and (30), are solved simultaneously to yield the critical values of displacement $\hat{U}_{cr}$ and the critical value of load $\hat{P}_{cr}$.

A typical set of the family of dimensionless load-deflection curves is shown in figure (5-c), for various values of the parameter K.

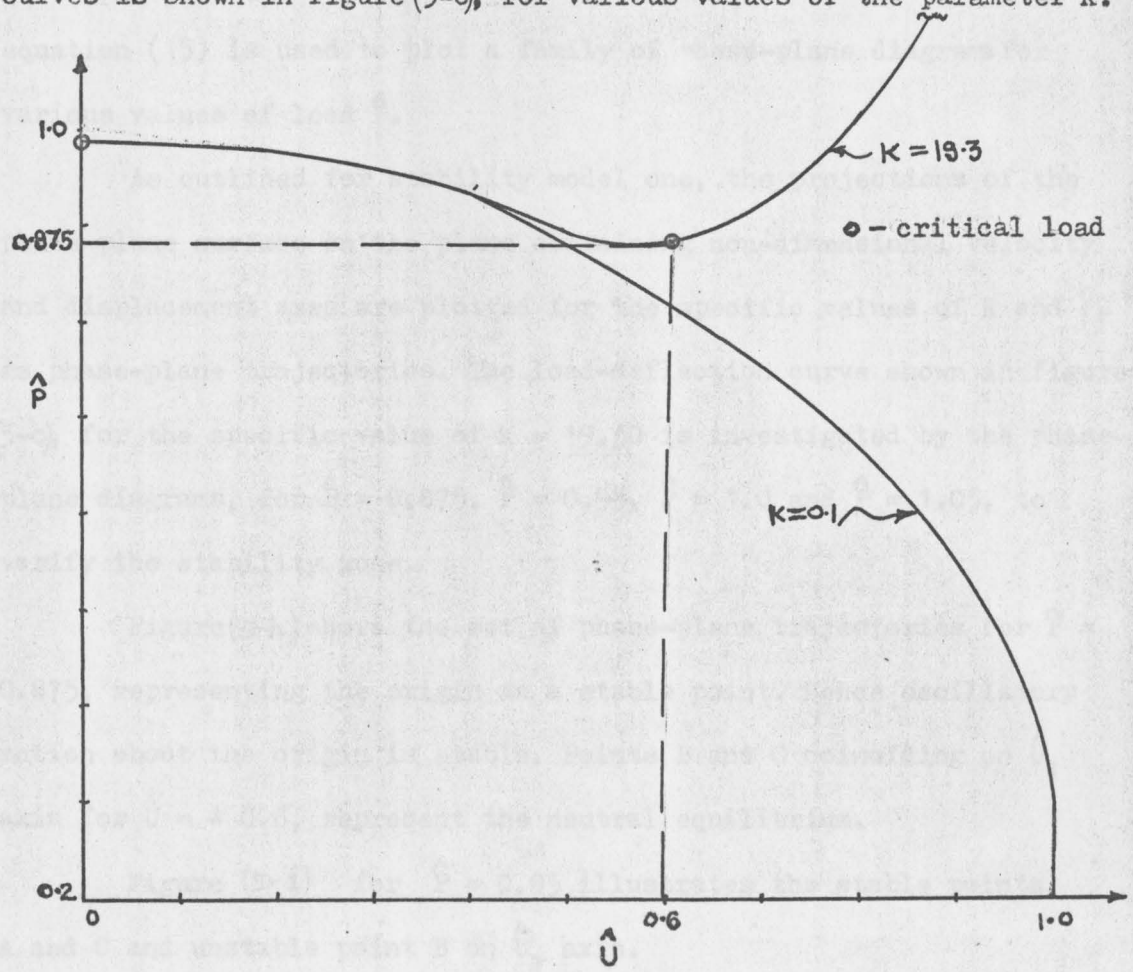

Typical load Vs displacement Figure (5-c)

Refering figure (5-c), it follows that for K = 19.30, and $0 \leq \hat{U} \leq 1$, the slope of the curve changes from negative value to positive value, and the slope is zero at $\hat{U} = 0.6$

The point corresponding to $\hat{P} = 1$ and $\hat{U} = 0$, is in neutral equilibrium since $\hat{V}' = 0$ and $\hat{V}'' = 0$ for K = 19.30. For K = 19.30, $0.875 < \hat{P} < 1$, and $0 < \hat{U} < 0.6$, all points on the load deflection curve are unstable, since V' = 0 and V" is negative in magnitude. The points on the curve corresponding to K = 19.30, $\hat{P} > 0.875$, and $\hat{U} > 0.6$ are in stable equilibrium since $\hat{V}' = 0$ and $\hat{V}''$ is positive in magnitude.

5.2 DYNAMIC ANALYSIS

Adopting a procedure outlined in chapter two, the basic form of equation (15) is used to plot a family of phase-plane diagrams for various values of load $\hat{P}$.

As outlined for stability model one, the projections of the phase-plane surface on the plane containing non-dimensional velocity and displacement axes are plotted for the specific values of K and $\hat{P}$, as phase-plane trajectories. The load-deflection curve shown in figure (5-c), for the specific value of K = 19.30 is investigated by the phase-plane diagrams, for $\hat{P} = 0.875$, $\hat{P} = 0.95$, $\hat{P} = 1.0$ and $\hat{P} = 1.05$, to verify the stability zone.

Figure (5-h) shows the set of phase-plane trajectories for $\hat{P} = 0.875$, representing the origin as a stable point. Hence oscillatory motion about the origin is stable. Points B and C coinciding on $\hat{U}_1$ axis for $\hat{U} = \pm 0.6$, represent the neutral equilibrium.

Figure (5-i) for $\hat{P} = 0.95$ illustrates the stable points A and C and unstable point B on $\hat{U}_1$ axis.

Figures (5-J) and (5-K) illustrate the phase-plane plots for $\hat{P} = 1.0$ and $\hat{P} = 1.05$ respectively. The points A and B coincide at the origin, hence origin is an unstable point while point C on $\hat{U}_1$ axis is a stable point.

Thus, for K = 19.30 as the magnitude of dimensionless load $\hat{P}$ increases beyond $\hat{P} = 0.875$, point B showing position of unstable point, moves towards the origin and approaches point A. For $\hat{P} \geq 1$, points A and B coincide and form an unstable point.

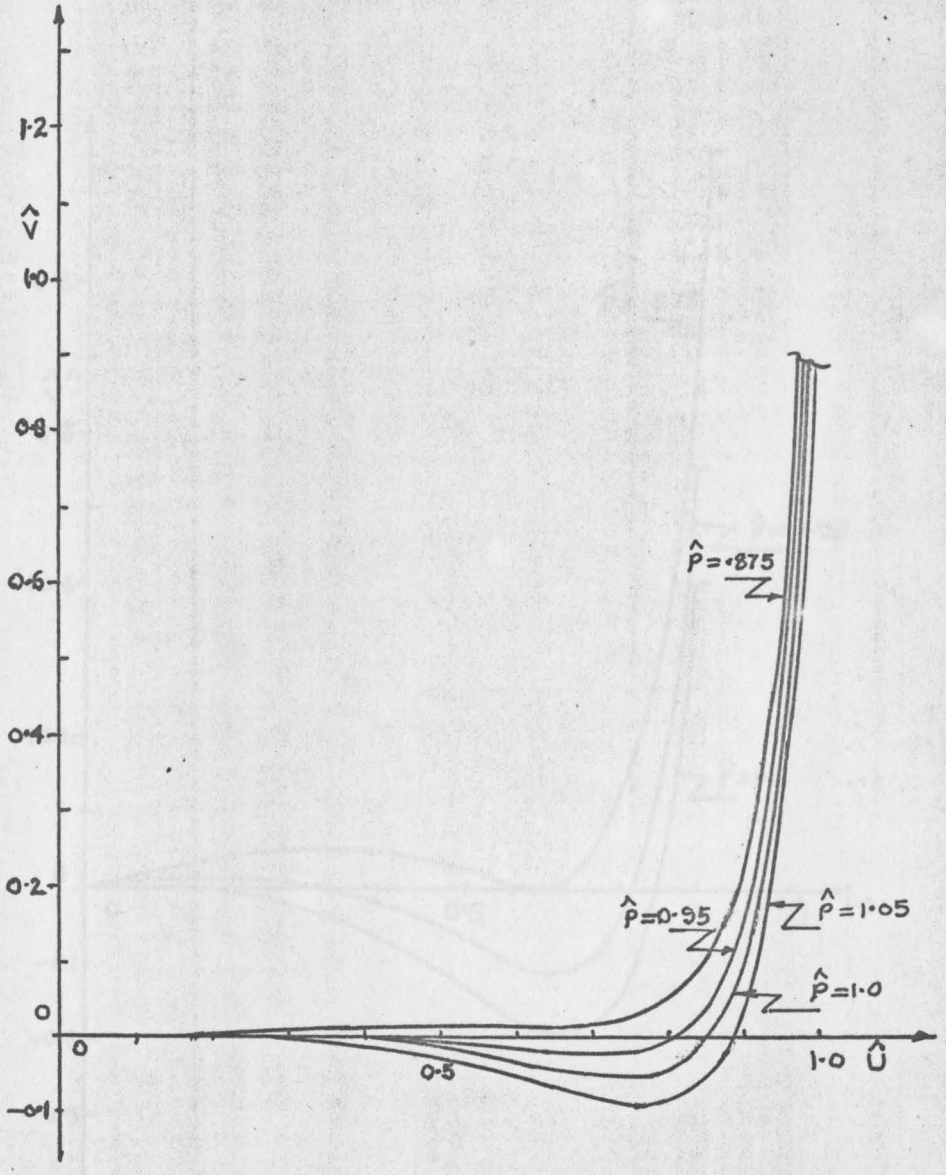

Potential energy Vs displacement

Figure (5-e)

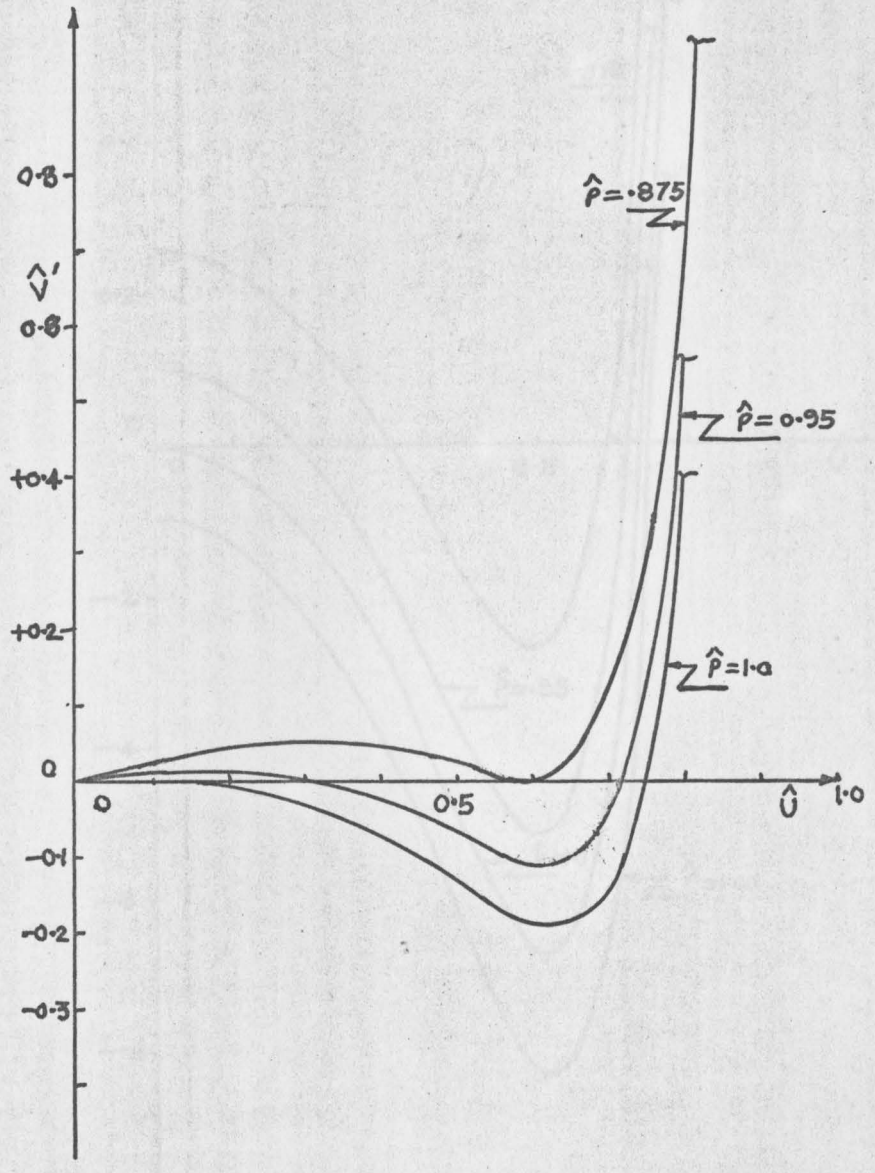

$\hat{V}'$ Vs displacement

Figure(5-f)

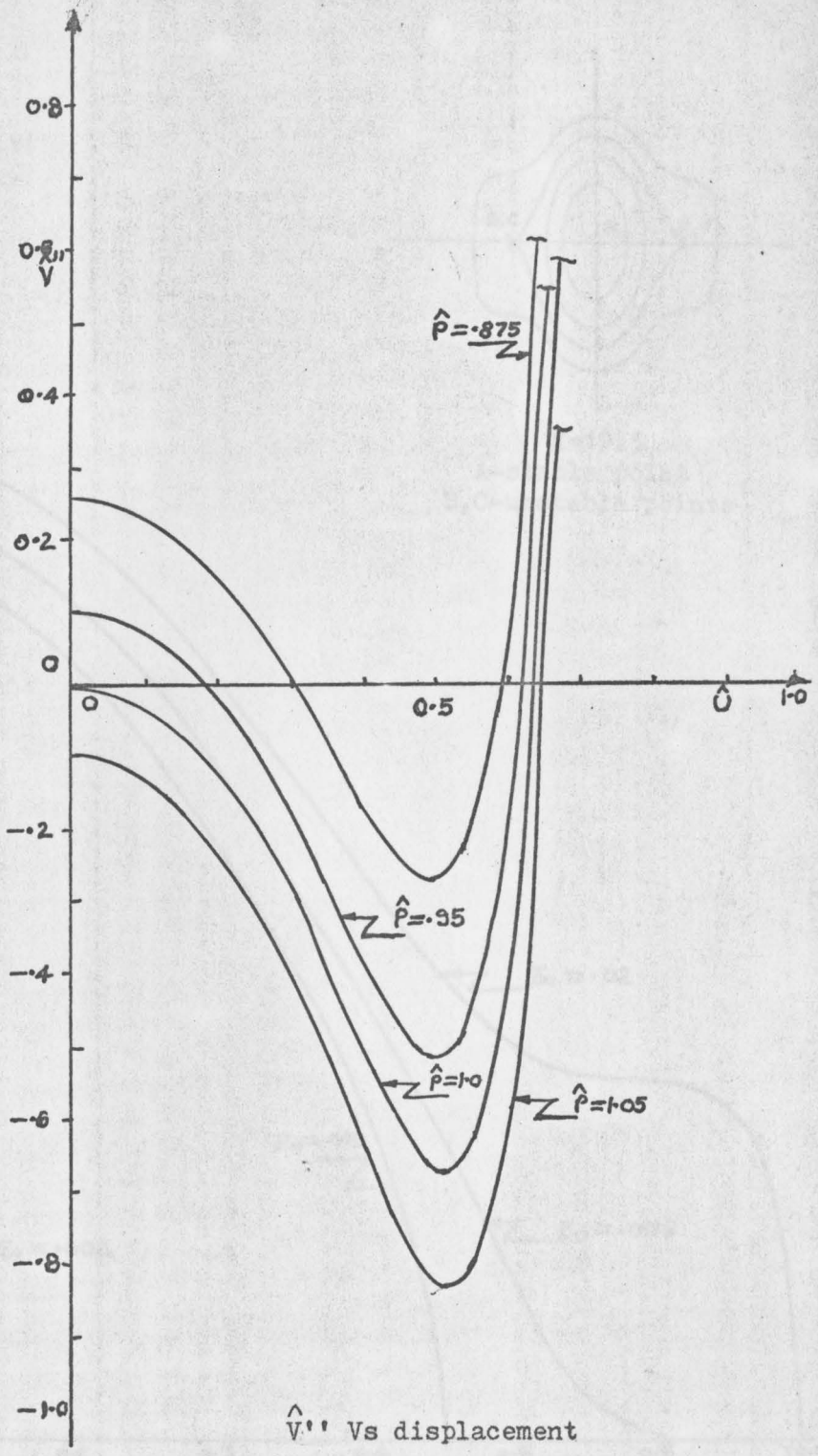

$\hat{V}''$ Vs displacement

Figure (5-g)

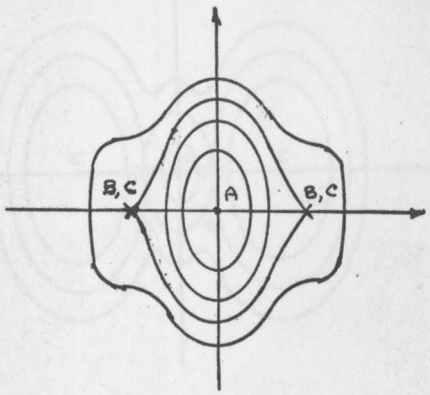

K=19.3
A-stable point
B,C-unstable points

Phase-plane plot for $\hat{P}$=0.875

Figure (5-h)

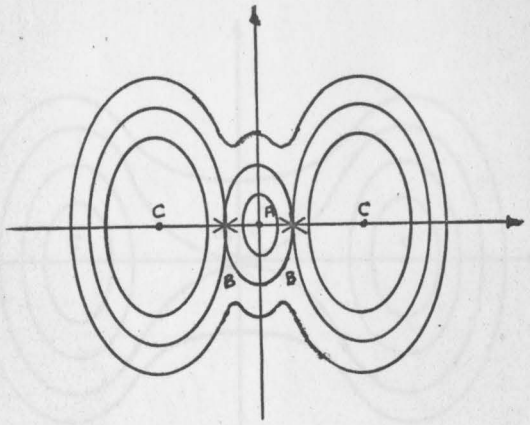

K=19.3
A,C-stable points
B-unstable points

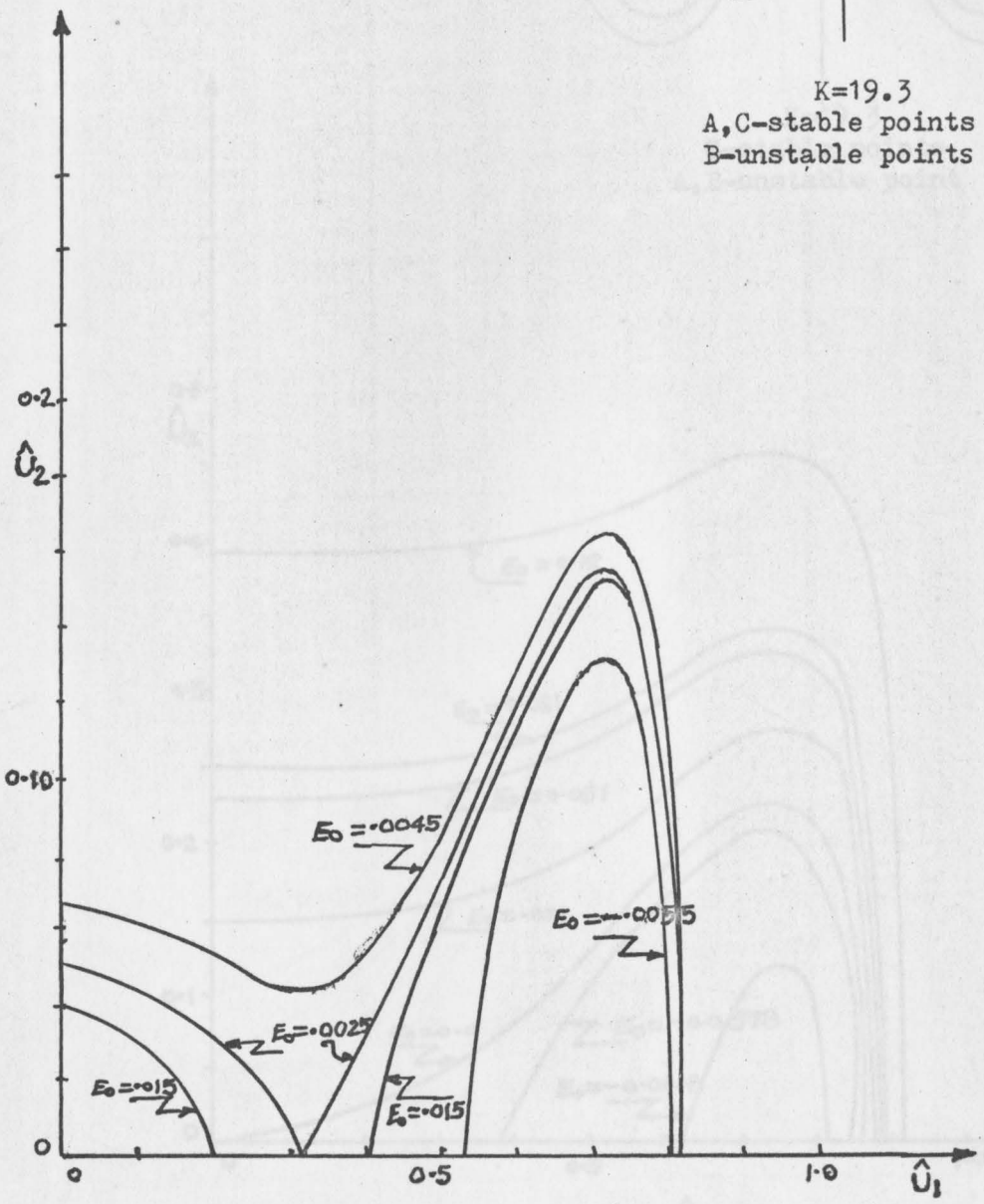

Phase-plane plot for $\hat{P}$= 0.95

Figure (5-1)

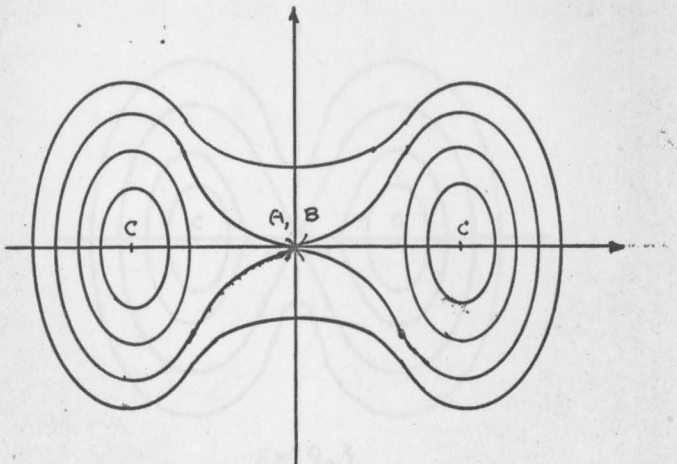

K=19.3
C-stable points
A,B-unstable point

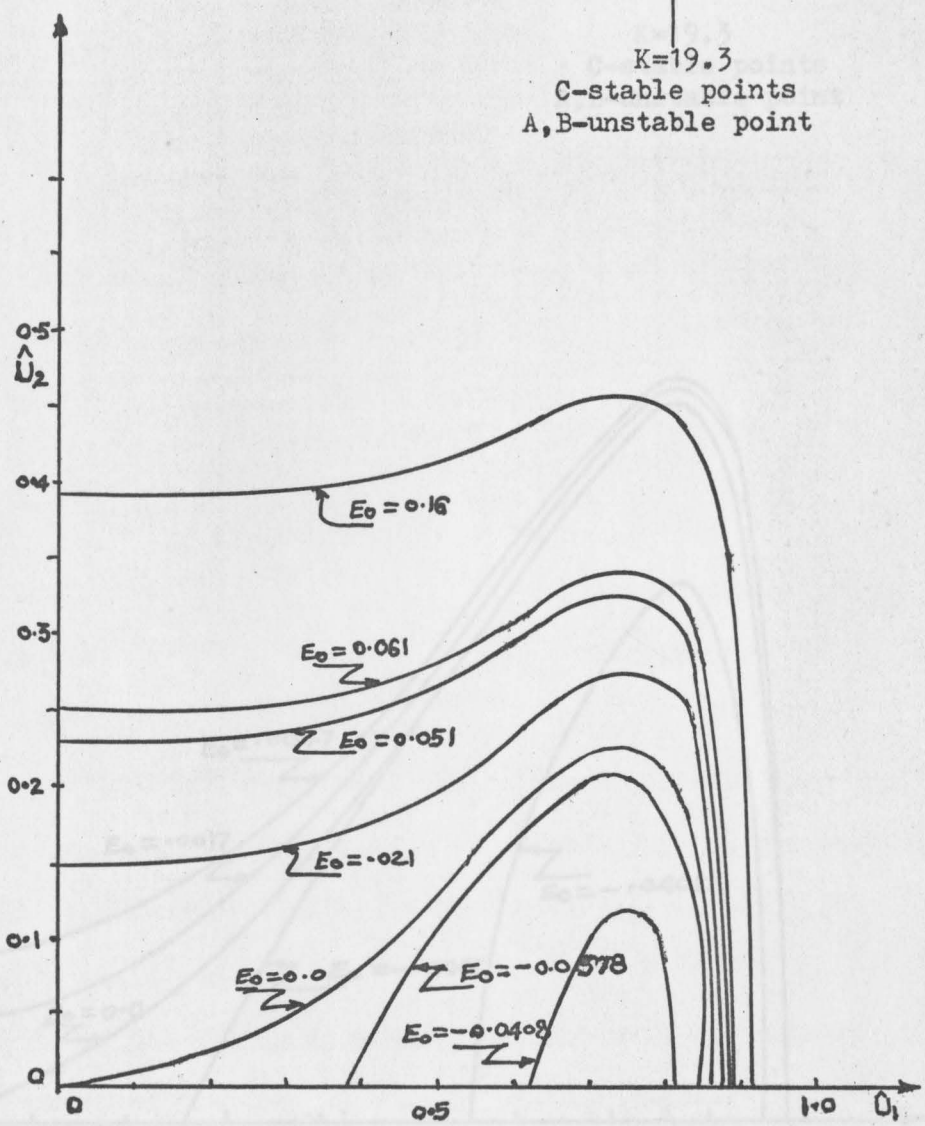

Phase-plane plot for $\hat{P}$=1.0

Figure (5-I)

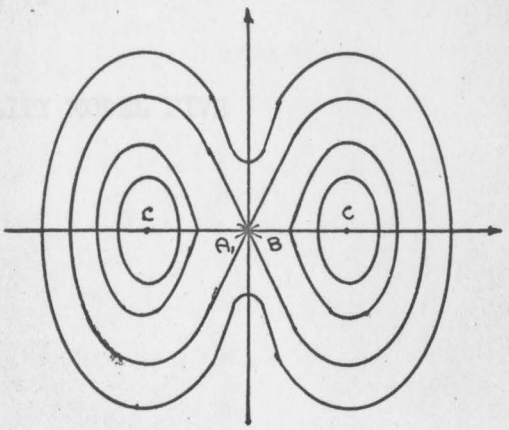

K=19.3
C-stable points
A,B-unstable point

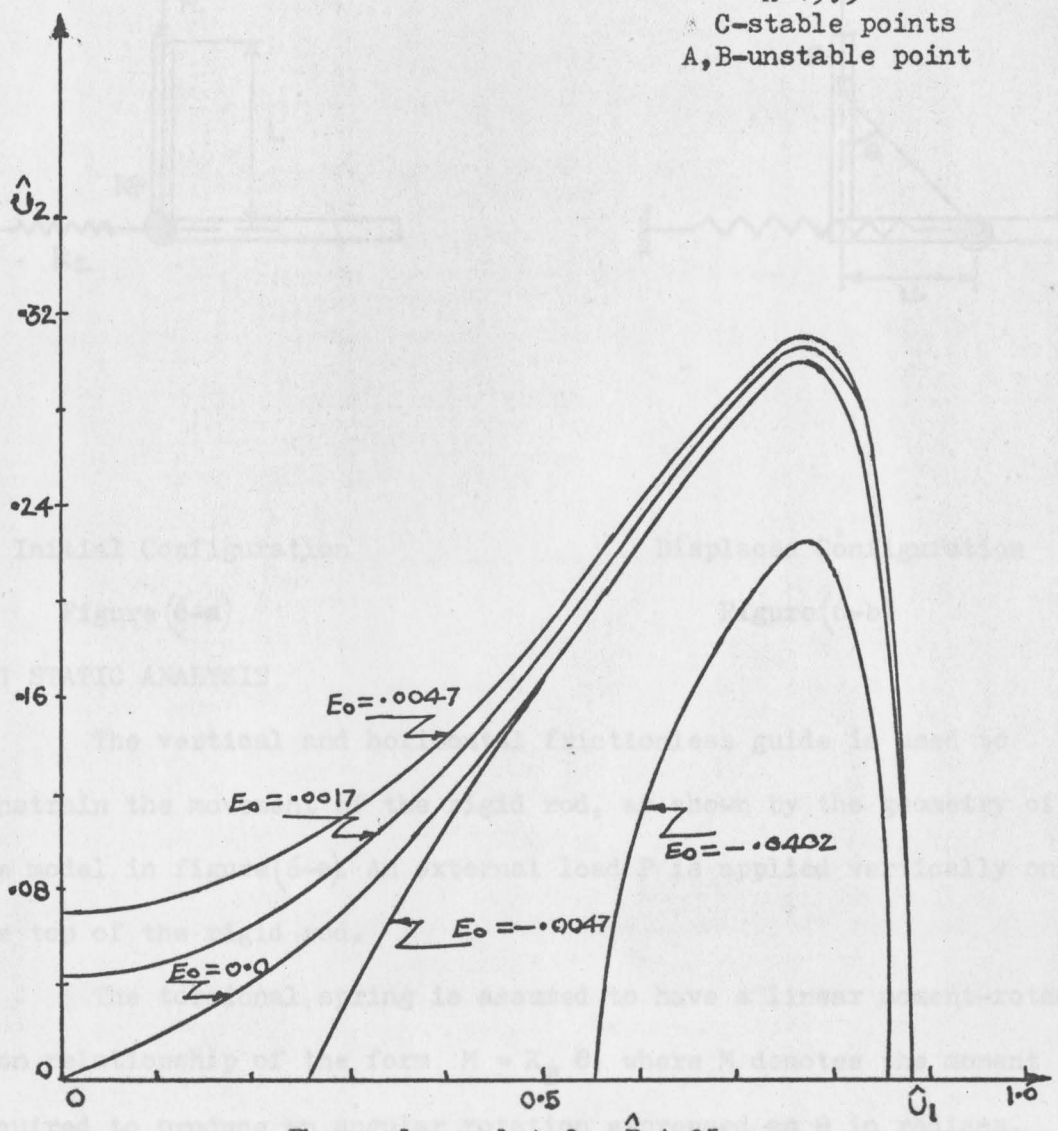

Phase-plane plot for $\hat{P}$=1.05

Figure (5-k)

CHAPTER VI

ANALYSIS OF STABILITY MODEL FIVE

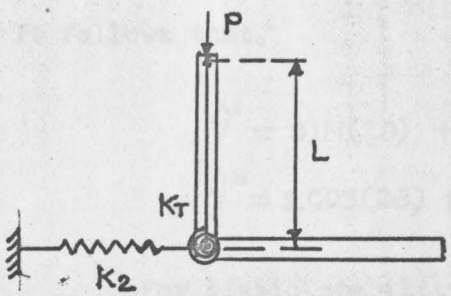

Initial Configuration

Figure (6-a)

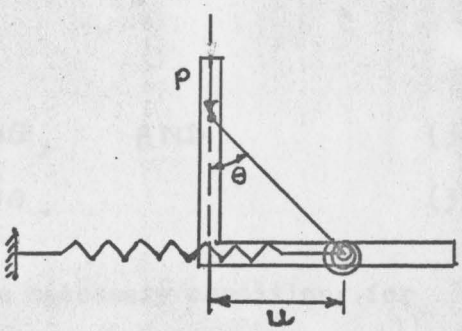

Displaced Configuration

Figure (6-b)

6.1 STATIC ANALYSIS

The vertical and horizontal frictionless guide is used to constrain the movement of the rigid rod, as shown by the geometry of the model in figure (6-a). An external load P is applied vertically on the top of the rigid rod.

The torsional spring is assumed to have a linear moment-rotation relationship of the form $M = K_T \theta$, where M denotes the moment required to produce an angular rotation expressed as θ in radians. The other basic assumptions are same as described previously.

Figure (6-b) representing the displaced configuration of the model yields the dimensionless potential energy function as

$$\hat{V} = (\sin\theta)^2 + K(\theta)^2 + 2\hat{P}[\cos\theta - 1], \tag{31}$$

where

$\hat{P} = P/K_2L$,

$\hat{V} = V/\frac{1}{2}K_2L^2$, and

$K = K_T/K_2L^2$.

It follows that,

$$\hat{V}' = \sin(2\theta) + 2K\theta - 2\hat{P}\sin\theta, \quad \text{AND} \tag{32}$$

$$\hat{V}'' = 2\cos(2\theta) + 2K - 2\hat{P}\cos\theta . \tag{33}$$

For static stability analysis, the necessary condition, for the existence of a possible equilibrium state at $\theta = \theta_0$ is that, $\hat{V}' = \frac{d\hat{V}}{d\theta} = 0$, this condition yields,

$$\hat{P} = \cos\theta + K\theta/\sin\theta . \tag{34}$$

Equation (34) gives a relation between non-dimensional load $\hat{P}$ and angular rotation θ.

The sufficiency condition for neutral equilibrium is given by the condition $\hat{V}'' = \frac{d^2\hat{V}}{d\theta^2} = 0$, this condition yields,

$$\hat{P} = [\cos(2\theta) + 2K]/\cos\theta . \tag{35}$$

Equation (34) and (35) can be solved simultaneously to evaluate the critical value of angular rotation θ_{cr} and the critical value of load $\hat{P}_{cr}$.

A plot of the dimensionless load versus angular rotation is shown in figure (6-c) for the specific value of the parameter K.

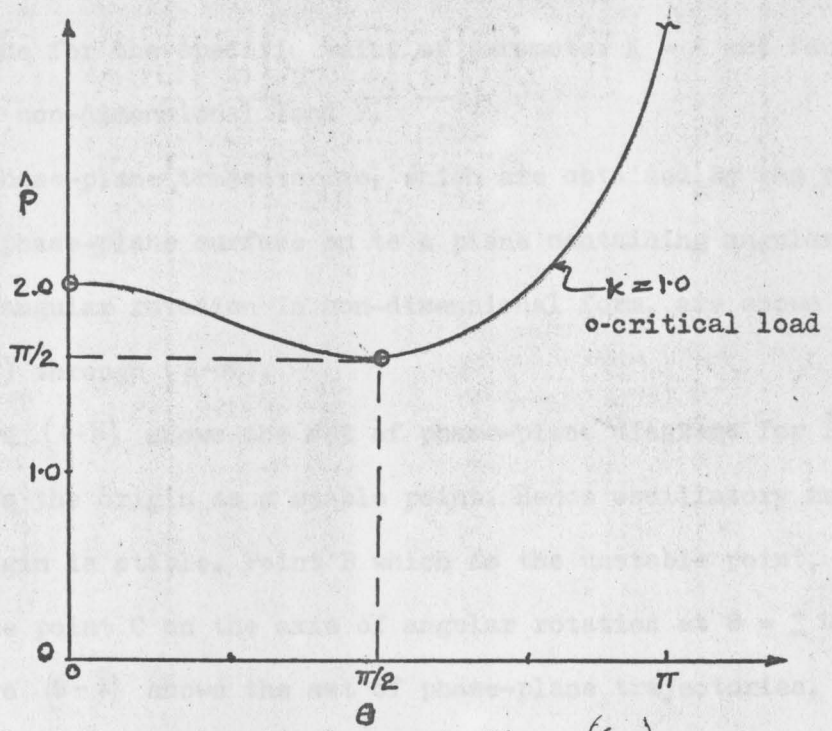

Typical load Vs angular displacement Figure (6-c)

Refering figure (6-c) it follows that, for K = 1 and $0 \leq \theta \leq \pi$, the slope of the load-rotation curve changes from negative to positive and slope is zero at $\theta = \pi/2$.

The point corresponding to $\hat{P} = 2$ and $\theta = 0$, is in neutral equilibrium, since $\hat{V}' = 0$ and $\hat{V}'' = 0$. For $1.57 < \hat{P} < 2$ and $0 < \theta < \pi/2$, all points on the load-rotation curve are unstable, since $\hat{V}' = 0$ and $\hat{V}''$ is negative in magnitude. The points on curve corresponding to the condition $\hat{P} > 1.57$ and $\theta > \pi/2$ are in stable equilibrium.

6.2 DYNAMIC ANALYSIS

Using the basic form of equation (15), the non-dimensional angular velocity of motion can be evaluated for the specific value of the initial energy E_o of the elastic system at any time t, for the known value of the dimensionless potential energy.

The phase-plane concept is used to investigate dynamic stability conditions for the specific value of parameter K = 1 and for various values of non-dimensional load $\hat{P}$.

The phase-plane trajectories, which are obtained by the projection of the phase-plane surface on to a plane containing angular velocity and angular rotation in non-dimensional form, are shown in figures (6-h) through (6-K).

Figure (6-h) shows the set of phase-plane diagrams for $\hat{P} = \frac{\pi}{2}$ and represents the origin as a stable point. Hence oscillatory motion about the origin is stable. Point B which is the unstable point, coincides with the point C on the axis of angular rotation at $\theta = \pm \pi/2$.

Figure (6-i) shows the set of phase-plane trajectories, for $\hat{P} = 1.8$ and illustrates the stable points A and C, and an unstable point B on the axis of angular rotation.

Figures (6-J) and (6-K) illustrate phase-plane trajectories, for $\hat{P} = 2$ and $\hat{P} = 2.2$ respectively. The unstable point B coincides with point A at the origin, hence the origin is an unstable point and point C is a stable point.

Thus, for K = 1, as the value of load P increases beyond $\pi/2$, unstable point B moves towards the origin and approaches point A. For $\hat{P} \geq 2$, points A and B coincide to form an unstable equilibrium at the origin.

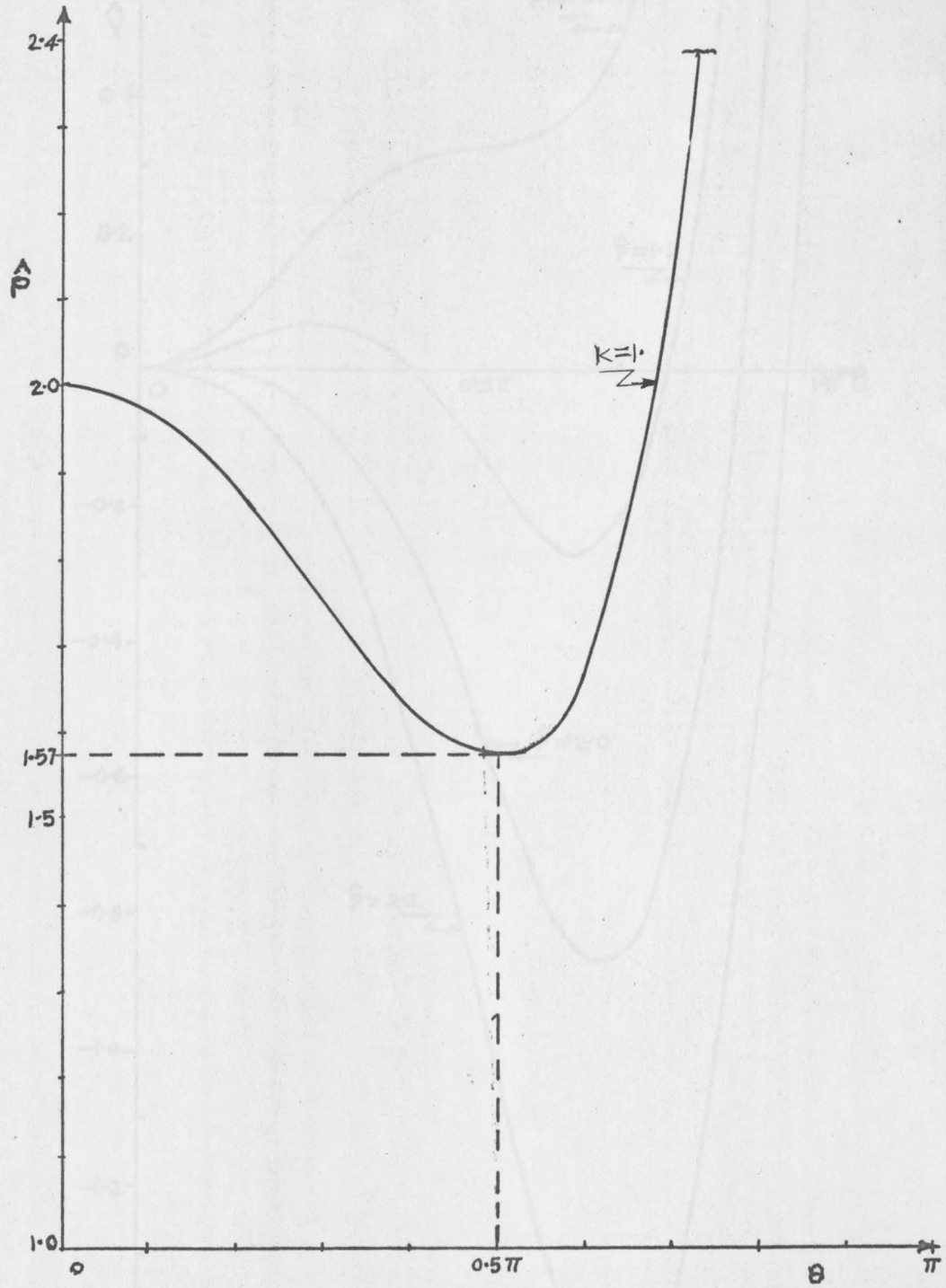

Load Vs angular displacement

Figure (6-d)

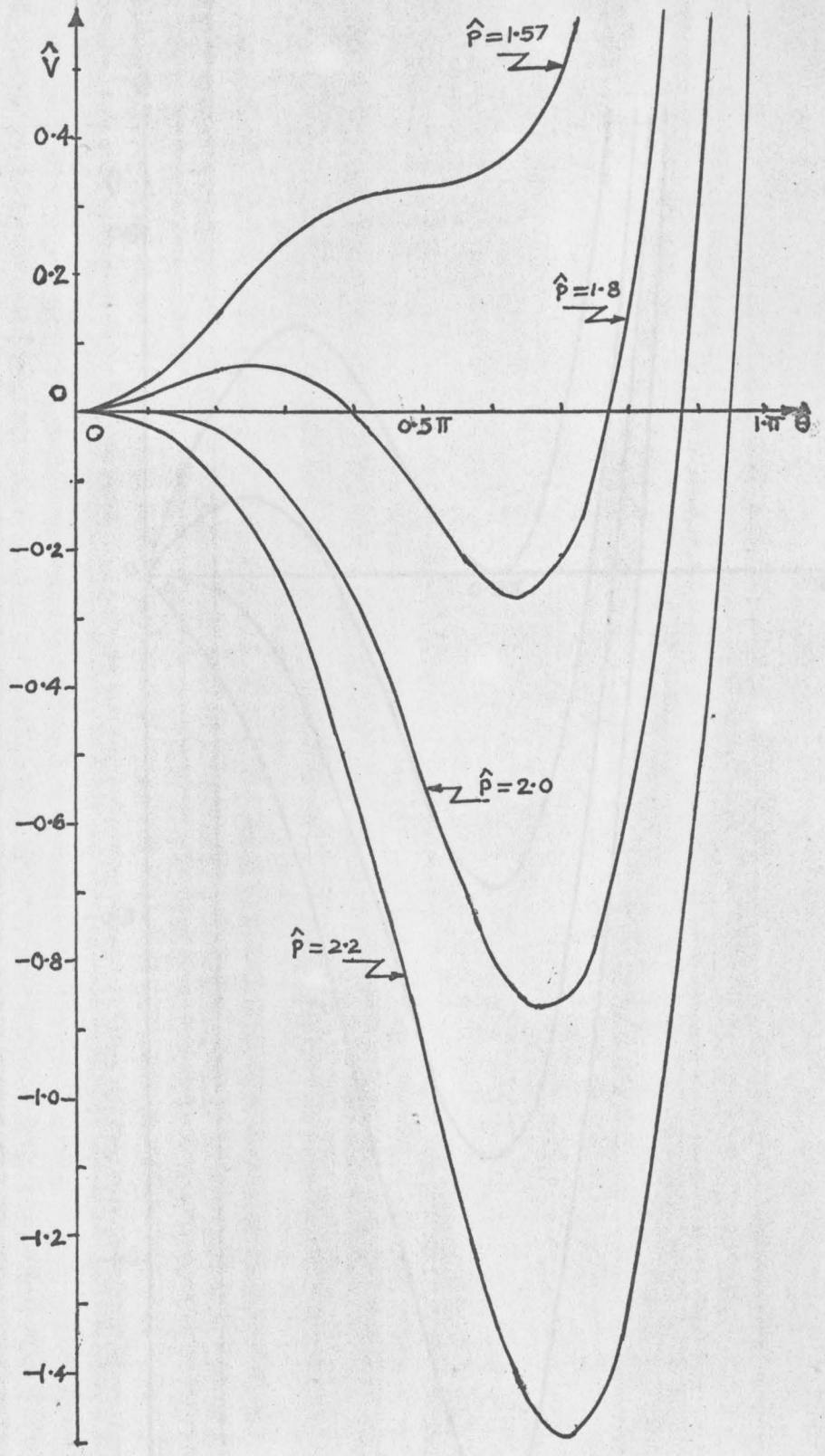

Potential energy Vs angular displacement Figure(6-e)

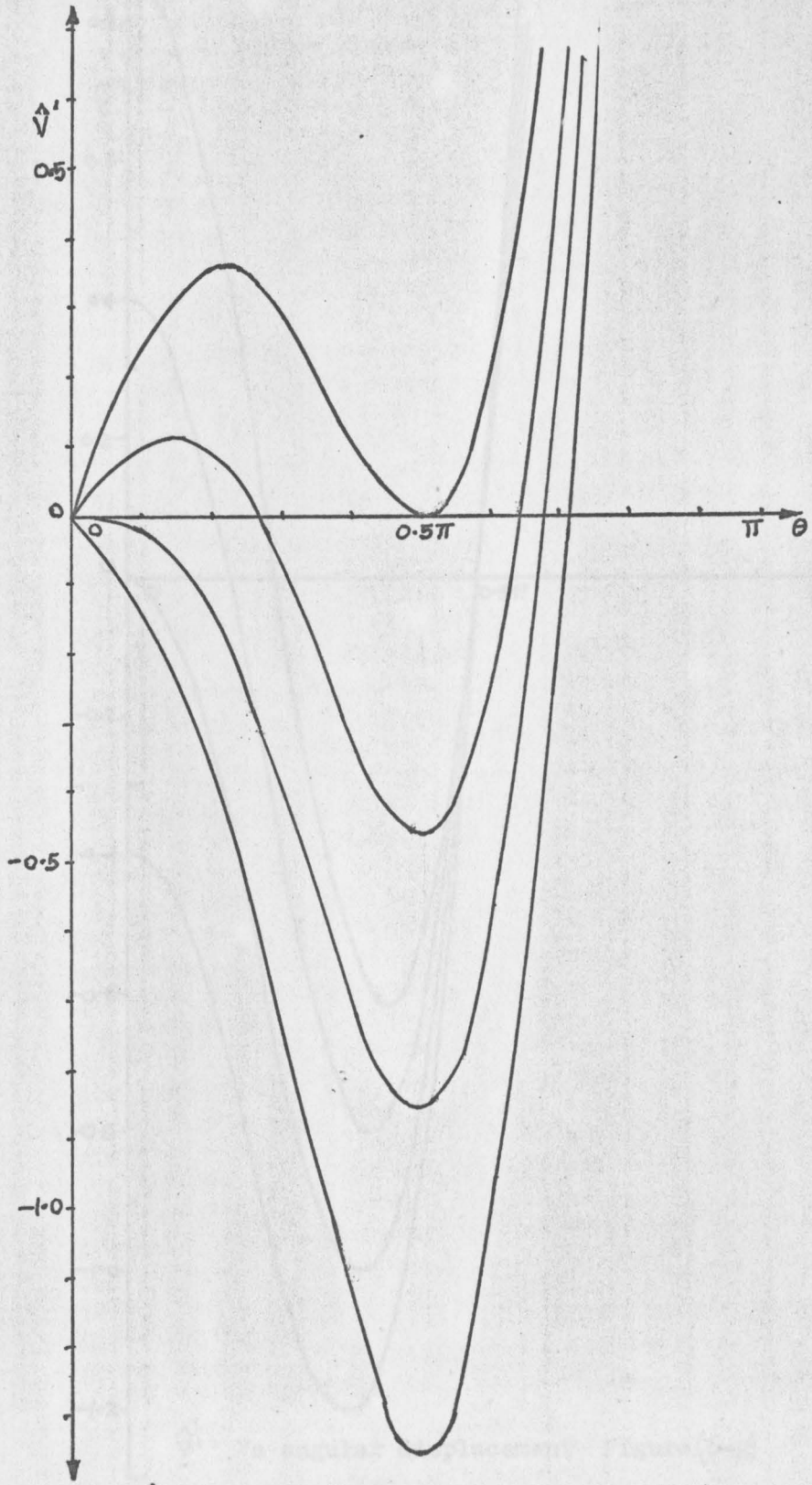

$\hat{V}'$ Vs angular displacement Figure (6-f)

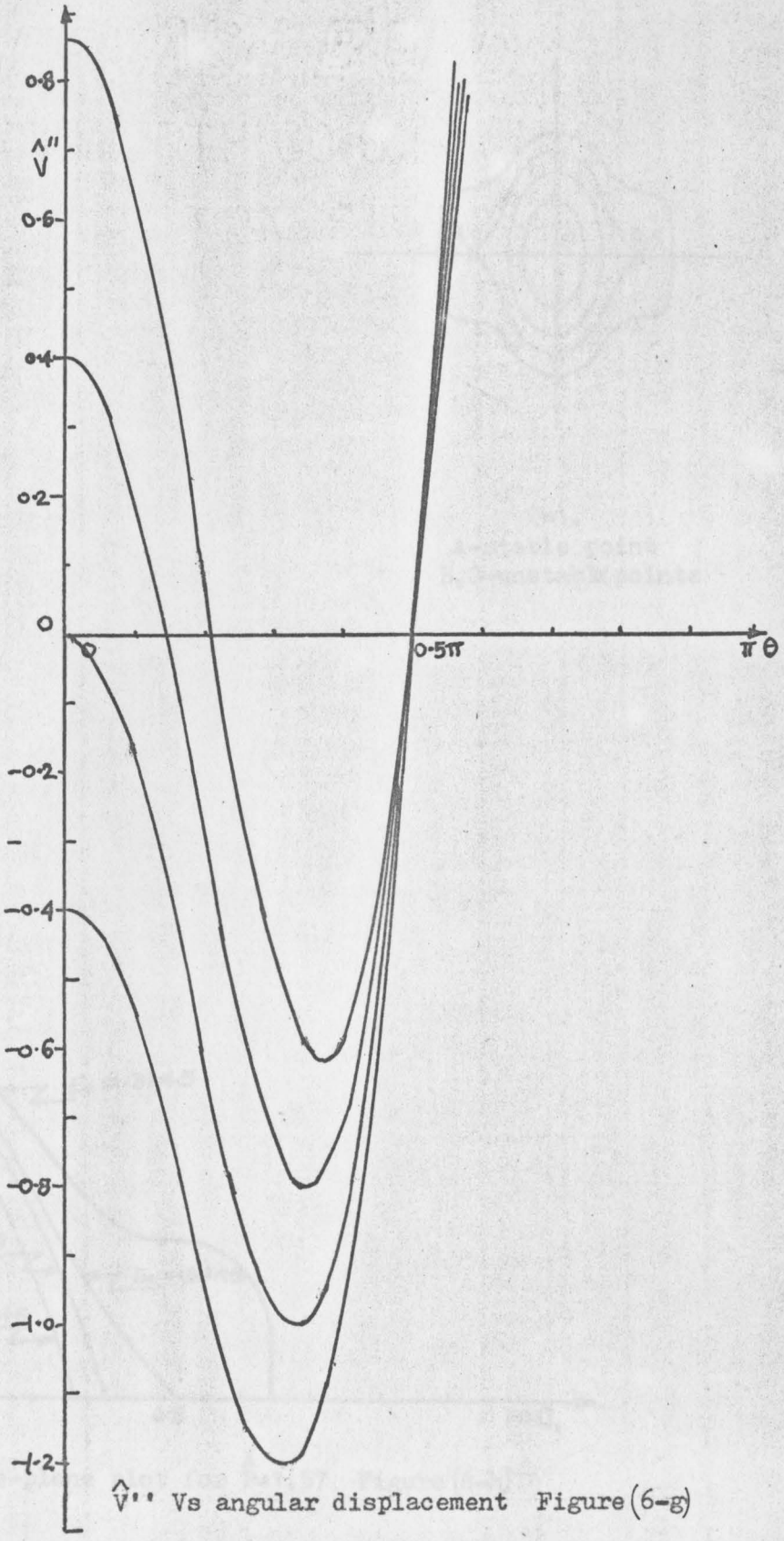

$\hat{V}''$ Vs angular displacement Figure (6-g)

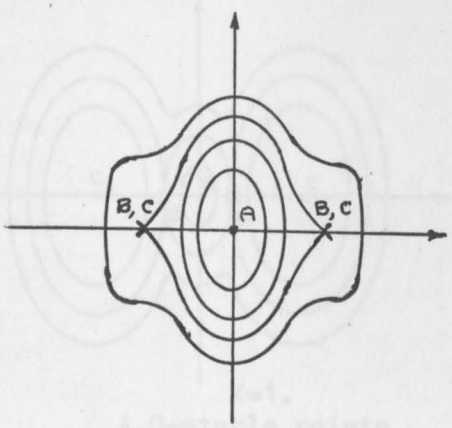

K=1.
A-stable point
B,C-unstable points

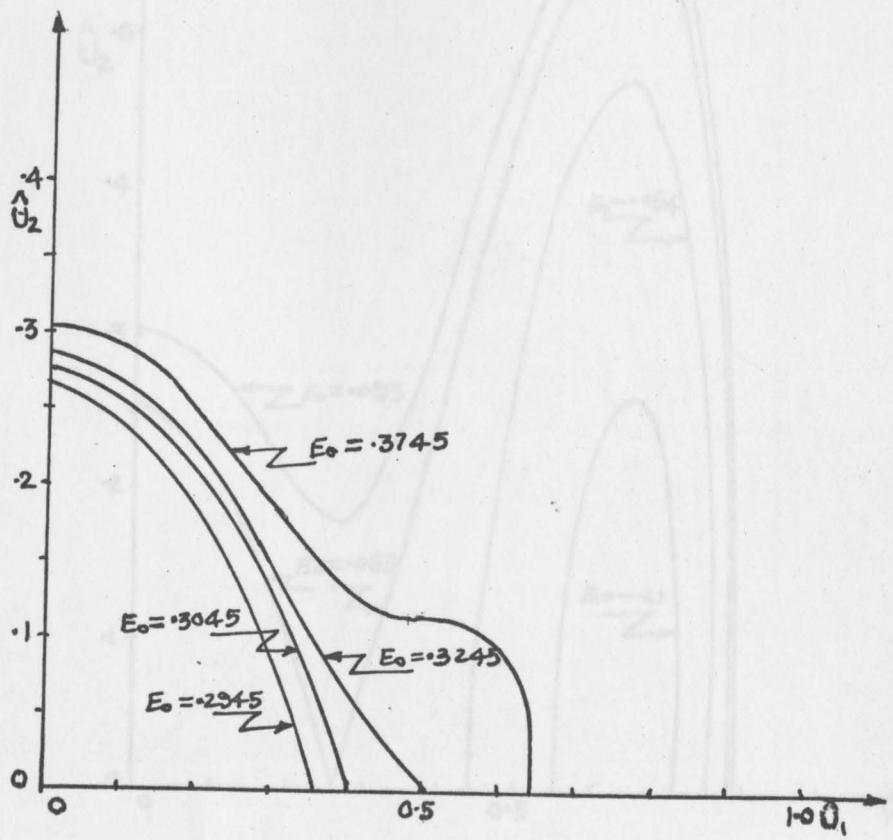

Phase-plane plot for $\hat{P}$=1.57 Figure (6-h)

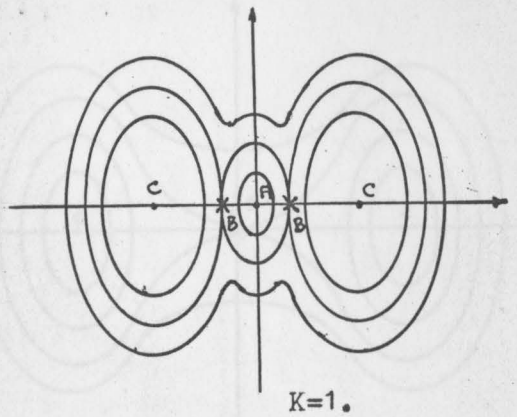

K=1.
A,C-stable points
B-unstable point

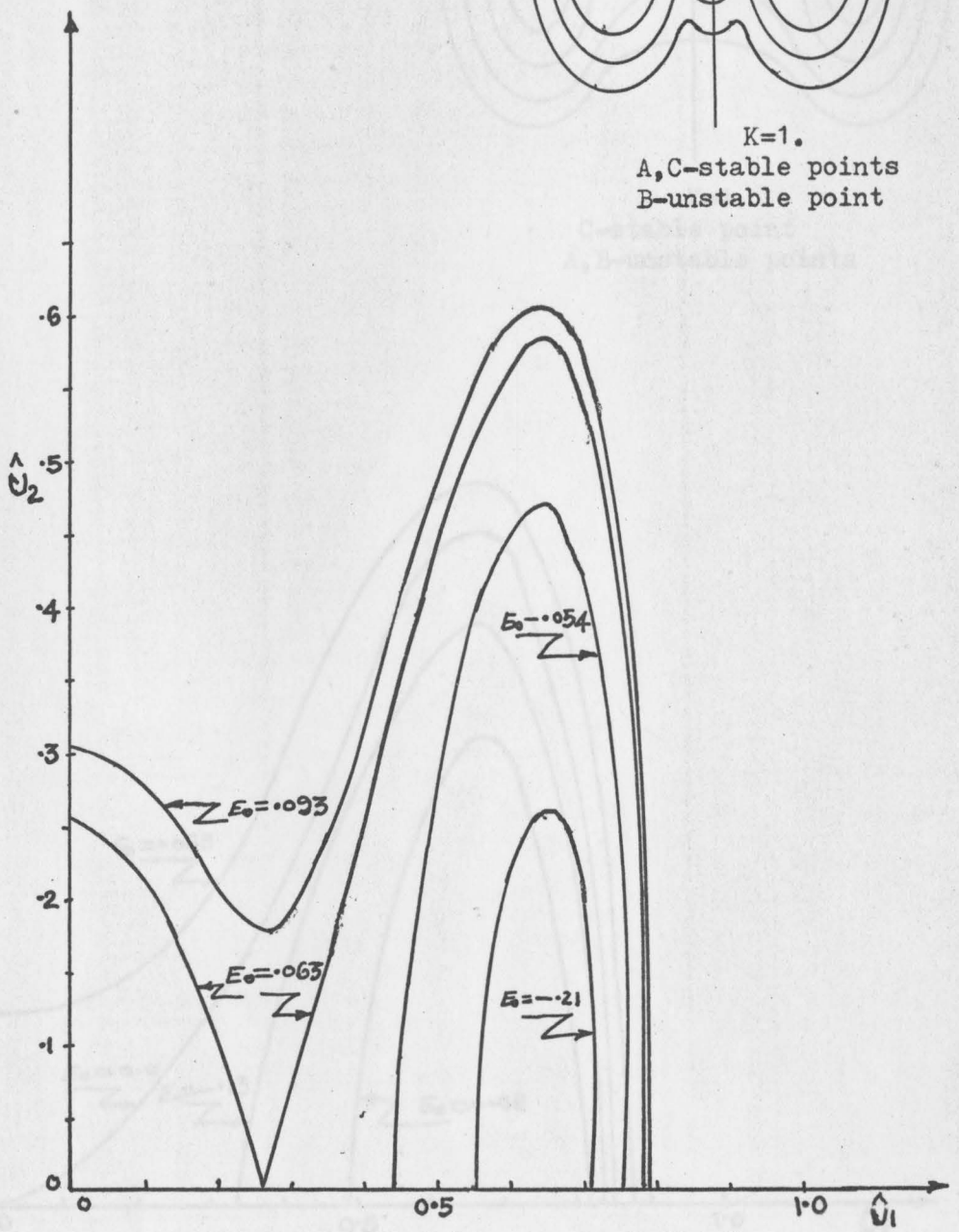

Phase-plane plot for $\hat{P}$=1.80 Figure (6-i)

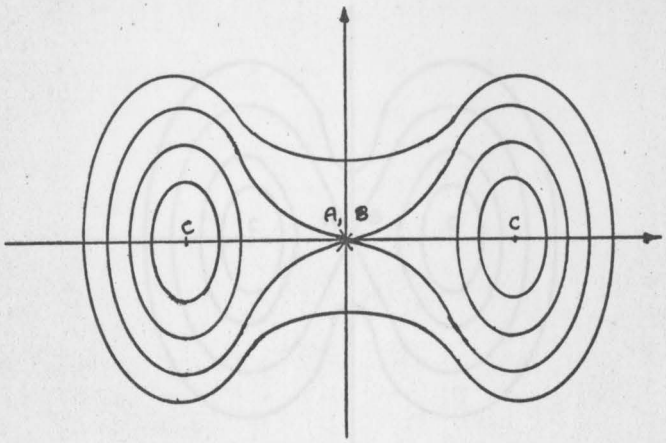

K=1.
C-stable point
A,B-unstable points

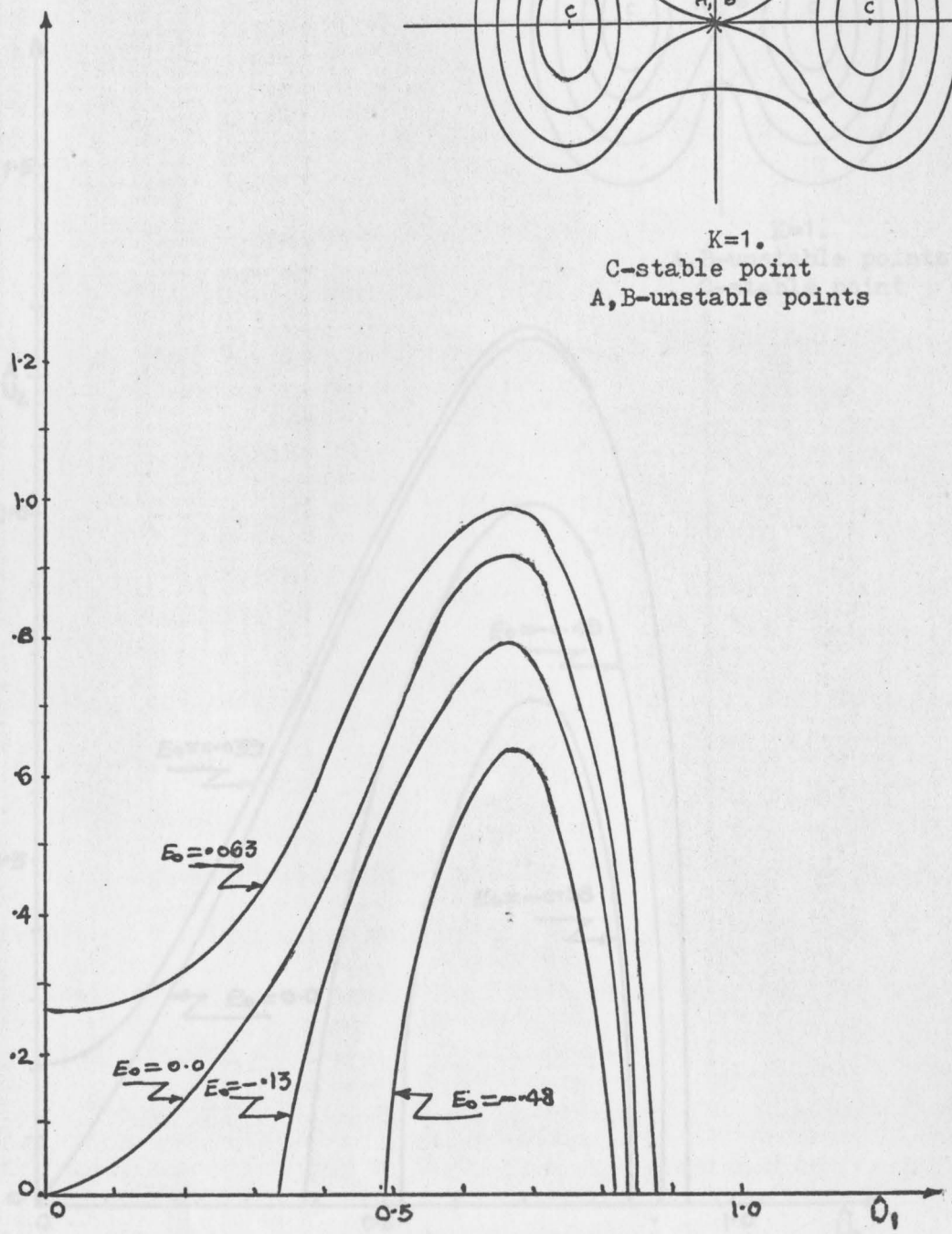

Phase-plane plot for $\hat{P}=2.0$ Figure (6-V)

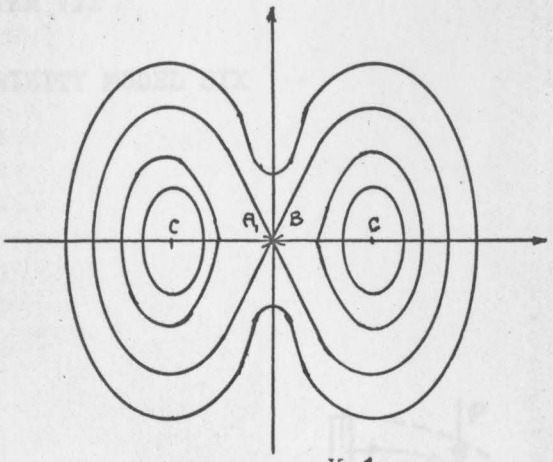

K=1.
A,B-unstable points
C-stable point

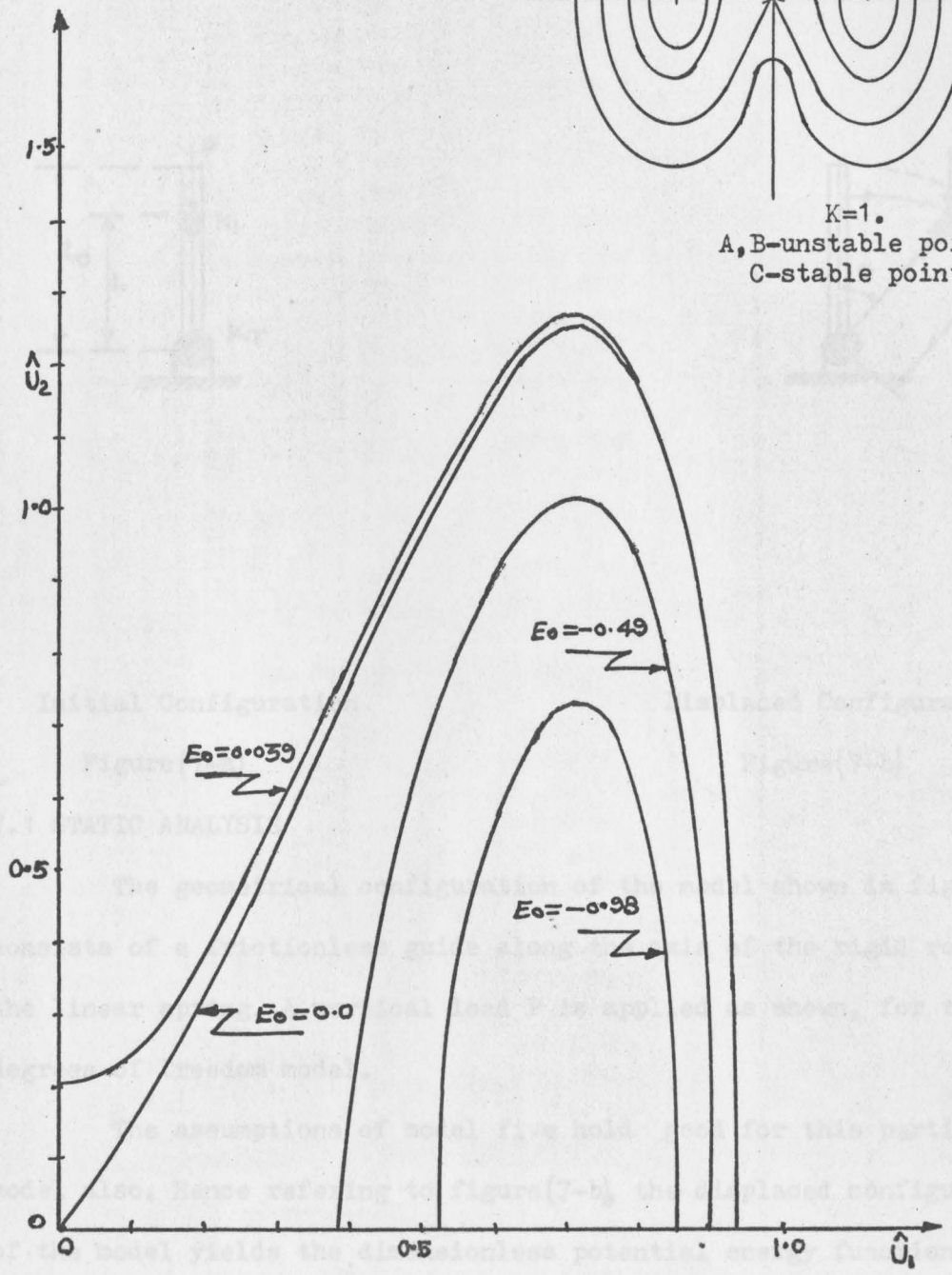

Phase-plane plot for $\hat{P}$=2.20 Figure (6-K)

CHAPTER VII

ANALYSIS OF STABILITY MODEL SIX

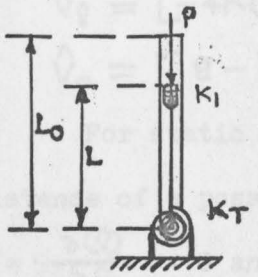

Initial Configuration

Figure(7-a)

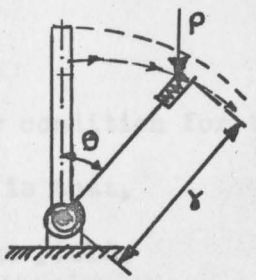

Displaced Configuration

Figure(7-b)

7.1 STATIC ANALYSIS

The geometrical configuration of the model shown in figure(7-a) consists of a frictionless guide along the axis of the rigid rod for the linear spring. A vertical load P is applied as shown, for this two degrees of freedom model.

The assumptions of model five hold good for this particular model also. Hence refering to figure(7-b), the displaced configuration of the model yields the dimensionless potential energy function as,

$$\hat{V}_{(\hat{\gamma},\theta)} = (\theta^2/2 + 2\hat{K}(1-\hat{\gamma})^2 + \hat{P}\hat{\gamma}\cos\theta - \hat{P}). \qquad (36)$$

where,

$$\hat{V} = \frac{V(\hat{\gamma},\theta)}{K_T} ,$$

$$\hat{P} = \frac{PL_o}{K_T} ,$$

$$\hat{r} = \gamma/L_o \quad , \text{ and}$$

$$K = K_1 L_o^2/4K_T .$$

It follows that,

$$\hat{V}_{\hat{\gamma}} = [-4K(1-\hat{\gamma}) + \hat{P}\cos\theta], \tag{37}$$

$$\hat{V}_{\theta} = [\theta - \hat{P}\hat{\gamma}\sin\theta]. \tag{38}$$

For static stability analysis, the necessary condition for the existence of a possible equilibrium state at $\theta = \theta_o$ is that, $\hat{V}_{\hat{\gamma}} = \frac{\partial(\hat{V})}{\partial\hat{\gamma}} = 0$ and $\hat{V}_{\theta} = \frac{\partial(\hat{V})}{\partial\theta} = 0$, these conditions yield,

$$\hat{\gamma}_{1,2} = 1/2[1 \mp (1 - \theta(K\tan\theta)^{-1})^{1/2}], \tag{39}$$

Combining equations (36) and (39), yields

$$\hat{V}_{(\theta)1,2} = \theta^2/2 + K/2[1 \mp (1 - \theta(K\tan\theta)^{-1})^{1/2}]^2 + 1/2\hat{P}\cos\theta[1 \pm (1-\theta(K\tan\theta)^{-1})^{1/2}] - \hat{P}, \tag{40}$$

It follows that,

$$\hat{V}_1' = [K(1-D) - \hat{P}\cos\theta/2]\times [(1+D)\tan\theta + (2KD)^{-1}(\tan\theta - \theta\sec^2\theta)(\tan^2\theta)^{-1}] \tag{41-a}$$

$$\hat{V}_2' = [K(1+D) - \hat{P}\cos\theta/2] \times \{[-2(KD)^{-1}(\tan\theta - \theta\sec^2\theta)\times(\tan^2\theta)^{-1} + (1-D)\tan\theta]\}. \tag{41-b}$$

where,

$$D = [1 - \theta(K\tan\theta)^{-1}]^{1/2}.$$

$$\hat{V}''_{(\theta)1} = \left[\left\{(1+D)\tan\theta + (2KD)^{-1}(\tan\theta - \theta\sec^2\theta)(\tan^2\theta)^{-1}\right\}\times \left\{(\tan\theta - \theta\sec^2\theta)(2D\tan^2\theta)^{-1} + \tfrac{1}{2}\hat{P}\sin\theta\right\}\right] + \left[\left\{-\tan\theta(\tan\theta - \theta\sec^2\theta)(2DK\tan^2\theta)^{-1} + (1+D)(\cos^2\theta)^{-1} + (\tan\theta - \theta\sec^2\theta)^2 \times (4K^2D^3\tan^4\theta)^{-1} + (DK\sin^2\theta)^{-1}(-1 + \theta\cos\theta/\sin\theta)\right\}\right]\times \left[K(1-D) - \tfrac{1}{2}\hat{P}\cos\theta\right], \quad (42\text{-a})$$

and

$$\hat{V}''_{(\theta)2} = \left[\left\{(1-D)\tan\theta - (2KD)^{-1}(\tan\theta - \theta\sec^2\theta)(\tan^2\theta)^{-1}\right\}\times \left\{-(\tan\theta - \theta\sec^2\theta)(2D\tan^2\theta)^{-1} + \tfrac{1}{2}\hat{P}\sin\theta\right\}\right] + \left[\left\{+\tan\theta(\tan\theta - \theta\sec^2\theta)(2DK\tan^2\theta)^{-1} + (1-D)(\cos^2\theta)^{-1} - (\tan\theta - \theta\sec^2\theta)^2 \times (4K^2D^3\tan^4\theta)^{-1} + (DK\sin^2\theta)^{-1}(-1 + \theta\cos\theta/\sin\theta)\right\}\right]\times \left[K(1+D) - (\hat{P}\cos\theta)\tfrac{1}{2}\right]. \quad (42\text{-b})$$

where,

$D = \left[1 - \theta(K\tan\theta)^{-1}\right]^{1/2}$, and

$\hat{V}''_{(\theta)} = \dfrac{d^2\hat{V}}{d\theta^2}$.

For static stability analysis, the necessary condition for the existence of a possible equilibrium state at $\theta = \theta_o$ is that, $\hat{V}' = \dfrac{d\hat{V}}{d\theta} = 0$, this condition yields

$$\hat{P}_{1,2} = 2(\cos\theta)^{-1}\{K[1 \mp (1 - \theta(K\tan\theta)^{-1})^{1/2}]\}. \qquad (43)$$

Equation (43) gives relations between dimensionless load $\hat{P}$ and angular rotation θ in radians.

The sufficiency condition for the neutral equilibrium is given by the condition that, $\hat{V}'' = \frac{d^2\hat{V}}{d\theta^2} = 0$. Hence the critical values of rotation $(\theta_{1,2})_{cr}$ and critical values of load $(\hat{P}_{1,2})_{cr}$ are evaluated by using the conditions that, $(\hat{V}_{1,2})' = 0$ and $(\hat{V}_{1,2})'' = 0$, simultaneously.

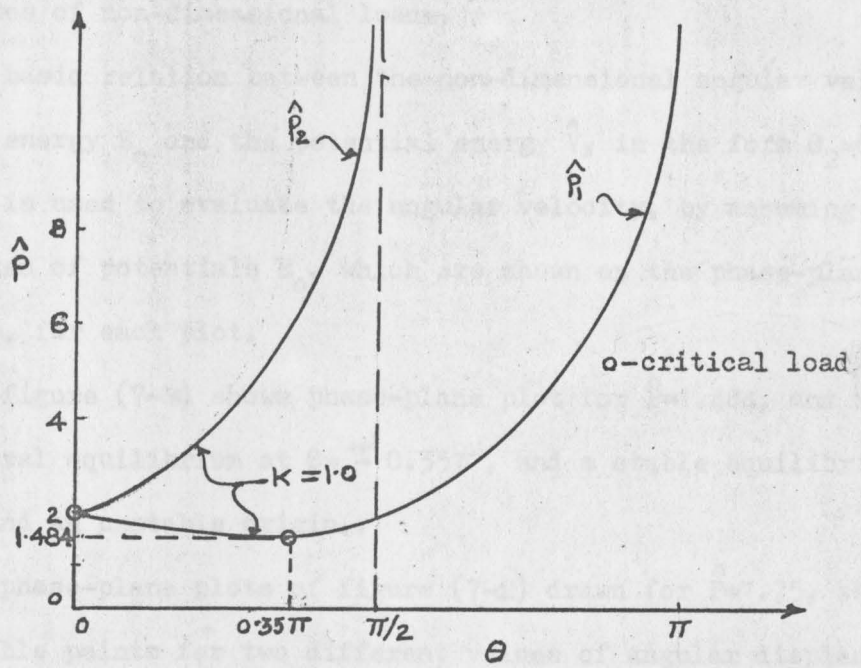

Typical load Vs angular displacement Figure (7-c)

A plot of the family of dimensionless load $\hat{P}$ versus rotation θ curves is shown in figure (7-c) for various values of parameter K.

For K=1, $\hat{P}_1=2$ and $\theta=0$, the corresponding point on the load rotation curve is in neutral equilibrium, since $\hat{V}_1'=0$ and $\hat{V}_1''=0$. For $\hat{P}_1>1.484$ and $0.35\pi<\theta<\pi$, all points on the curve are in stable equilibrium for K=1.

For K=1, $\hat{P}_2=2$ and $\theta=0$, the corresponding point is in stable equilibrium, since $\hat{V}_2'=0$ and $\hat{V}_2''$ is positive. For K=1, $\hat{P}_2>2$ and $0<\theta<\pi/2$ all points on the curve are in stable equilibrium, since $\hat{V}_2'=0$ and $\hat{V}_2''$ is positive.

7.2 DYNAMIC ANALYSIS

The phase-plane concept is used to investigate the dynamic stability of the model, for a specific value of parameter K and for various values of non-dimensional loads.

The basic relation between the non-dimensional angular velocity, the initial energy E_o and the potential energy $\hat{V}$, in the form $\theta_2=\dot{\theta}_1=\pm(E_o-\hat{V})^{1/2}$, is used to evaluate the angular velocity, by assuming various values of potentials E_o, which are shown on the phase-plane trajectories, for each plot.

The figure (7-k) shows phase-plane plot for $\hat{P}=1.484$, and represents neutral equilibrium at $\theta=\pm 0.35\pi$, and a stable equilibrium at $\theta=0.14\pi$ and an unstable origin.

The phase-plane plots of figure (7-l) drawn for $\hat{P}=1.75$, shows a set of stable points for two different values of angular displacements and a set of unstable points which includes the origin.

The phase-plane plots of figures (7-m), (7-n) and (7-o) drawn for $\hat{P}_1=2.0$, $\hat{P}_1=4.0$ and $\hat{P}_1=8.0$, respectively show a set of stable points including the origin and an unstable point in between the two stable points.

Figure (7-p) shows phase-plane plots for $\hat{P}_2$=2.0 and represents a stable origin.

The phase-plane plots shown in figure (7-q) and (7-r) for $\hat{P}_2$=4.0 and $\hat{P}_2$=8.0 respectively, represent the origin as an unstable point and a stable point on an angular displacement axis for different values of θ corresponding to the points on the load-deflection curve.

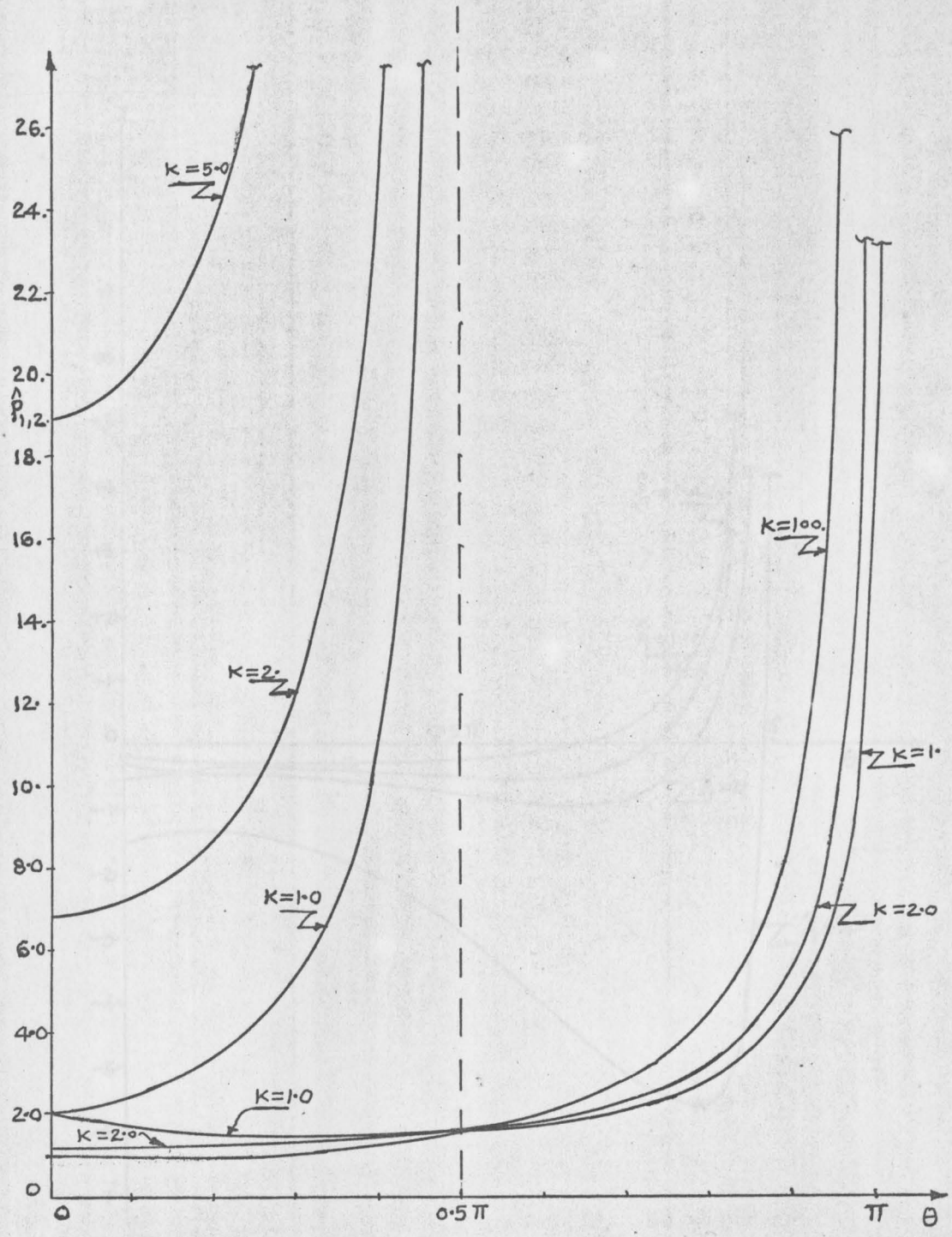

Load Vs angular displacement

Figure (7-d)

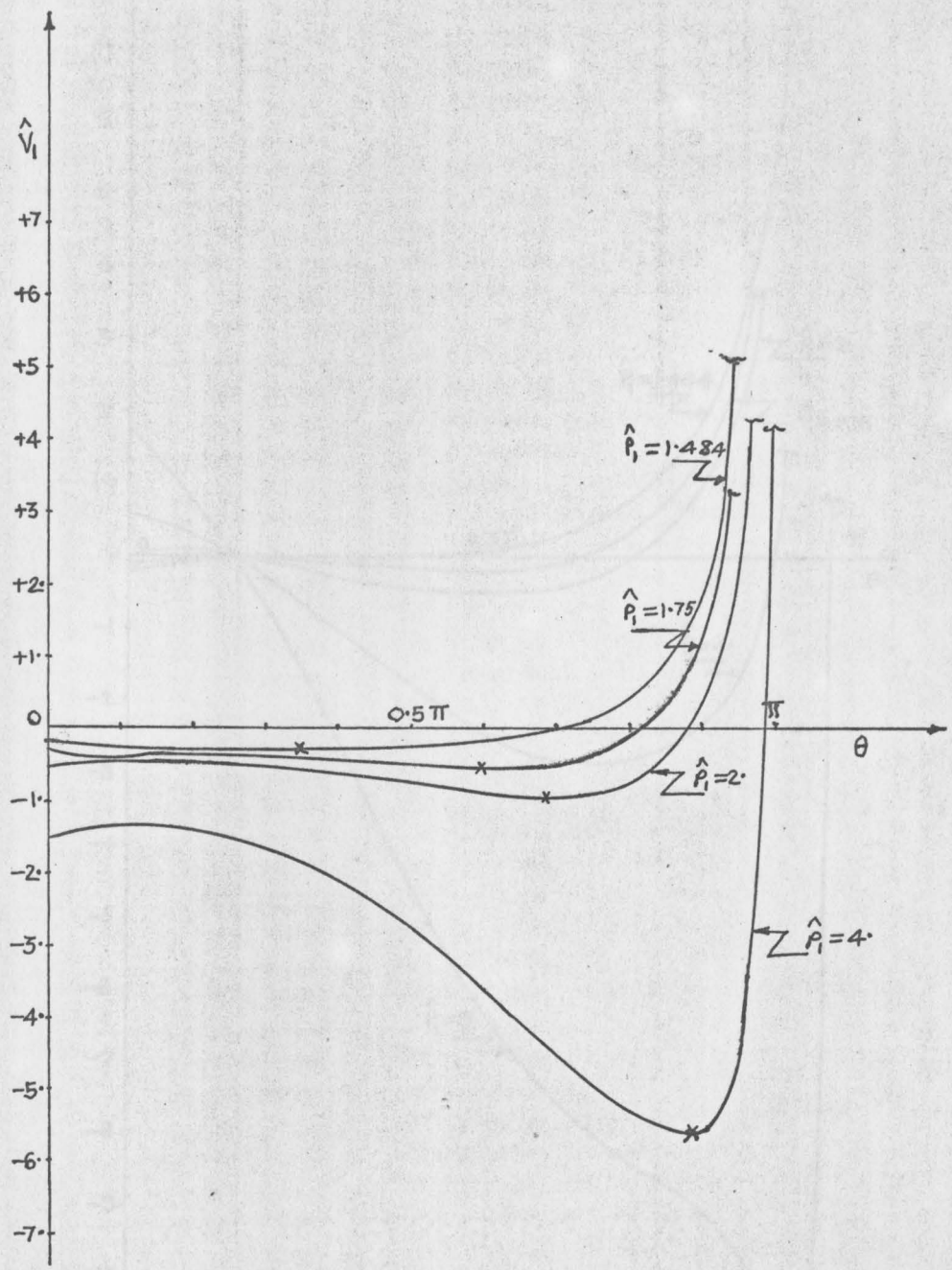

Potential energy Vs angular displacement

Figure (7-e)

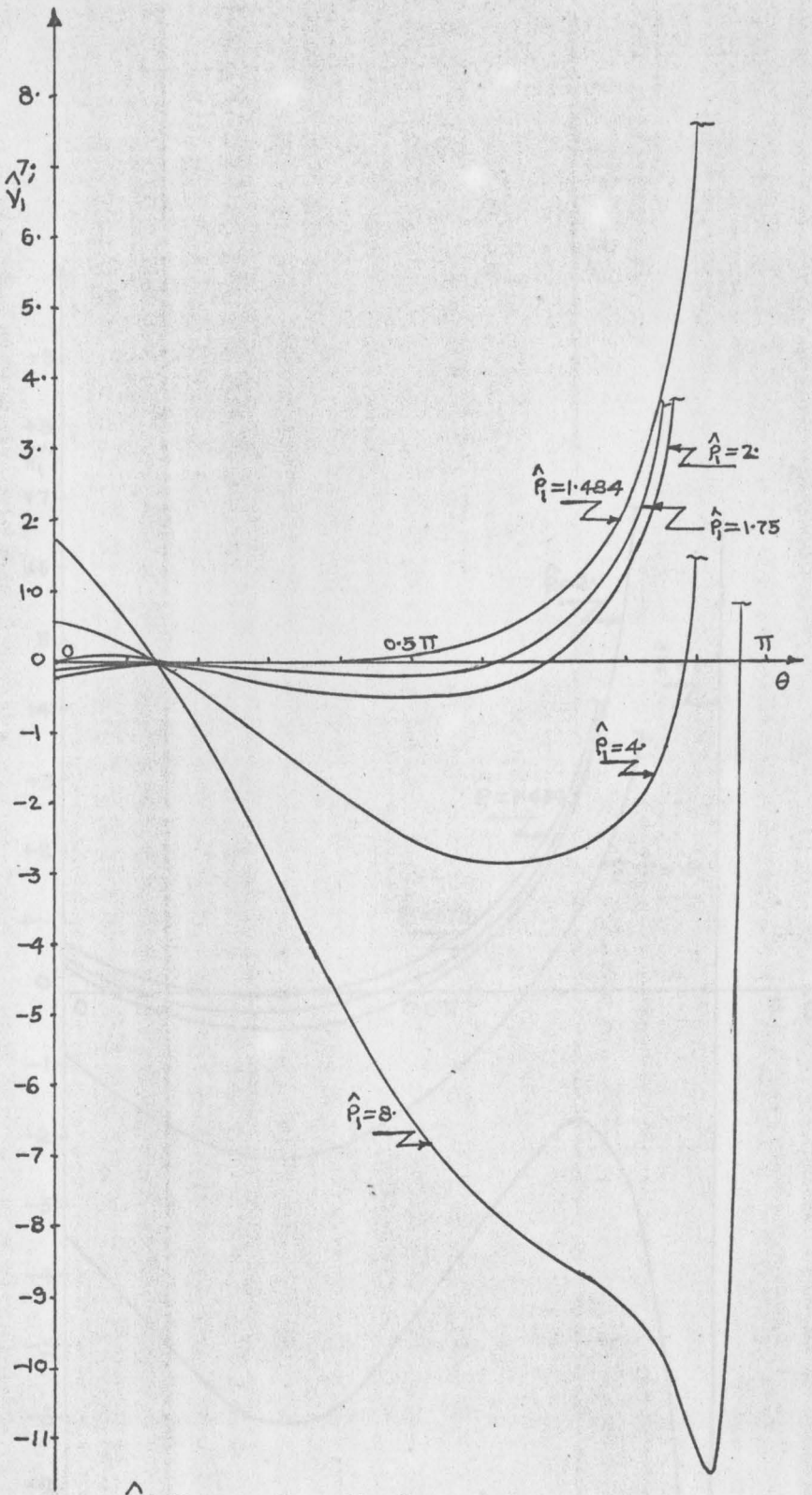

$\hat{V}_1$ Vs angular displacement

Figure (7-f)

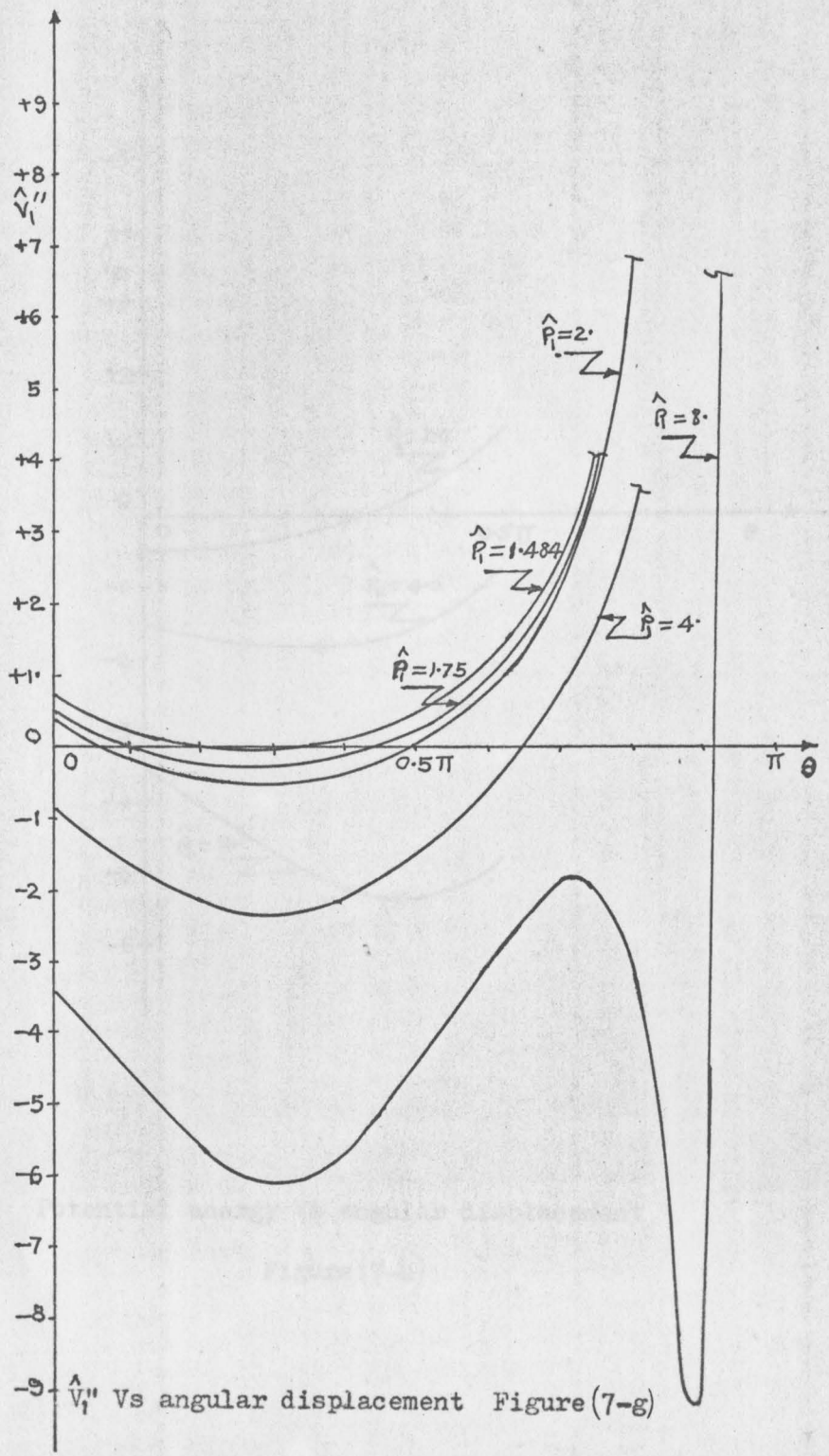

$\hat{V}_1''$ Vs angular displacement Figure (7-g)

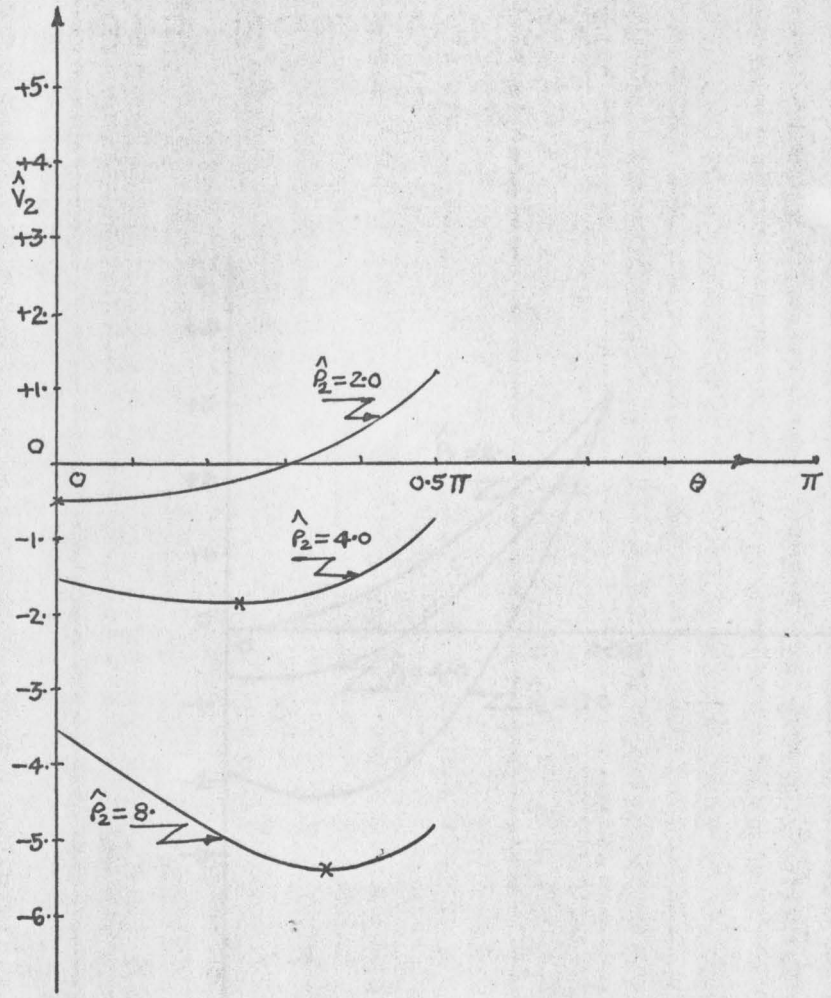

Potential energy Vs angular displacement

Figure (7-h)

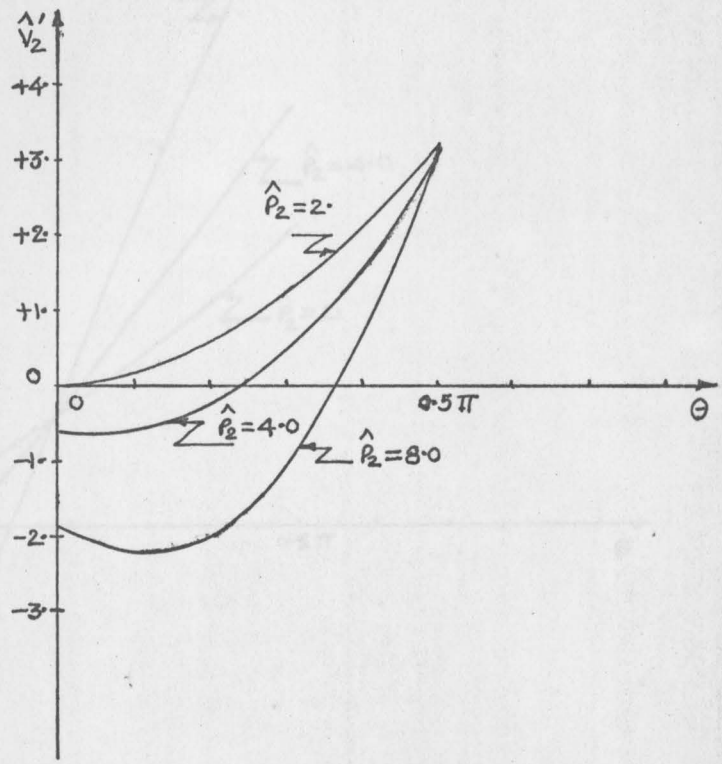

$\hat{V}_2'$ Vs angular displacement

Figure (7-i)

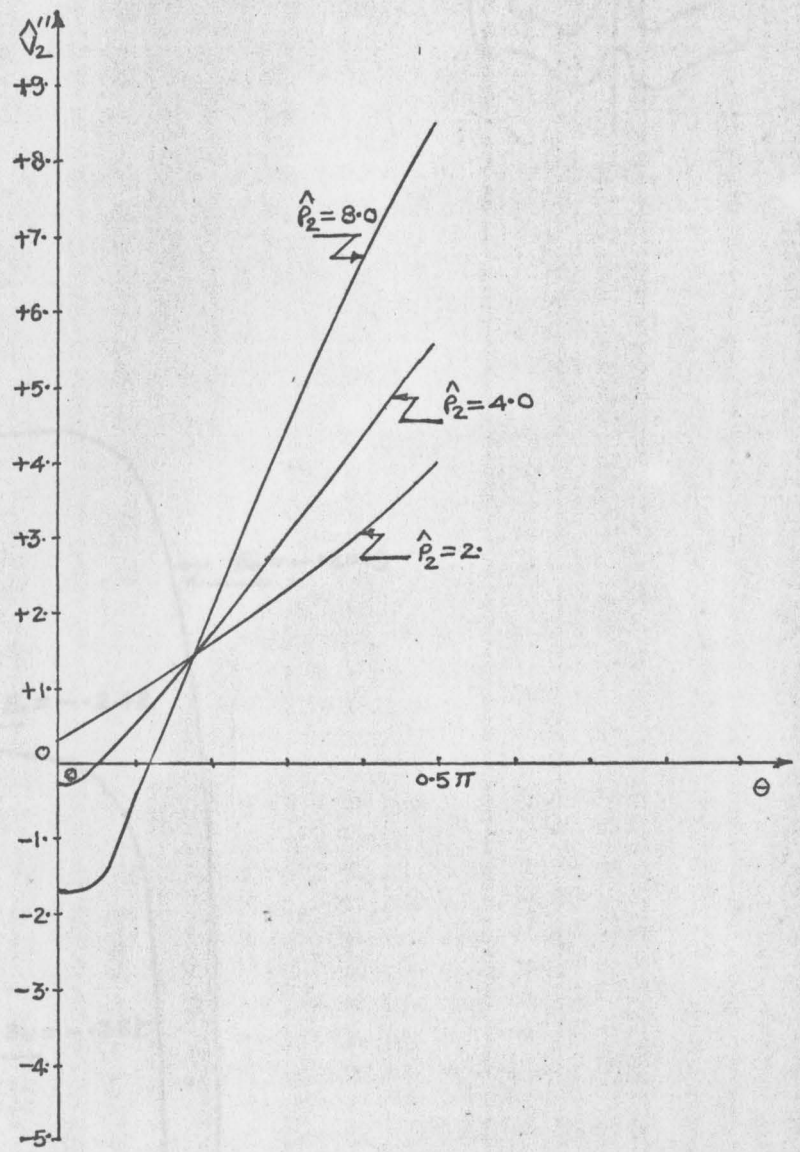

$\hat{V}_2''$ Vs angular displacement

Figure (7-J)

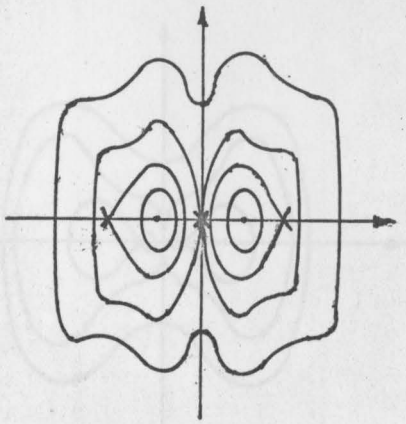

K=1.

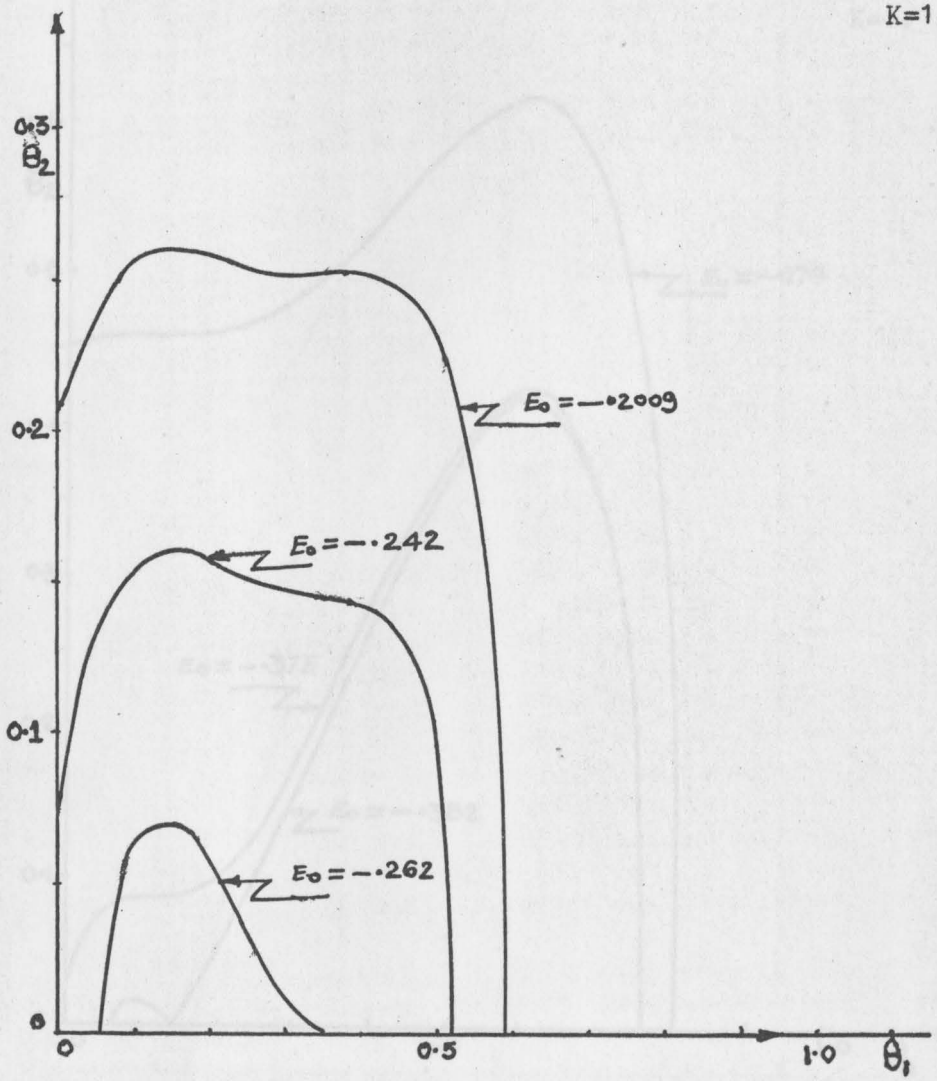

Phase-plane plot for $\hat{P}_i$= 1.484

Figure (7-K)

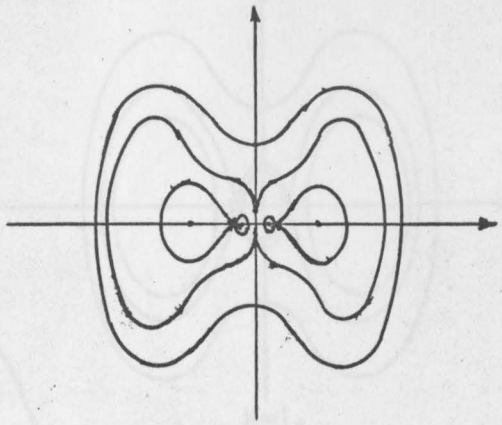

K=1.

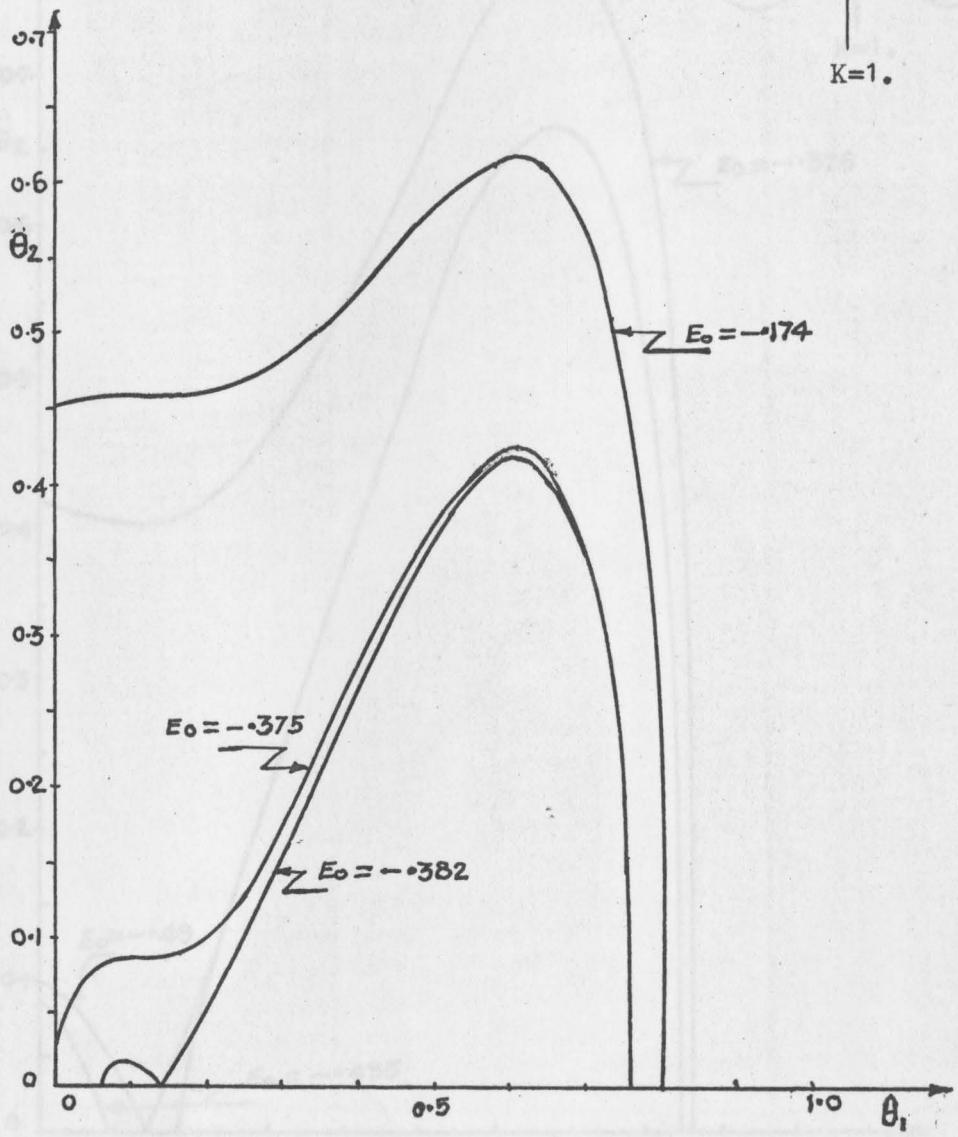

Phase-plane plot for $\hat{P}_1$=1.750

Figure(7-1)

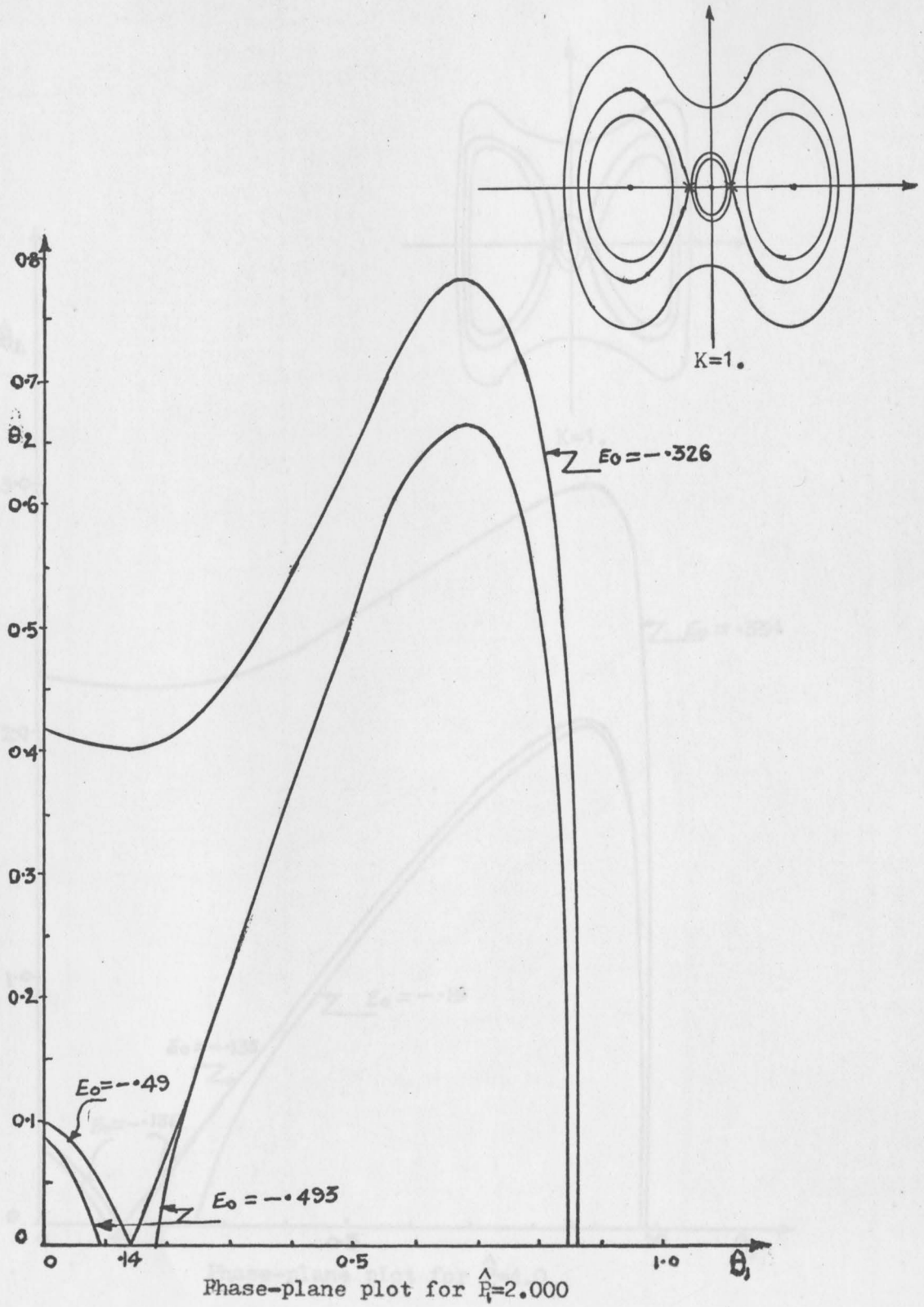

Phase-plane plot for $\hat{P}_i$=2.000

Figure (7-m)

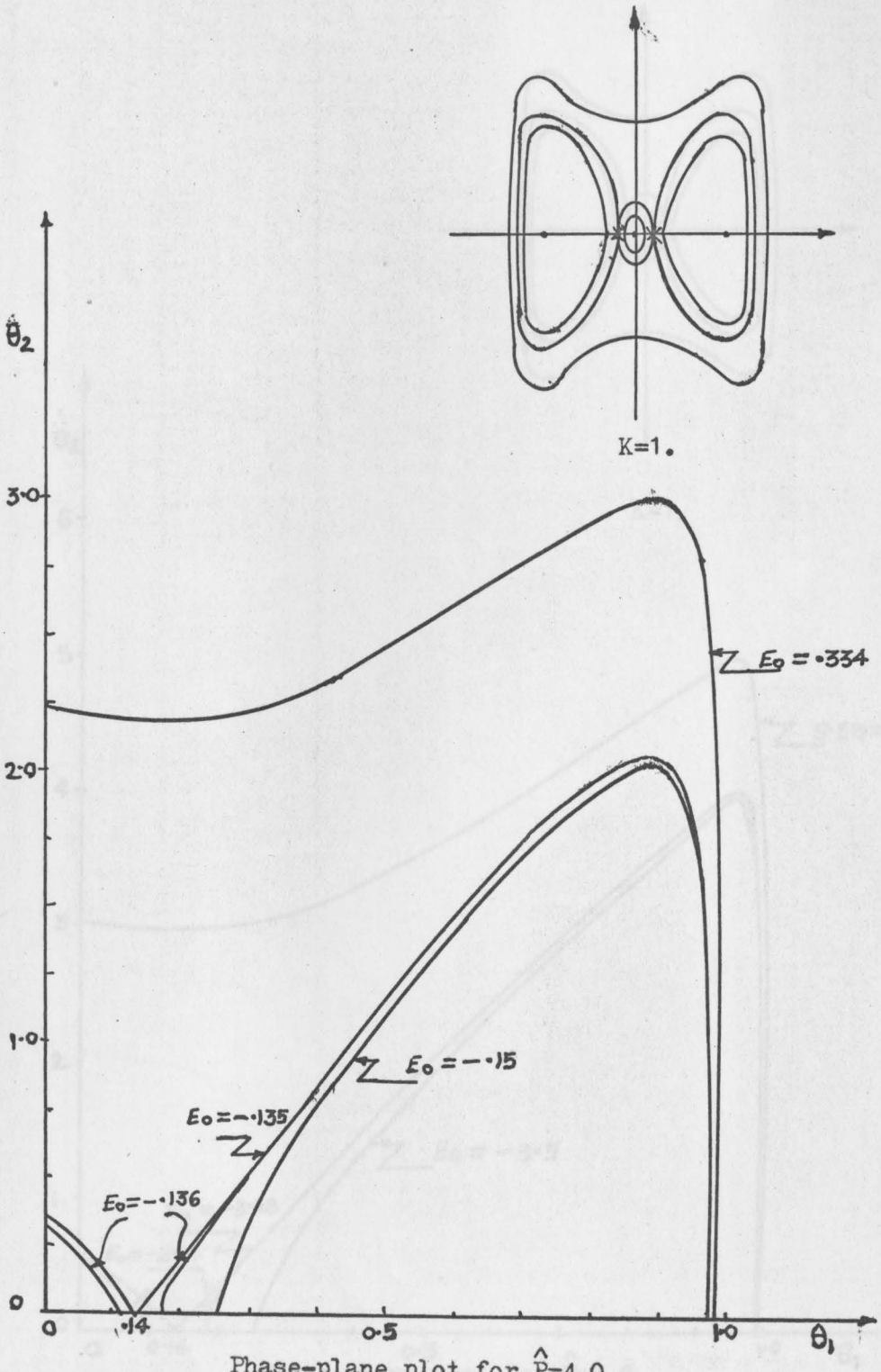

Phase-plane plot for $\hat{P}_j$=4.0

Figure (7-n)

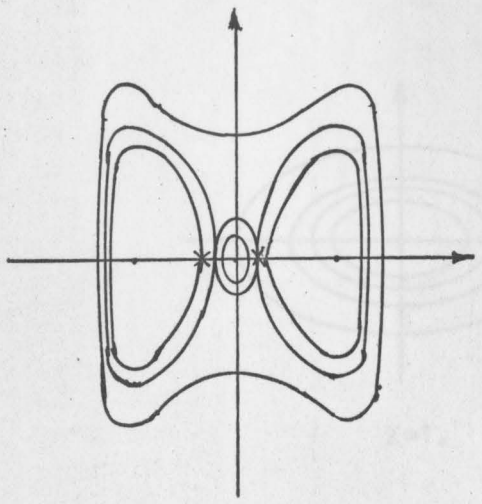

K=1.

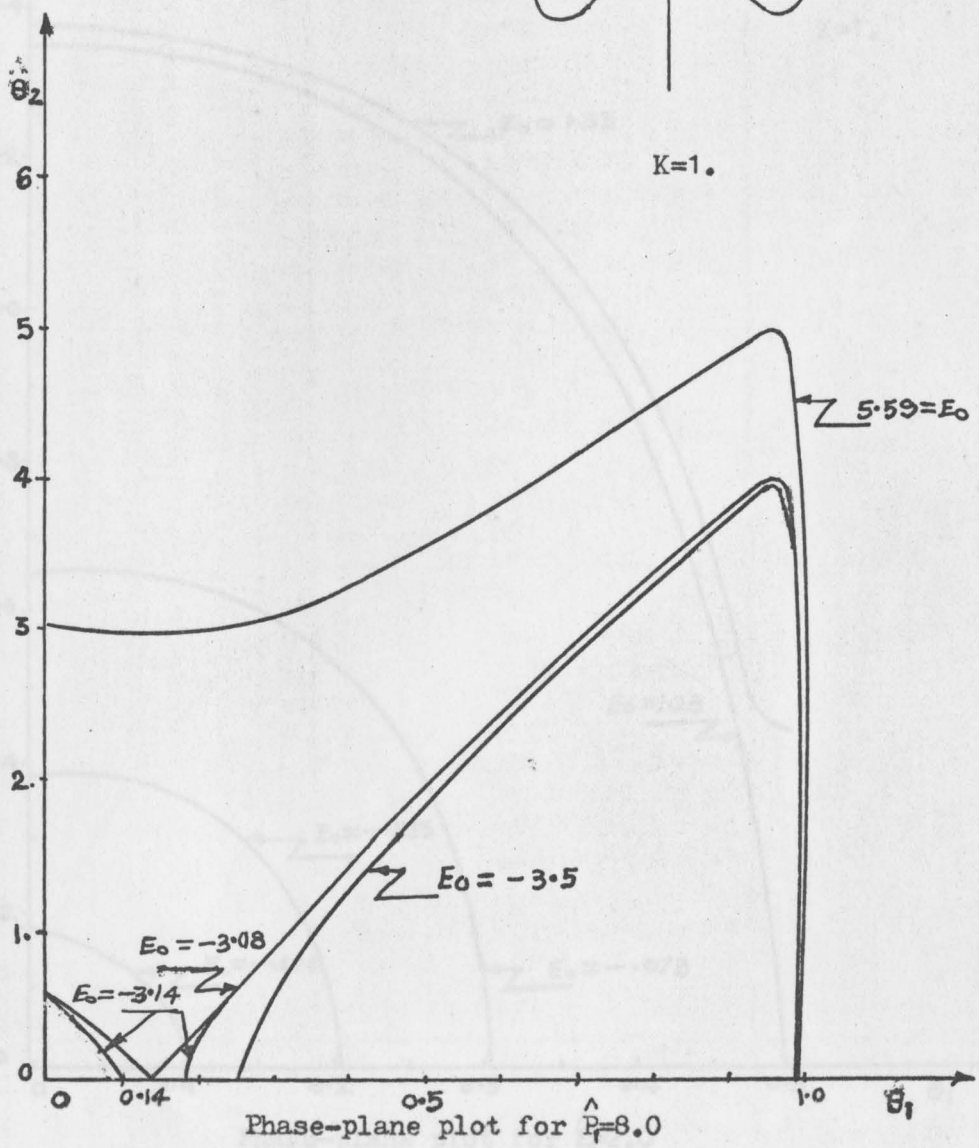

Phase-plane plot for $\hat{P}_f$=8.0

Figure(7-a)

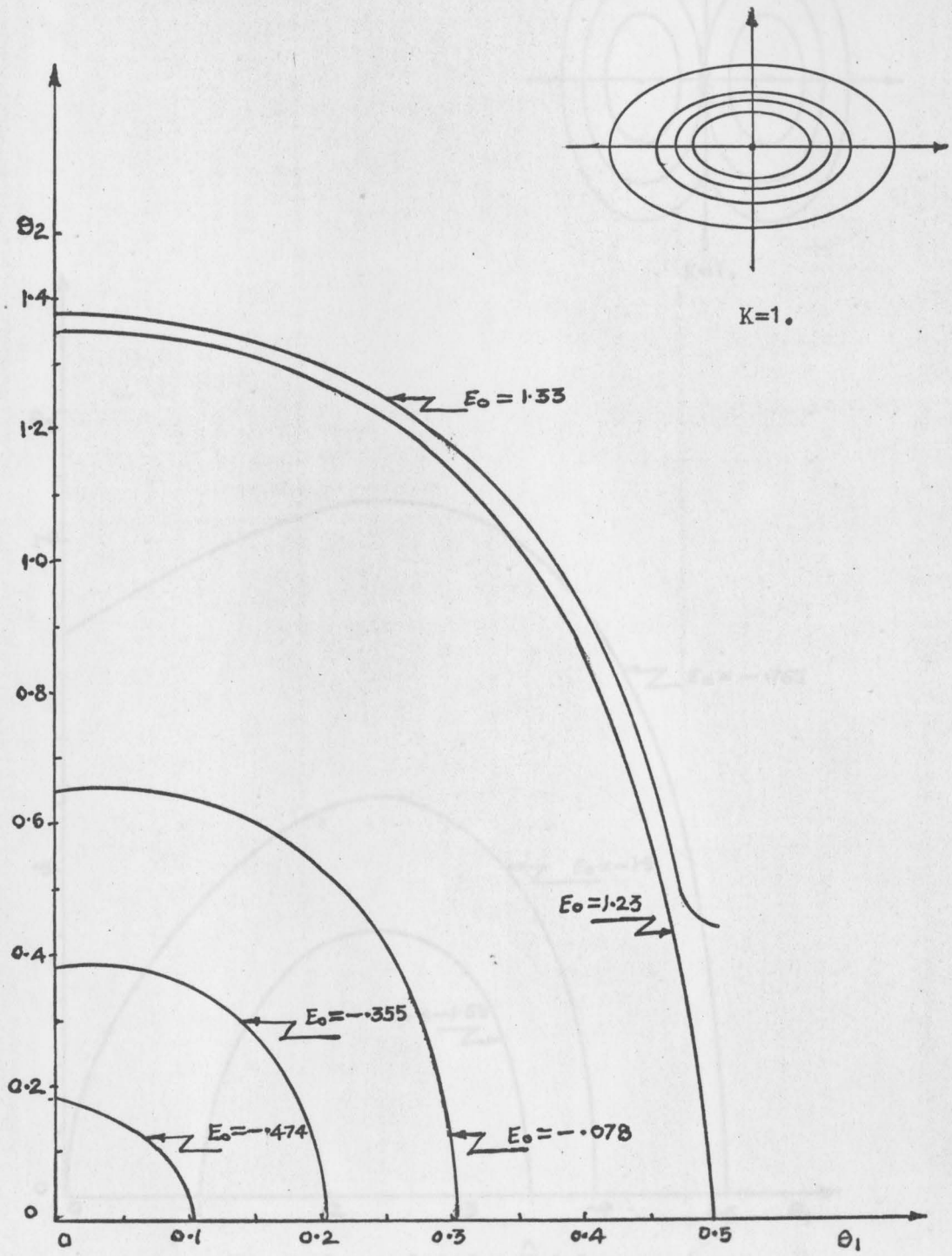

Phase-plane plot for $\hat{P}_\Sigma = 2.0$

Figure (7-p)

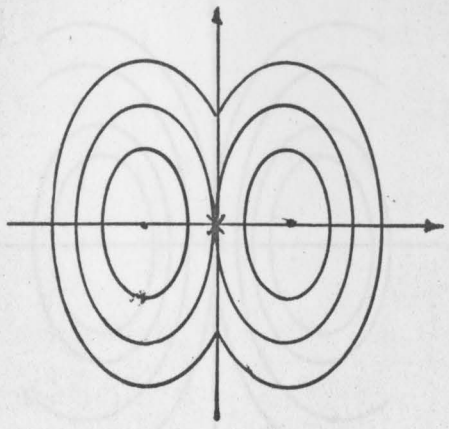

K=1.

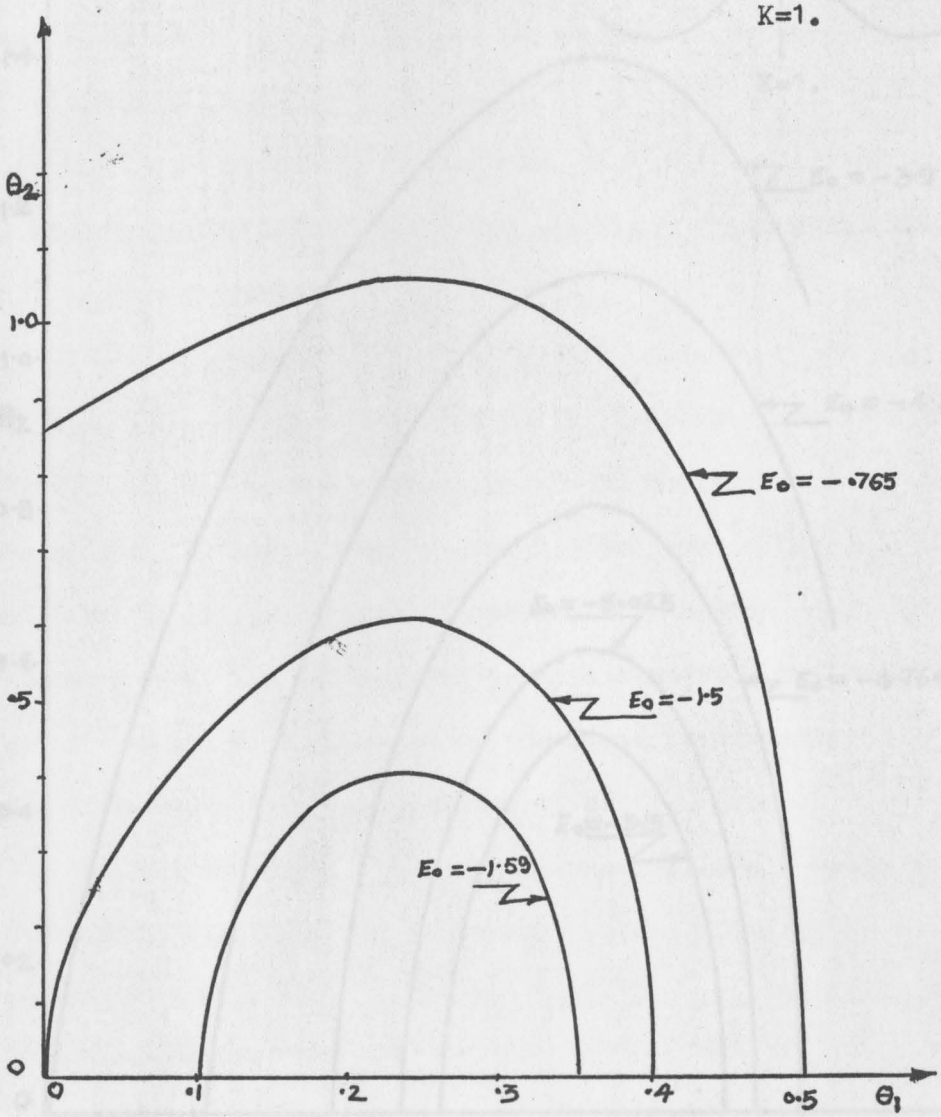

Phase-plane plot for $\hat{P}_Z$=4.0

Figure (7-Q)

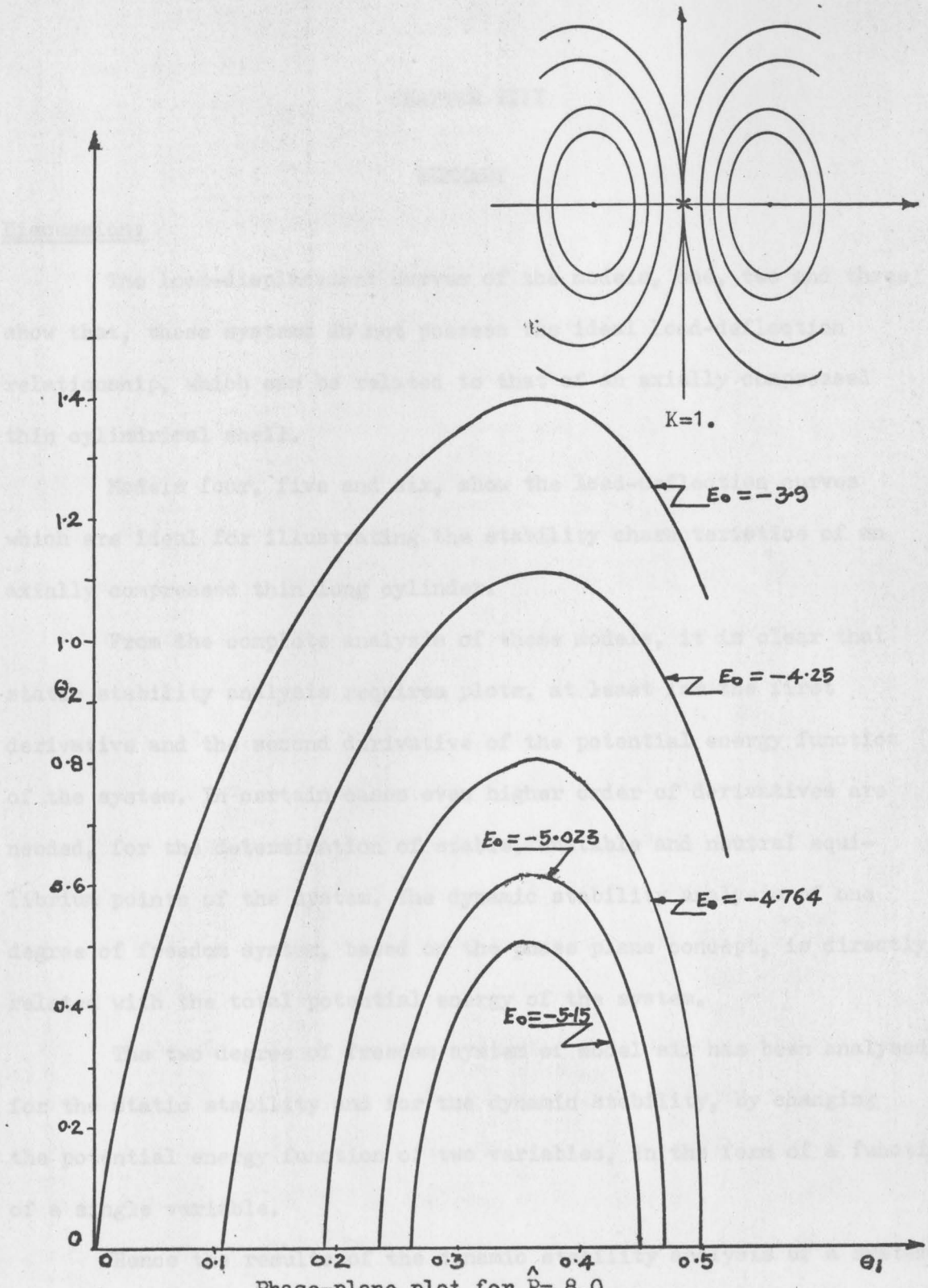

Phase-plane plot for $\hat{P}_2 = 8.0$

Figure (7-7)

CHAPTER VIII

SUMMARY

Discussion:

The load-displacement curves of the models, one, two and three show that, these systems do not possess the ideal load-deflection relationship, which can be related to that of an axially compressed thin cylindrical shell.

Models four, five and six, show the load-deflection curves which are ideal for illustrating the stability characteristics of an axially compressed thin long cylinder.

From the complete analysis of these models, it is clear that static stability analysis requires plots, at least for the first derivative and the second derivative of the potential energy function of the system. In certain cases even higher order of derivatives are needed, for the determination of stable, unstable and neutral equilibrium points of the system. The dynamic stability analysis of one degree of freedom system, based on the phase plane concept, is directly related with the total potential energy of the system.

The two degree of freedom system of model six has been analysed for the static stability and for the dynamic stability, by changing the potential energy function of two variables, in the form of a function of a single variable.

Hence the results of the dynamic stability analysis of a system complement the results of the static stability analysis. Thus the combination of a static and a dynamic analysis of the stability for a system

gives a precise interpretation of the stability based on the lateral displacement criteria.

Conclusion:

The system of model six, even for such a simple geometrical configuration, involves a complicated mathematical analysis. The load-deflection plot for the system shown by model five, gives a finite value of non-dimensional load for zero deflection. As the deflection starts increasing beyond zero, the curve follows a well defined downward trend, showing an unstable segment between the two neutral equilibrium points. Once the deflection starts increasing beyond the second neutral equilibrium point, the curve shows a stable segment and thus reverses the earlier downward trend. Hence the model five is chosen as the most appropriate model to illustrate the lateral-deflection criteria of the elastic stability of an axially compressed thin cylindrical shell, in a most simplified manner.

Throughout this thesis, non-linearity is induced geometrically, while material properties have been assumed to possess a linear load-deflection relationship. Even a simple non-linear form of geometrical configuration involves a complicated mathematical analysis as seen from the analysis of model two.

Hence the effect of the non-linearity of the material may be investigated for the simple models of one degree of freedom systems, which are presented in this thesis, to verify the possibility of a further simplification of the analysis of the models.

REFERENCES

1. Leipholz, H. , Stability Theory (translated by scientific translation service), Academic Press, New York, 1970.

2. Oden, J. T. , Mechanics of Elastic Structures, McGraw-Hill, New York, 1967.

3. Panovko, Y. G. and Gubanova, I. I. , Stability and Oscillations of Elastic Systems, Nauka Press, Moscow, 1964.

4. Stoker, J. J. ,Nonlinear Vibrations, Interscience Publishers, Wiley and Sons, Inc., New York, 1966.